AMERICAN UNIVERSITY OF BEIRUT

OPTIMIZED ONLINE CONTROL STRATEGY OF COMBINED CHILLED CEILING AND DISPLACEMENT VENTILATION SYSTEMS FOR ENERGY SAVINGS

by
AMER MAHER KEBLAWI

A thesis
submitted in partial fulfillment of the requirements
for the degree of Master of Engineering
to the Department of Mechanical Engineering
of the Faculty of Engineering and Architecture
at the AmericanUniversity of Beirut

Beirut, Lebanon
June 2010

AMERICAN UNIVERSITY OF BEIRUT

OPTIMIZED ONLINE CONTROL STRATEGY OF COMBINED CHILLED CEILING AND DISPLACEMENT VENTILATION SYSTEMS FOR ENERGY SAVINGS

by

AMER MAHER KEBLAWI

Approved by:

_____

Dr. Nesreen Ghaddar, Professor — Advisor
Department of Mechanical Engineering

_____

Dr. Kamel Ghali, Associate Professor — Member of Committee
Mechanical Engineering

_____

Dr. Daniel Asmar, Assistant Professor — Member of Committee
Mechanical Engineering

Date of thesis defense: June 09, 2010

AMERICAN UNIVERSITY OF BEIRUT

THESIS RELEASE FORM

I, Amer Maher Keblawi

☐ authorize the American University of Beirut to supply copies of my thesis to libraries or individuals upon request.

☐ do not authorize the American University of Beirut to supply copies of my thesis/dissertation/project to libraries or individuals for a period of two years starting with the date of the thesis defense.

_____
Signature

_____
Date

ACKNOWLEDGMENTS

I would like to thank my advisors at the American University of Beirut for the help and dedicated support that spanned for the time taken for this work to be accomplished. I am sincere to Prof. Nesreen Ghaddar and Prof. Kamel Abou Ghali for their dedicated help and support during work time at AUB and during Holidays and weekends.

The motivation of my advisors Prof. Ghaddar and Prof. Ghali was very essential to initiate and boost this work. Their guidance was very helpful for me to be able to complete the years spent on accomplishing my master's degree at AUB.

I would like to thank Prof. Daniel Asmar for bearing with me and reviewing my thesis as a member of my thesis committee in a short notice.

I would like to acknowledge the support and help of the faculty at the Mechanical Engineering Department for enhancing my scientific knowledge, analytical and learning skills.

I would like to thank the staff at the American University of Beirut for their great help from their positions at AUB.

Thanks to all my friends and colleagues with whom I have shared unforgettable moments at AUB and who supported me during my research work time. I would especially like to thank Abed Al-Kader Al-Saidi, Ralph Saade, Mohammad Al-Othmani, Mohammad Kanaan, Adnan Akhdar, Jack Abboud, and Ezzat Al-Jaroudi.

Last but not least, I would like to greatly thank my family for their great patience and support in the period during which this work was finalized; if it wasn't for my family's support I would not have been at this place at this time.

AN ABSTRACT OF THE THESIS OF

Amer Maher Keblawi for Master of Engineering
Major: Mechanical Engineering

Title: Optimized Online Control Strategy of Combined Chilled Ceiling and Displacement Ventilation Systems for Energy Savings

The chilled ceiling displacement ventilation (CC/DV) system is a promising hybrid energy efficient air-conditioning system for the Middle East. The CC/DV operation involves several variables to be controlled unlike conventional systems. These variables include supply air flow rate, temperature and humidity, and the chilled ceiling temperature. Energy consumption is strongly dependent on the settings of these variables.

The objective is to develop an optimized supervisory control tool for the CC/DV system to determine optimal set points of the control variables using conventional and optimized operation modes (strategies) to minimize energy consumption while creating the best indoor air quality (*IAQ*) and thermal comfort. The optimized supervisory control tool will use inline dynamic control models that are based on simplified relations derived from the physical behavior of the system and cooled space. An innovative methodology is proposed to relate the chilled ceiling load to total load ratio to the system control variables to simplify the optimization process under transient loading. A dynamic multi-variable objective cost function for the supervisory control of the CC/DV system performance indices and constraints will be formulated and solved using genetic algorithms that will interact with the online model of the CC/DV plume-multi-layer thermal space model and the system components models to insure feasible solutions that meet both physical constraints, *IAQ* as determined from the stratification height of the fresh air zone and carbon dioxide concentration, and thermal comfort as determined by the vertical temperature gradient and percent people dissatisfied. Grey box models are used to determine the inherent displacement ventilation parameters including the stratification height and temperature gradient inside the cooled zone.

The contribution of the proposed work is in the development of a robust online control methodology with optimized supervisory control for CC/DV systems to improve the hybrid system energy efficiency. Recommendations will be forwarded through a case study for system operation under climatic conditions of Beirut using typical construction.

CONTENTS

ILLUSTRATIONS

Figure Page

TABLES

Dedication addressed

To my family

CHAPTER 1

INTRODUCTION

In real life applications, the process of improving thermal comfort and indoor air quality inside a conditioned space increases the HVAC system's energy consumption. Also maintaining healthy indoor conditions may sometimes conflict with human thermal comfort. Tradeoffs between these desired targets must be done to reach an acceptable compromise. Moreover, a heating, ventilation and air-conditioning system first cost is an important parameter to calculate the overall cost of the system.

Conventional HVAC applications use mixed air systems, where the warm room in the air is conditioned by diluting it with a certain quantity of cold air. The source of the introduced cold air may be either from totally fresh air or partially fresh air (fresh + recycled), and the second case is commonly used. These conventional heating, ventilation and air-conditioning (HVAC) systems are supposed to consume additional energy because the air conditioning process is being applied to the whole air volume of the zone while the actual need is to condition the air in a part of the zone where the occupancy is concentrated.

The displacement ventilation combined with a chilled ceiling (CC/DV) system under study eliminates this problem by introducing conditioned air to a certain level where the occupants' sensation is limited. The Displacement Ventilation is a system where completely (or partially) fresh air is introduced to the system at a relatively higher temperature than the conventional system; air enters the zone from ducts mounted at a low level near the ground (floor-supply). The introduced air builds up in

the room until it reaches a certain level. The level at which air circulating mass becomes negligible is called the "Stratification Height Level". Reaching the stratification height, air density gradient is supposed to increase and virtual sheet of air is created separating lower fresh and cold air from the upper mixed hotter and contaminated air. Return air then leaves from the upper part of the zone (ceiling-exhaust) taking with it the air that was slightly heated by the dynamic load and contaminated by the generation of carbon dioxide from people or other contaminating sources. On the other hand Displacement Ventilation Systems have limited load removal capacity and is estimated to be 40 W/m^2 according to ASHRAE studies; that is, as the load increases either the temperature of the introduced air must be lowered or the mass flow rate of the supply air must be increased and consequently the speed must be increased, and in both cases limitations exist to assure thermal comfort concerning temperature sensation and draft sensation [Jiang et al. (1995)]. Introducing a chilled ceiling to the system increases the load removal capacity to 100 W/m^2. The chilled ceiling assists in removing part of the sensible load by its radiative effect. The overall thermal load removal capacity of the system will certainly increase, and the system is now more complex to operate because more controlled parameters are introduced. Now the operation of such a multi component system may have many scenarios that result in the desired thermal comfort and indoor air quality (IAQ) constraints, only one of these scenarios is considered the best if it is associated with the minimum energy consumption.

The objective of this thesis is to control the chilled ceiling displacement ventilation system to operate at a minimal running cost. Thus, it is essential to optimize the running cost of the CC/DV system by finding the optimum operational cost in an online fashion. To be able to perform the online optimization, simplified inline

dynamic models are used that are relatively fast and usable over small simulation time intervals.

Several reasons render the optimization of the total cost of the CC/DV system a complex task. The first challenge is that the performance of the system cannot be predicted using simple systematic equations with defined variables, but rather the performance is predicted in transient by simulating several lumped non-linear coupled equations, so that the performance parameters are considered to be an output of a black box in which number of simulations and iterations are performed internally. Such a black box system gives no information about differential quantities which are necessary information for conventional optimization routines to search for the minimum in the system. This challenge directed us toward evolutionary derivative-free optimization routines such as Simulated Annealing, Pattern Search, Particle Swarm and Genetic Algorithm. Derivative free algorithms don't need any information about the differential quantities as conventional optimization routines do, but rather apply certain strategies depicted from natural phenomenon to search for the minimum in the system.

Another challenge is how to optimize with time, the derivative-free optimization routines optimize for discrete events, and the challenge is then focused to how to find the optimum design variables in which the continuous series of events is considered as a single discrete event, during each prediction period the optimized variables are supposed to be constant and not varying with time.

A third challenge is that the optimization routine shall be able to cope with the real system dynamics; i.e. the optimization should be made and terminated within the specified prediction period upon which the control is set.

The aim of the optimization is to be able to get the control set-points for which the controller would operate on, after the set-points are determined, it is not difficult to determine the voltage required for the actuator to set the valve ratio.

CHAPTER 2

LITERATURE REVIEW

Buildings equipped with energy management control systems (*EMCS*s) allow optimizing the supervisory control for *HVAC* (Heating, Ventilation, and Air conditioning) systems to establish optimal operation mode and set points while providing the desired indoor comfort and environment quality at minimum cost. One of the HVAC systems that has potential for energy savings at optimized operation is the combined chilled ceiling and displacement ventilation (*CC/DV*) systems [Novoselac & Sebric (2002), Mossolly et al. (2008)]. The *CC/DV* system at loads not exceeding 100 W/m^2 offers an improved indoor air quality (*IAQ*) at lower energy consumption and operational cost [Ghali et al. (2007)].

Many studies have used system based optimal control strategies in simulating the space response to changes in the controlled variables and have shown considerable energy savings when used compared to conventional strategies. Nassif et al. (2005) utilized a two-objective genetic algorithm to optimize model parameters of model-based supervisory control strategy for building HVAC systems. Their optimization process was applied to an existing variable air volume (VAV) conventional HVAC system and resulted in 16% savings in energy use over two summers. House and smith (1995) showed that energy savings as high as 20% are achieved through optimized control strategies based on physical models of VAV system. The complexity of the optimization control strategy problem increases with the use of detailed physical models which is the case of a CC/DV system. Detailed physical models would definitely lead to more accurate simulation results but at higher computational cost and computer

memory [Wang and Ma, 2008]. Depending on the optimization technique, the issue of computer time will be compounded if multiple iterations are required between the optimizer that sets the trial set points of the controlled variables and the physical models to predict thermal response and performance.

Neural network black-box models have been utilized to construct supervisory control strategies for HVAC systems without relying on any assumptions of the system or process [Curtiss et al. (1994), Massie (2002), Chow et al. (2002), Dodier and Henze (2004), Zhang et al. (2005)]. Artificial neural network (ANNs) can be used for the optimal on-line control strategy of the CC/DV system. However, the accuracy of the neural network model depends on the size of data used to train the model. Use the neural network model outside the range of training data may result in significant errors as reported by Xu et al. (2005).

The CC/DV is a special air-conditioning system characterized by a complex interactive nature between its two subsystem air conditioning components: chilled ceiling and the displaced supply air. The two subsystem components are responsible in providing the required load and in maintaining the required thermal comfort and indoor air quality. However, the load portions removed by the two subsystems are determined by detailed physical space model of energy, mass and flow balances to insure a stratification height above 1 m and a temperature gradient below 2.5 K/m. Increasing the load removed by the DV subsystem will enhance the indoor air-quality at a higher energy cost and lower thermal comfort due to the increase of the temperature gradient. Whereas increasing the load removed by the CC subsystem will enhance the thermal comfort to some extent at a lower indoor air quality. This complex interactive nature of the two subsystems accompanied with their complex models due to non-linearity model

equations will render the use of the detailed physical models impossible for on-line applications.

Inline dynamic models represent a viable alternative to formulate optimized supervisory control methods (Wang and Jin 1999). Mathematical or statistical correlations could be developed based on simplifying the complicated physical model to allow the use of the empirical relations for a wide range of operating conditions in transient settings at a lower computational cost. The highest computational cost in CC/DV system simulation is the prediction of the space thermal response Ghaddar et al. (2008), whilst the CC/DV system components models such as the chiller, pump, fan coil, fans, reheat, and chilled ceiling loop are well developed in literature and are computationally inexpensive. To develop an optimized online supervisory control method for the CC/DV system, it is essential to derive correlations between the control variables of the system and the desired comfort and IAQ parameters.

Correlation models that could be used for optimization settings were developed for the CC/DV system inherent parameters in feasible load regions (Keblawi, et al. 2009). These correlations are based on the ratio of the CC cooling load to the total load (*R*), the thermal comfort represented by the temperature gradient (*dT/dZ*), IAQ determined by stratification height *H*, and the amount of displaced air parameter (P = ratio of total load to supply air mass flow rate). These models are accompanied with on-line lumped CC/DV system space dynamic model to find all the required indoor air quality and thermal comfort parameters in an online fashion. The design chart parameters for steady state operation include the temperature ranges of the supply air temperature and the chilled ceiling for any *R* in the feasible design regions where *dT/dZ* is less than 2.5 K/m and with the facility to read off the stratification height *H* and

insure that it is above 1.2 m. In addition, statistical correlations were derived between the desired comfort and IAQ values were also derived for different load ranges using Ayoub et al. (2006) wall-plume-multilayer model (Ghaddar, et al. 2008). These correlations, although important in developing quasi-steady optimized supervisory control method for the CC/DV system, they are not generally suitable for use when significant energy storage is present due to transient internal and external space load, this problem is simply solved by using small prediction time periods (equivalent to 10 minutes) after modeling the storage elements. The dynamic optimization involves determining a trajectory of set points during operation. A detailed physical space model can be used to generate transient operation correlations between physical and comfort variables to form the basis of an effective optimized online supervisory control of the CC/DV system.

There are several possibilities of operational control strategies to associate with a selected design of CC and DV subsystem to meet peak load. The performance of a selected combined system under transient loading conditions varies depending on the complexity (number of control variables) of the selected control strategy to meet demand [Mossolly et al (2008)]. It is of great interest to investigate the possible optimal combinations of size of subsystems, control strategy, and associated operational parameters over the load cycle of the system operation to optimize system cost. Typical control strategies derived specifically for CC/DV systems reported by Novoselac & Sebric (2002) and Mumma and Conory (2001) concentrate on controlling the temperature of the cooling panel. Displacement ventilation systems may use in general more fan but less chiller energy compared to conventional systems [Lau and Chen (2006)]. The control of panel temperature was also associated with dew point control in

the room (Reffat et al (2004). Spercher at al. (1995) investigated night cooling aspect of cooled ceiling panel control strategy to offset heat storage in walls and save energy. Condensation prevention control strategies have also been proposed in literature by adjusting supply air temperature, humidity and flow rate. Simmonds et al. (2006) presented concepts on how condensation can be prevented on the cooled ceiling by controlling supply water temperature to the panels to reach higher temperature than air dew point. It is also possible to dehumidify supply air temperature by sub-cooling to the desired humidity and then heat the air by a reheat coil to the set supply temperature. The control of radiant ceiling panel temperature is normally done by either using variable water flow / fixed supply water temperature system or fixed flow/ variable water temperature system [Strand and Baumgartner (2004), Conory and Mumma (2001)]. Conory and Mumma (2001) cooling loop control strategy was based on modulating chilled water flow rate to the ceiling panel in response to space thermostat. Niu et al. (1995) used, while assessing a CC/DV system performance, a control strategy by which the supply air flow rate and temperature are kept constant at design values of ventilation requirements and temperature of 15 °C, and further cooling requirement is met by activating the ceiling panel.

Although, many researchers tackled the general optimization problem of the CC/DV system but none has developed a robust optimized dynamic online supervisory control methodology that stems from accurate predictions of interaction of physical space and system components models to determine the trajectory of the system set points.

In this work, an optimized, effective, and advanced supervisory control methodology will be developed using online dynamic models to design and

implementan online controller for the optimized operation of the CC/DV under the optimal strategy based on controlling both DV and CC system variables that include the chilled ceiling temperature and supply air flow and thermal conditions.

CHAPTER 3

PROBLEM STATEMENT

The main objective of this work is to control the chilled ceiling displacement ventilation in an optimal cost fashion where the operational cost of the system is minimized in an online manner holding in mind that the minimization of the operational cost leads to sacrifices in the thermal comfort and internal air quality. The operational cost includes the cost of running the chiller, pump, reheat and fan; it is worth to note that the major component of the cost is the cost of the chiller and reheat.

To be able to calculate the operational cost, the optimization tool and control strategies of a combined chilled-ceiling and DV air conditioning (CC/DV) system shall be defined to predict optimal controller set-points to improve the operating performance while satisfying thermal comfort and indoor air quality taking into account controlling the system. The specific objectives of this research work are the following:

1) Minimize the system operational cost in an online manner using an evolutionary direct search derivative free optimization methodology, for this work the genetic algorithm is selected. To be able to optimize the operational cost in an online fashion, online dynamic models have been developed; these models also include derived statistical correlations that are used in this work.
2) Develop a controller that would control the system to the optimally found operational control variables settings. The controller is chosen to be the proportional integral derivative controller (PID) for the fan and reheat. Non-linear model predictive control is used for the three way valves.

The control strategies work will result in optimal setting of parameters for a given control strategy of CC/DV of system. The contribution of the proposed work is to develop a robust evaluation tool of control strategies for CC/DV systems for low energy requirement.

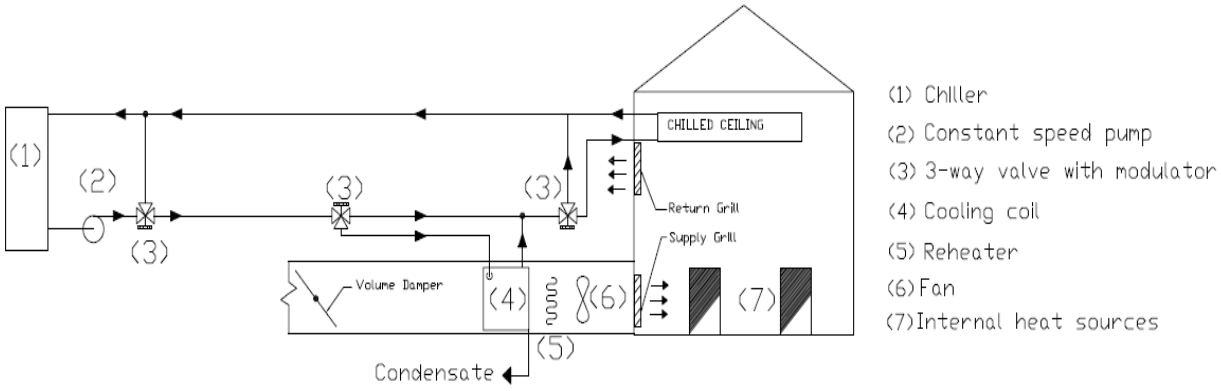

Fig.3.1: Schematic of a single zone cooled and ventilated by a combined chilled ceiling and displacement ventilation system.

A schematic of the CC/DV system is shown in Fig.3.1that shows a tentative chilled water circuit and the primary system equipment and components. A first step to formulate the optimization problem based on first and operating cost is to develop suitable simulation models for the ceiling panel and the fan coil unit (air handling unit), and suitable performance prediction models of water chiller, fans, and pumps [Lu et al (2005]. In addition, a computationally effective transient physical model of the space cooled by the CC/DV system is necessary to predict indoor environment level of thermal comfort and indoor air quality as a function of the load and system operational variables. The space model will be coupled with models of primary equipment and air handling unit, air fans and pumps as well as models predicting the cost of the various components.

Detailed simulation models have been developed to be able to simulate the actual system; nevertheless, these models could not be used in online optimization for their large computational time. For this reason, online simplified dynamic models were derived to be able to optimize the system in an online fashion.

The simulation models of the following subsystems and components will be as considered:

1) Modeling of the ceiling panel will be done using Conroy and Mumma (2001) to predict the ceiling temperature transient response.
2) Modeling of the fan coil unit will follow the model of (Zhou, Braun and Zeng September 2007)to predict the point at which the cooling coil switches between the wet and dry conditions and the coil dynamic performance.
3) The chiller, pumps, and fans performance at part load will be predicted using empirical correlations and cost functions.
4) The CC/DV cooled space thermal model will use a simplified transient dual layer plume model taking into consideration heat gain by walls and changes in internal loads schedules.

CHAPTER 4

SIMULATION MODELS

The simulation models are used to simulate the actual operation and processes in a combined chilled ceiling and displacement ventilation air conditioned system, these models are more accurate, precise and need a more computational time than their counterpart dynamic models.

Four different simulation models are presented in this work: the wall simulation model, the chilled ceiling displacement ventilation simulation model, the cooling coil simulation model and the chilled ceiling simulation model.

4.1. Wall Simulation Model

This text discusses the one-dimensional heat transfer through a wall considering the transient storage effects. Before the computations are made, the sol-air temperature would be defined and a method of computation of the sol-air temperature is discussed.

4.1.1. The External Sol-air Temperature

Solar radiation absorbed by the exterior surfaces of the walls often provides the majority of the energy added to the surface in summer conditions. To obtain an accurate energy balance on the walls, the absorbed solar energy, infrared radiation exchange, and convective heat gain or loss on the exterior surface are to be included in the analysis. Each component may be analyzed separately; however, an alternative method may be used by utilizing the sol-air temperature. The sol-air temperature is

defined as “a fictitious outdoor dry bulb temperature such that in the absence of solar radiation, the surface would exchange the same net amount of energy to air at the sol-air temperature as exchanged in the actual environment”.

Consider an external surface of a building that is not transparent to solar radiation. The surface absorbs a portion of the incident direct (I_D), diffuse (I_d), and reflected (I_R) solar radiation. The total absorbed amount becomes (provided that the solar absorptivity is equal for all three components):

$$q_s'' = \left(I_D + I_d + I_R\right)\alpha_s = I_T\alpha_s \tag{4.1.1}$$

The exterior wall surface also absorbs heat by convection from the surrounding ambient air based on the temperature between the wall surface (t_w) and the air dry-bulb temperature (t_o):

$$q_c'' = h_{o,c}\left(t_o - t_w\right) \tag{4.1.2}$$

The infrared radiation emitted by the surface is:

$$q_{IR,out}'' = \varepsilon_w \sigma T_w^{\,4} \tag{4.1.3}$$

The infrared radiation absorbed by the surface originates from a variety of other surfaces and the sky:

$$q_{IR,in}'' = \sum_{i=1}^{n}\left(\varepsilon_i F_{w,i}\sigma T_i^4\right) \tag{4.1.4}$$

The net energy flux to the surface becomes:

$$q_{net}'' = q_s'' + q_c'' + q_{IR,in}'' - q_{IR,out}'' = I_T\alpha_s + h_{o,c}\left(t_o - t_w\right) + \sum_{i=1}^{n}\left(\varepsilon_i F_{w,i}\sigma T_i^4\right) - \varepsilon_w \sigma T_w^{\,4} \tag{4.1.5}$$

To simplify the foregoing expression, the following assumptions may be made:

All infrared emissivity values are equal; i.e. $\varepsilon_i = \varepsilon_w = \varepsilon$. This is a good assumption for non-metal surfaces where $0.9 \le \varepsilon \le 0.95$. The net infrared radiation to the surface then becomes:

$$q_{IR,net} = \varepsilon\sigma\left[\left(\sum_{i=1}^{n} F_{w,i} T_i^4\right) - T_w^{\ 4}\right] \tag{4.1.6}$$

The infrared radiation is linearized as the temperature differences are small. This eliminates the need for the absolute temperature and introduces a radiative heat transfer coefficient.

The temperatures of all surfaces, except the one taken into consideration, are at the local air dry-bulb temperature, t_o. This is a reasonable approximation, although the sky temperature is usually lower than the local dry-bulb temperature and surrounding surfaces receiving solar radiation have a higher temperature. A correction factor is introduced to account for the error introduced with this assumption. This correction factor is noted by $\varepsilon\,\Delta R$.

Using the above assumptions, the foregoing equation may be written as:

$$q''_{net} = I_T \alpha_s + h_{o,c}\left(t_o - t_w\right) + h_{o,R}\left(t_o - t_w\right) - \varepsilon\,\Delta R \tag{4.1.7}$$

Using the definition $h_o = h_{o,c} + h_{o,R}$, the above equation is written as:

$$q''_{net} = I_T \alpha_s + h_o\left(t_o - t_w\right) - \varepsilon\,\Delta R \tag{4.1.8}$$

From the definition of the sol-air temperature, t_e, we could write the same net energy transfer to the surface:

$$q''_{net} = h_o \left(t_e - t_w \right) \tag{4.1.9}$$

Combing the above two equations, the following equation is found for the sol-air temperature:

$$t_e = t_o + \frac{I_T \alpha_s}{h_o} - \frac{\varepsilon \Delta R}{h_o} \tag{4.1.10}$$

ASHRAE recommends that the correction factor ($\varepsilon \Delta R / h_o$) be given a value of 4 ^{0}C for horizontal surfaces facing up. Thus the sol-air temperature is 4 ^{0}C cooler due to the reduced infrared radiation coming from the sky. The correction factor is specified to be zero for vertical surfaces, as warmer sunlit surfaces compensate for the cooler sky temperature. An estimate for the correction factor for other tilt angles is found by using the following equation:

$$\frac{\varepsilon \Delta R}{h_o} = 4 \cos \Sigma \ ^0\text{C} \tag{4.1.11}$$

whereΣ is the surface tilt angle between the normal and the vertical.

The ratio α_s / h_o is a function of the color of the surface. For dark colors $\alpha_s / h_o = 0.052\,\text{m}^2\text{-}^0\text{C/W}$.On the other hand, for light colors $\alpha_s / h_o = 0.026\,\text{m}^2\text{-}^0\text{C/W}$.

4.1.2. Evaluating the External Heat Transfer Coefficient

The external heat transfer coefficient is dependent on the temperature difference between the wall temperature and the outdoor air, and the outdoor air velocity and direction with respect to the wall. According to the mobile window thermal test model(Yazdanian and Klems 1994), the external convective heat transfer coefficient may be written as

$$h_o = \sqrt{\left[C_t\left(\Delta T\right)^{1/3}\right]^2 + \left[aV_o^{\,b}\right]^2} \qquad (4.1.12)$$

In equation (4.1.12), the parameters are

ΔT	Temperature difference between the exterior surface and external air
C_t	Turbulent natural convection constant
a and b	Constants (refer to)
V_o	Wind speed at standard conditions

The values of the constants and coefficients of the mobile window thermal test model are summarized in Table 4.1.

Table 4.1: mobile window thermal test model constants

Wind Direction	C_t [W m^{-2} K$^{-4/3}$]	a [W m^{-2} K (m s^{-1})^b]	b
Windward	0.84	2.38	0.89
Leeward	0.84	2.86	0.617

4.1.3. Heat Gain Through Walls

4.2. As mentioned in the previous section, the wall absorbs solar energy, infrared radiation exchange, and convective heat gain or loss on the exterior surface; the sol-air temperature was defined to include the solar energy and the infrared radiation exchange in a fictitious outdoor temperature. Therefore, the sol-air temperature becomes the

external thermal boundary condition. The boundary conditions are coupled to solid wall by using the convective-radiative surface film coefficients. Therefore, the transient wall problem becomes a problem where the solid has convective coefficients on both sides with the fluid temperatures changing during the day.

The most important assumptions in the analysis are:

- Internal heat transfer is by conduction only (or pseudo-conduction if natural convection and infrared radiation are present in air cavities or in porous insulation).
- Contact resistances between layers of material are neglected.
- Air infiltration/exfiltration through the wall or roof construction is negligible.
- Heat flows only in the direction perpendicular to the exposed surfaces. Thus the heat transfer is one-dimensional.

Considering a multilayered wall; if the coordinate perpendicular to the wall surface is *x*, the governing equation within each layer is:

$$\frac{\partial T}{\partial t} = \alpha_j \frac{\partial^2 t}{\partial x^2} T \qquad (4.1.13)$$

The temperature and heat flux must be equal in both materials at an interface between them at the same value of *x*:

$$k_j \left.\frac{\partial t}{\partial x}\right|_j = k_{j+1} \left.\frac{\partial t}{\partial x}\right|_{j+1} \qquad (4.1.14)$$

The boundary condition on the inside surface is:

$$q_i'' = h_i \left(t_{w,i} - t_i \right) \tag{4.1.15}$$

The boundary condition on the outside surface is:

$$q_o'' = h_o \left(t_e - t_{w,o} \right) \tag{4.1.16}$$

Note that the heat flux is positive when the energy is moving into the building.

4.1.4. Numerical Methods

Although a large number of wall or roof constructions have been solved analytically, different structures which have not been analyzed may be encountered. Moreover, the internal wall temperatures may be of interest along with the internal wall temperature and heat flux. For this reason numerical solutions are employed to analyze the transient thermal response of a wall.

To have a numerical solution, the one-dimensional unsteady heat equation has to be discretized to convert the partial differential equation to an algebraic equation. Two methods of discretization are considered: the Taylor Series Expansion (TSE) method and the Integration over a Control Volume (IOCV) method.

The most general form of the one dimensional unsteady heat equation is

$$\frac{\partial}{\partial x}\left[kA\frac{\partial T}{\partial x} \right] + q'''A = \rho A\frac{\partial (CT)}{\partial t} \tag{4.1.17}$$

Note that in this work *T* stands for the temperature and *t* stands for time. The following notes are made on the foregoing equation:

- The equation is most general. It permits variation of medium properties ρ, *k*, and *C* with respect to *x* and/or *t*.
- The equation permits variation of cross-sectional area *A* with *x*.
- The equation also permits variation of q''' with *T* or *x*.
- The foregoing equation is to be solved for boundary condition at *x* = 0 and *x* = L. Thus $0 \le x \le L$ specifies the domain of interest.

To discretize the one dimensional unsteady heat equation, a grid is to be chosen. A sample grid is shown in the figure below

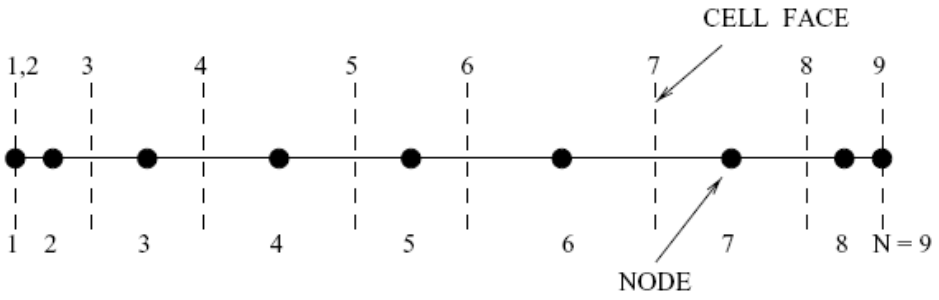

Fig.4.1: The Grid Layout

If the considered node is node P, the nodes to the east and west of P are denoted as E and W respectively. A figure is shown below to illustrate this notation:

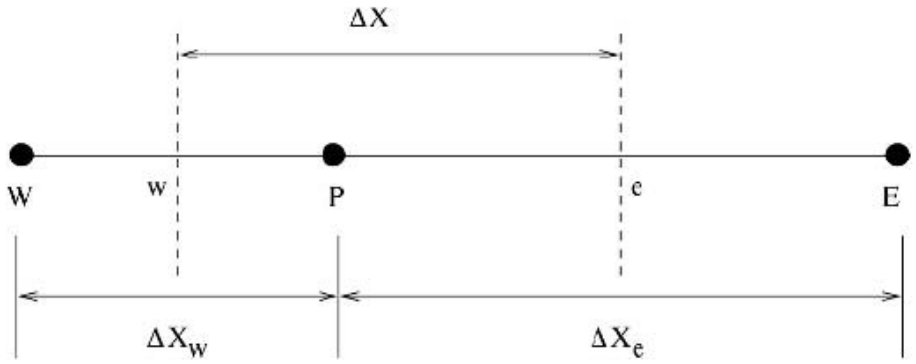

Fig.4.2: A Typical Node P with West and East Nodes

4.1.4.1. The Taylor Series Expansion Method

To employ this method, the one dimensional unsteady heat equation is written in the form

$$kA\frac{\partial^2 T}{\partial x^2}+\frac{\partial(kA)}{\partial x}\frac{\partial T}{\partial x}+q'''A=\rho A\frac{\partial(CT)}{\partial t} \tag{4.1.18}$$

The left hand side (LHS) and the right hand side (RHS) of the above equation are:

$$LHS\big|_P=kA\frac{\partial^2 T}{\partial x^2}+\frac{\partial(kA)}{\partial x}\frac{\partial T}{\partial x}+q'''A \tag{4.1.19}$$

$$RHS\big|_P=\rho A\frac{\partial(CT)}{\partial t} \tag{4.1.20}$$

The left hand side may be evaluated at a time t, or at a time $t + \Delta t$, or at a time intermediate between t and $t + \Delta t$. In general, the one dimensional unsteady heat equation may be written as

$$\zeta\left(LHS\right)_P^n+(1-\zeta)\left(LHS\right)_P^o=RHS\big|_P \tag{4.1.21}$$

Where ζ is a weighting factor, superscript *n* refers to the new time $t + \Delta t$, superscript *o* refers for the old time *t*. If $\zeta = 0$, then the discretization is called implicit; if $\zeta = 1$, then the discretization is called explicit; and if $0 < \zeta < 1$, then the discretization is called semi-implicit or semi-explicit.

The foregoing equation contains first and second derivatives of *T* with respect to *x*. To represent these derivatives a Taylor series expansion is employed:

$$T_E = T_P + \Delta x_e \left.\frac{\partial T}{\partial x}\right|_P + \frac{\left(\Delta x_e\right)^2}{2} \left.\frac{\partial^2 T}{\partial x^2}\right|_P + \cdots \tag{4.1.22}$$

$$T_W = T_P - \Delta x_w \left.\frac{\partial T}{\partial x}\right|_P + \frac{\left(\Delta x_w\right)^2}{2} \left.\frac{\partial^2 T}{\partial x^2}\right|_P + \cdots \tag{4.1.23}$$

From these two expressions, it is shown that:

$$\left.\frac{\partial T}{\partial x}\right|_P = \frac{\left(\Delta x_w\right)^2 T_E - \left(\Delta x_e\right)^2 T_W + \left(\left(\Delta x_e\right)^2 - \left(\Delta x_w\right)^2\right) T_p}{\Delta x_e \Delta x_w \left(\Delta x_e + \Delta x_w\right)} \tag{4.1.24}$$

$$\left.\frac{\partial^2 T}{\partial x^2}\right|_P = \frac{\Delta x_w T_E + \Delta x_e T_W - \left(\Delta x_e + \Delta x_w\right) T_p}{\Delta x_e \Delta x_w \left(\Delta x_e + \Delta x_w\right)/2} \tag{4.1.25}$$

Note that in the Taylor series expansion, terms involving derivative of order larger than two are ignore. Thus the foregoing derived expressions are called second-order accurate representations of first and second order derivatives with respect to *x*.

Evaluating the time derivative

$$\left(CT\right)_p^n = \left(CT\right)_p^o + \Delta t \left.\frac{\partial \left(CT\right)}{\partial t}\right|_P + \cdots \tag{4.1.26}$$

Therefore,

$$\left.\frac{\partial(CT)}{\partial t}\right|_P = \frac{(CT)_p^n - (CT)_p^o}{\Delta t} \tag{4.1.27}$$

In the Taylor series expansion, derivatives of order higher than one are ignored. Therefore the foregoing equation is a first-order-accurate representation of the time derivative.

Re-substituting into the heat equation, we obtain

$$\left[\left.\frac{\rho \Delta V C^n}{\Delta t}\right|_P + \zeta(AE + AW)\right] T_p^n = \zeta\left[AE\,T_E^n + AW\,T_W^n\right] + S \tag{4.1.28}$$

With

$$AE = \frac{2}{\Delta x_e}\left[(K\,A)_P + \frac{\Delta x_w}{2}\left.\frac{d(k\,A)}{dx}\right|_P\right]\frac{\Delta x}{(\Delta x_e + \Delta x_w)}$$

$$AW = \frac{2}{\Delta x_w}\left[(K\,A)_P - \frac{\Delta x_e}{2}\left.\frac{d(k\,A)}{dx}\right|_P\right]\frac{\Delta x}{(\Delta x_e + \Delta x_w)}$$

$$S = \left[\zeta q_p^{\prime\prime\prime,n} + (1-\zeta) q_p^{\prime\prime\prime,o}\right]\Delta V + (1-\zeta)\left[AE\,T_E^o + AW\,T_W^o\right] + \left[\left.\frac{\rho \Delta V C^o}{\Delta t}\right|_P - (1-\zeta)(AE + AW)\right] T_P^o$$

The following observations may be made on the Taylor Series Expansion method:

- Calculation of the coefficients *AE* and *AW* require the evaluation of the derivative $\left.d(kA)/dx\right|_P$
- For certain variations of *(kA)* and choices of Δx_e and Δx_w, *AE* and/or *AW* can become negative.

- For certain choices of Δt, the multiplier of T_p^o can become negative.
- In steady state problems, $\Delta t = \infty$ and T^o has no meaning. Therefore, steady state problems are solved implicitly and $\zeta = 1$

4.1.4.2. The Integration over a Control Volume method

In this method, the *RHS* and *LHS* of equation 2.5 are integrated within over a control volume Δx and over a time step Δt. Thus

$$Int\left(LHS\right) = \int_t^{t'} \int_w^e \frac{\partial}{\partial x}\left[kA\frac{\partial T}{\partial x} \right] dx\, dt + \int_t^{t'} \int_w^e q''' A dx\, dt \qquad (4.1.29)$$

Where $t' = t + \Delta t$. It is assumed that the integrands are constant over the time interval Δt. Further, q''' is assumed constant over the control volume. Since the second-order derivative is evaluated at a constant time, we have

$$Int\left(LHS\right) = \left[kA\frac{\partial T}{\partial x}\bigg|_e - kA\frac{\partial T}{\partial x}\bigg|_w \right]\Delta t + q_P''' A\Delta x \Delta t \qquad (4.1.30)$$

It is further assumed that T varies linearly with x between adjacent nodes. Therefore,

$$\frac{\partial T}{\partial x}\bigg|_e = \frac{T_E - T_P}{\Delta x_e}, \qquad \frac{\partial T}{\partial x}\bigg|_w = \frac{T_P - T_W}{\Delta x_w}$$

Note that when the cell faces are mid-way between the nodes, the representations of the derivatives are second order accurate. Replacing the derivatives in the original equation, we obtain

$$Int\left(LHS\right)=\left[\left.\frac{kA}{\Delta x}\right|_{e}\left(T_{E}-T_{P}\right)+\left.\frac{kA}{\Delta x}\right|_{w}\left(T_{W}-T_{P}\right)\right]\Delta t+q_{P}'''A\Delta x\Delta t \tag{4.1.31}$$

The right hand side of the equation is integrated as

$$Int\left(RHS\right)=\rho A\int_{t}^{t'}\int_{w}^{e}\frac{\partial\left(CT\right)}{\partial t}dx\,dt=\left(\rho A\Delta x\right)_{P}\left[\left(CT\right)^{n}-\left(CT\right)^{o}\right]_{P} \tag{4.1.32}$$

Re-substituting the integrals into integrated version of the one dimensional unsteady heat equation

$$\left[\left.\frac{\rho\Delta VC^{n}}{\Delta t}\right|_{P}+\zeta\left(AE+AW\right)\right]T_{P}^{n}=\zeta\left[AE\,T_{E}^{n}+AW\,T_{W}^{n}\right]+S \tag{4.1.33}$$

Where

$$AE=\left.\frac{kA}{\Delta x}\right|_{e}$$

$$AW=\left.\frac{kA}{\Delta x}\right|_{w}$$

$$S=\left[\zeta q_{P}^{'''n}+\left(1-\zeta\right)q_{P}^{'''o}\right]\Delta V+\left(1-\zeta\right)\left[AE\,T_{E}^{o}+AW\,T_{W}^{o}\right]+\left[\left.\frac{\rho\Delta VC^{o}}{\Delta t}\right|_{P}-\left(1-\zeta\right)\left(AE+AW\right)\right]T_{P}^{o}$$

Note that the equation derived by using the IOCV method has the following properties:

- Coefficients *AE* and *AW* can never be negative since $kA/\Delta x$ can only assume positive values.
- *AE* and *AW* represent thermal conductance.

- In steady state problems, $\zeta = 1$ because $\Delta t \to \infty$. In unsteady problems – for certain choices of Δt – the multiplier of T_P^o could still be negative. This is common with the TSE method.

4.1.5. Stability and Convergence

Designating each node by a running index $i = 1, 2, 3, ..., N$ where $i = 1$ and $i = N$ are boundary nodes, the discretized equation may be written in the following general form:

$$AP_i T_i = \zeta \left[AE_i T_{i+1} + AW_i T_{i-1} \right] + S_i, \qquad i = 2, 3, ..., N-1$$

The subscript *n* is dropped for convenience.

The discretized set of equations could be solved by using a variety of direct and iterative methods. These methods yield a converged solution if and only if a convergence criterion (also named Scarborough's criterion) is satisfied. This criterion may be stated in terms of the following equations:

$$\frac{\zeta \left[\left| AE_i \right| + \left| AW_i \right| \right]}{\left| AP_i \right|} \le 1 \text{ for all nodes}$$

$$\frac{\zeta \left[\left| AE_i \right| + \left| AW_i \right| \right]}{\left| AP_i \right|} < 1 \text{ for at least one node}$$

In unsteady problems, the convergence of the given set of discretized equation also requires that that coefficient of the term T_i^o be always positive. To satisfy this requirement, the following relation shall also be satisfied:

$$\Delta t < \left[\frac{\rho \Delta V_i C_i^o}{(1-\zeta)(AE_i + AW_i)} \right]_{\min}$$

Nevertheless, solution experience shows that for a given solution to converge:

$$\Delta t < \left[\frac{\rho \Delta V_i C_i^o}{(1-2\zeta)(AE_i + AW_i)} \right]_{\min} \qquad \text{for} \qquad \zeta < 0.5$$

For $\zeta \geq 0.5$ the time step Δt could be chosen without any restriction.

Note that for $\zeta = 0$, an explicit procedure is devised. For $\zeta = 1$ the implicit procedure s used and for $0 < \zeta < 1$ a partially implicit procedure is used. It is worth to note that by choosing $\zeta = 0.5$ the Crank-Nicholson method is used.

4.1.6. Choosing the Solution Methodology

The Taylor Series Expansion and Integration over a Control Volume method have been devised to discretize the one dimensional unsteady heat equation. The purpose of this section is to choose the methodology that is going to be used to solve the one dimensional wall problem: the discretization type and the unsteady solver approximation. Note that the following points may be made on the problem:

- Note that the Taylor Series Expansion (TSE) method casts the discretized algebraic equation in a non-conservative form while the Integration over a Control Volume (IOCV) method uses the as-derived conservative form.

- In the TSE, method the terms AE and AW have a little physical meaning. On the other hand, in the IOCV method, the terms AE and AW represent thermal conductance of the east and west faces respectively.
- In the TSE method, Scarborough's criterion may be violated. In the IOCVmethod, this can never happen. The question of invoking explicit procedure arises only when unsteady-state problems are considered. The implicit procedure, in contrast, can be invoked for both transient as well as steady-state problems. In fact, in steady-state problems ($t = \infty$) the implicit procedure is the only one possible.
- The explicit procedure imposes restriction on the largest time step to obtain stable solutions. The implicit and Crank-Nicholson procedures do not suffer from such a restriction.

In view of the above comments, the best combination is to use the Integration over a Control Volume (IOCV) method with the implicit procedure. Moreover, the implicit procedure is used for the analysis. Note that the crank Nicholson procedure is also considered.

4.1.7. Satisfying the Boundary Conditions

In one dimensional unsteady heat conduction problems, three types of boundary conditions may be encountered:

- Boundary temperatures T_1 and/or T_N are specified.
- Boundary heat fluxes q_1''or $q_N''$are specified.
- Boundary heat transfer coefficients h_1 and/or h_N are specified.

For each of the three types of boundary conditions shown above, the temperature at node 2 shall be derived for purposes of illustration.

4.1.7.1. Specified boundary temperature

In the specified boundary temperature, the temperature of the specified boundary node is known. Assuming that the temperature of node 1 (boundary node) is known, the temperature of the second node (node 2) is found to be:

$$\left(AP_2 + Sp_2\right)T_2^{l+1} = AE_2T_3^{l+1} + AW_2T_1^{l+1} + Su_2 \qquad (4.1.34)$$

Equation (4.1.34) is altered by inserting the boundary condition into the source term. This is done by using the following three step procedure:

$$Su_2 = Su_2 + AW_2\,T_1$$
$$Sp_2 = Sp_2 + AW_2$$
$$AW_2 = 0$$

4.1.7.2. Specified Heat Flux

In the specified boundary heat flux condition, the heat flux at the specified boundary node is known. For the purpose of illustration let the heat flux q_1'' be specified at $x = 0$. Then, temperature T_1 is unknown and the heat to node 1 is given as:

$$q_1 = A_1q_1'' = AW_2\left(T_1 - T_2\right)$$
$$T_1 = \frac{A_1q_1}{AW_2} + T_2$$

Therefore, the constant heat flux boundary condition may be applied by using the following procedure:

1. Calculate the temperature T_1 of node 1 from the foregoing equation.

2. Update $Su_2 = Su_2 + A_1 q_1$ and $Sp_2 = Sp_2 + 0$

3. Set $AW_2 = 0$.

Note that the above equations were derived assuming that heat flux enters into the boundary node. If heat exits from the boundary node, then the sign of the heat flux is changed. Moreover, if the heat flux is given at node N, then the q''_N boundary condition can be similarly dealt with by altering AE_{N-1} and Su_{N-1}.

4.1.7.3. Specified Heat Transfer Coefficient

In the specified boundary heat transfer coefficient condition, the convective heat transfer coefficient at the specified boundary node is known. For the purpose of illustration let h1 be the heat transfer coefficient and let T∞ be the temperature adjacent to the surface at x = 0. By performing an energy balance, it may be shown that

$$q_1 = A_1 q_1'' = A_1 h_1 \left(T_\infty - T_1\right) = AW_2 \left(T_1 - T_2\right)$$

Therefore

$$T_1 = \frac{T_2 + \left(A_1 h_1 / AW_2\right) T_\infty}{1 + \left(A_1 h_1 / AW_2\right)}$$

Therefore, the specified heat transfer coefficient boundary condition may be applied by using the following procedure:

1. Calculate the temperature T_1 of node 1 from the foregoing equation.

2. Update

$$Sp_2 = Sp_2 + \left[\frac{1}{A_1 h_1} + \frac{1}{AW_2}\right]^{-1} \text{ and } Su_2 = Su_2 + \left[\frac{1}{A_1 h_1} + \frac{1}{AW_2}\right]^{-1} T_\infty$$

3. Set $AW_2 = 0$.

4.1.8. The Multilayered Wall

If a multilayered wall is considered, the conductivity may change considerably between 2 nodes if each node was placed in a different layer. Assuming that nodes are placed such that the face between both nodes coincides with the interface between the layers, it is needed to find an effective value for the thermal conductivity at the layer boundary. Note that the density and heat capacitance need not be evaluated at the layer since only nodal values are needed. A schematic of the situation is shown below:

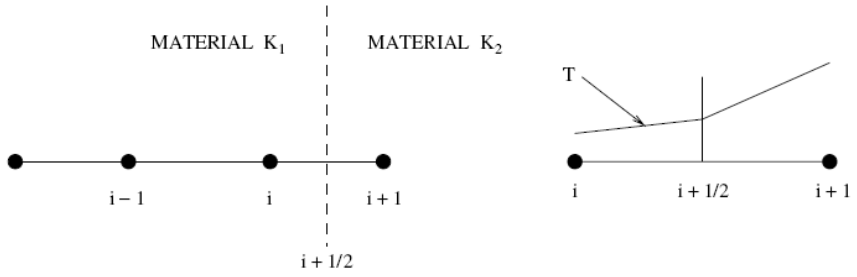

Fig.4.3: Case of a Multilayered Wall

In spite of the discontinuity between the two walls, the amount of heat transfer exiting a wall is equal to the amount of heat transfer entering the second wall; thus $Q_{i+½}$ on either side of the wall $i+½$ must be the same. Therefore:

$$Q_{i+½} = k_1 A_{i+½} \frac{T_i - T_{i+½}}{x_{i+½} - x_i}, \qquad k_1 = k_i$$

$$Q_{i+½} = k_2 A_{i+½} \frac{T_{i+½} - T_{i+1}}{x_{i+1} - x_{i+½}}, \qquad k_2 = k_{i+1}$$

Eliminating $T_{i+½}$ from the foregoing equations gives:

$$Q_{i+½} = A_{i+½} \left[\frac{x_{i+½} - x_i}{k_i} + \frac{x_{i+1} - x_{i+½}}{k_{i+1}} \right]^{-1} \left(T_i - T_{i+1} \right) \tag{4.1.35}$$

In Integration over a Control Volume method, the discretized equations were derived by assuming a linear temperature variation between nodes *i* and *i* + 1. This implies that

$$Q_{i+½} = \left. \frac{A}{\Delta x} \right|_{i+½} k_{i+½} \left(T_i - T_{i+1} \right) \tag{4.1.36}$$

Therefore, the effective thermal conductivity is found to be:

$$k_{i+½} = \Delta x_{i+½} \left[\frac{x_{i+½} - x_i}{k_i} + \frac{x_{i+1} - x_{i+½}}{k_{i+1}} \right]^{-1} \tag{4.1.37}$$

If the cell face was midway between the two nodes, the thermal conductivity is found to be:

$$k_{i+½} = 2 \left[\frac{1}{k_i} + \frac{1}{k_{i+1}} \right]^{-1} \tag{4.1.38}$$

Note that the thermal conductivity at a face midway between two nodes is found by applying a harmonic mean between the thermal conductivity of the first node and the thermal conductivity of the second node, the arithmetic mean is not used.

4.1.9. Solution Methodology

In the tri-diagonal matrix algorithm (TDMA) the discretized equation may be written in the following form:

$$T_i = a_i T_{i+1} + b_i T_{i-1} + c_i$$

The terms in the foregoing equation are defined as:

$$a_i = \frac{AE_i}{AP_i + Sp_i}, \qquad b_i = \frac{AW_i}{AP_i + Sp_i}, \qquad a_i = \frac{Su_i}{AP_i + Sp_i}$$

Note that since $Sp_i \geq 0$, a_i and b_i can only be fractions. There are (N-2) simultaneous algebraic equations that have to be solved. In matrix form, these equations may be written as $[\mathbf{A}][\mathbf{T}] = [\mathbf{C}]$, where the coefficient matrix [**A**] is shown on the next page.

Notice that the coefficient of T_i occupies the diagonal position of the matrix with $-a_i$ and $-b_i$ occupying the neighboring diagonal positions. All other elements of the matrix are zero.

$$\mathbf{A} = \begin{bmatrix} 1 & -a_2 & 0 & 0 & 0 & 0 & 0 & 0 & 0 & 0 \\ -b_3 & 1 & -a_3 & 0 & 0 & 0 & 0 & 0 & 0 & 0 \\ 0 & \ddots & 1 & \ddots & 0 & 0 & 0 & 0 & 0 & 0 \\ 0 & 0 & \ddots & 1 & \ddots & 0 & 0 & 0 & 0 & 0 \\ 0 & 0 & 0 & \ddots & 1 & \ddots & 0 & 0 & 0 & 0 \\ 0 & 0 & 0 & 0 & -b_i & 1 & -a_i & 0 & 0 & 0 \\ 0 & 0 & 0 & 0 & 0 & \ddots & 1 & \ddots & 0 & 0 \\ 0 & 0 & 0 & 0 & 0 & 0 & \ddots & 1 & \ddots & 0 \\ 0 & 0 & 0 & 0 & 0 & 0 & 0 & \ddots & 1 & -a_{N-2} \\ 0 & 0 & 0 & 0 & 0 & 0 & 0 & 0 & -b_{N-1} & 1 \end{bmatrix}$$

Therefore, the system of equations may be written in matrix form as:

$$\begin{bmatrix} 1 & -a_2 & 0 & 0 & 0 & 0 & 0 & 0 & 0 & 0 \\ -b_3 & 1 & -a_3 & 0 & 0 & 0 & 0 & 0 & 0 & 0 \\ 0 & \ddots & 1 & \ddots & 0 & 0 & 0 & 0 & 0 & 0 \\ 0 & 0 & \ddots & 1 & \ddots & 0 & 0 & 0 & 0 & 0 \\ 0 & 0 & 0 & \ddots & 1 & \ddots & 0 & 0 & 0 & 0 \\ 0 & 0 & 0 & 0 & -b_i & 1 & -a_i & 0 & 0 & 0 \\ 0 & 0 & 0 & 0 & 0 & \ddots & 1 & \ddots & 0 & 0 \\ 0 & 0 & 0 & 0 & 0 & 0 & \ddots & 1 & \ddots & 0 \\ 0 & 0 & 0 & 0 & 0 & 0 & 0 & \ddots & 1 & -a_{N-2} \\ 0 & 0 & 0 & 0 & 0 & 0 & 0 & 0 & -b_{N-1} & 1 \end{bmatrix} \begin{bmatrix} T_2 \\ T_3 \\ \vdots \\ \vdots \\ T_i \\ \vdots \\ \vdots \\ \vdots \\ \vdots \\ T_{N-1} \end{bmatrix} = \begin{bmatrix} C_2 \\ C_3 \\ \vdots \\ \vdots \\ C_i \\ \vdots \\ \vdots \\ \vdots \\ \vdots \\ C_{N-1} \end{bmatrix}$$

Notice that the coefficient of T_i occupies the diagonal position of the matrix with $-a_i$ and $-b_i$ occupying the neighboring diagonal positions. Thus matrix **A** has a diagonally dominant tri-diagonal structure. In this Tri-Diagonal Matrix Algorithm thus structure is exploited to solve the matrix. To exploit this structure, let:

$$T_i = A_i T_{i+1} + B_i, \qquad i = 2, \ldots, N-1$$

Thus, $T_{i-1} = A_{i-1} T_i + B_{i-1}$

Substituting this equation into the equation $T_i = a_i T_{i+1} + b_i T_{i-1} + c_i$, we would obtain:

$$T_i = \left[\frac{a_i}{1 - b_i A_{i-1}} \right] T_{i+1} + \left[\frac{b_i B_{i-1} + c_i}{1 - b_i A_{i-1}} \right]$$

Comparing with the foregoing equation, it is noted that:

$$A_i = \frac{a_i}{1 - b_i A_{i-1}}$$

$$B_i = \frac{b_i B_{i-1} + c_i}{1 - b_i A_{i-1}}$$

Thus A_i and B_i can be evaluated by recurrence. The procedure of the TDMA approach may be outlined by the following steps:

1. Prepare a_i, b_i and c_i for i = 2 to N-1 from knowledge of the previous time step temperature distribution.
2. Set $A_2 = a_2$and $B_2 = c_2$ (because if you refer to the matrix equation, you may incur that $b_2 = 0$). Evaluate A_i and B_i for i = 3 to N–1 by recurrence using the equations:

$$A_i = \frac{a_i}{1 - b_i A_{i-1}}$$
$$B_i = \frac{b_i B_{i-1} + c_i}{1 - b_i A_{i-1}}$$

3. Evaluate T_i by backwards substitution using; i.e. from $i = N$ –1 to 2. Note that since the boundary conditions are prescribed such that AE_{N-1}= 0, it follows that A_{N-1}= 0.
4. Evaluate the fractional change (FC) and go to step 1 if the convergence criterion is not satisfied.

The TDMA algorithm is a forward elimination and a backward substitution procedure in which temperatures at all i are updated simultaneously in step 3.

4.2. Chilled Ceiling Displacement Ventilation Simulation Model

This section describes the space models used for zones conditioned by using the Chilled Ceiling Displacement Ventilation (CC DV) system. The space is divided into two different zones, a thermally comfortable zone with an acceptable air quality and a stratified zone where neither the thermal nor the indoor air quality is of a concern.

In this model, the temperature and humidity are found in each zone as well as the temperature gradient, stratification height and the lumped CO2 concentration. The effects of radiation are included in the model (radiation between the walls and between the different walls and the human being).

Steady state and transient models for the space temperature and humidity variation are made to incorporate the transient effects consisting of heat storage in the walls and air inside the conditioned zone, humidity storage in air inside the room.

4.2.1. Lumped Models

In order to incorporate radiation effects inside the room effectively, the temperature of the different surfaces inside the room are considered to be uniform. Thus a lumped model is needed to calculate the internal walls – surfaces – temperatures. For steady state analysis a steady state lumped model is developed; the model is then extended to include transient effect for transient calculations.

4.2.1.1. Generalized Air-side Energy Balance

The generalized convective heat transfer energy balance applied on air inside a lumped room may be written in terms of the sensible and latent load added from the internal space (electric load q_{elec}, lighting load q_{light}, sensible people load $q_{people,sens}$ and latent people load $q_{people,lat}$), load added due to exposed or external walls q_{wall}, the infiltration rate ACH, the supply air mass flow rate and temperature. In this energy

balance, it is assumed that the leaving air temperature is *equal* to the temperature of air inside the occupied zone.

Therefore, the internal sensible load may be written as

$$q_{\text{int},sens} = q_{elec} + q_{light,conv} + q_{people,sens} \tag{4.2.1}$$

Applying the first law of thermodynamics, equation (4.2.2) is obtained

$$m_a c_{p,a} \frac{dT_a}{dt} = \sum q_{wall,conv} + q_{\text{int},sens} - \dot{m}_a c_{p,a}\left(T_a - T_{a,in}\right) - ACH\left(\frac{\rho\forall}{3600}\right) c_{p,a}\left(T_a - T_{a,\infty}\right) \tag{4.2.2}$$

Noting that the convective heat transfer from the wall may be written in terms of the convective heat transfer coefficient h, the corresponding wall temperature and the internal air temperature by using Newton's law of cooling, equation (4.2.2) may be written in the form

$$\begin{aligned} m_a c_{p,a} \frac{dT_a}{dt} = {} & \sum_{j=1}^{N} h_{conv} A_j \left(T_{wall,j,0} - T_a\right) + q_{\text{int},sens} - \dot{m}_a c_{p,a}\left(T_a - T_{a,in}\right) \\ & - ACH\left(\frac{\rho\forall}{3600}\right) c_{p,a}\left(T_a - T_{a,\infty}\right) \end{aligned} \tag{4.2.3}$$

4.2.1.2. Generalized Air-side Moisture Balance

There are two different types of cooling load, sensible and latent types. In this section latent heat gains are taken into consideration. Unlike the sensible heat gains that mainly affect the temperature inside the building space, moisture heat gain changes the humidity ratio content inside the room yielding to a change in the relative humidity that affects the predicted mean vote of a person. The relative humidity and predicted mean

vote are important thermal comfort parameters along with the temperature of the air inside the conditioned room.

The humidity ratio change inside the conditioned space depends on moisture transport through building and fabric elements (most notably external walls), the latent load of human beings inside the conditioned zone, the rate of moisture generation inside the space (due to cooking, foodstuffs, liquid water exposed to the air, etc…) the amount of infiltration into the room and the humidity ratio of air supplied to the room.

$$m_a \frac{dw_a}{dt} = \sum_{i=1}^{N} A_{w,i} h_{d,i} \left(w_{wall,i,0} - w_a \right) + \left(\sum \dot{m}_{w,\text{int}} + \frac{q_{\text{int},lat}}{h_{fg}} \right) - \dot{m}_a \left(w_a - w_{a,s} \right) + ACH \left(\frac{\rho \cancel{V}}{3600} \right) \left(w_{a,\infty} - w_a \right) \quad (4.2.4)$$

In non-hygroscopic building elements where the diffusion of water content may be neglected in the external walls, it is safe to neglect the moisture transfer trough the elements, thus equation (4.2.4) may be written as

$$m_a \frac{dw_a}{dt} = \left(\sum \dot{m}_{w,\text{int}} + \frac{q_{\text{int},lat}}{h_{fg}} \right) - \dot{m}_a \left(w_a - w_{a,s} \right) + ACH \left(\frac{\rho \cancel{V}}{3600} \right) \left(w_{a,\infty} - w_a \right) \quad (4.2.5)$$

Equation (4.2.5) is safe to use if the external walls are water proofed or painted against water absorption due to humidity differences between the external air humidity ratio and the internal air humidity ratio.

4.2.1.3. Generalized Internal Air Quality Balances

In many applications, the internal air quality is an important factor that determines the amount of ventilation a certain cooling space needs. One of the main

carbon dioxide sources in the cooling space is the living personnel inside the considered space who spontaneously emit carbon dioxide into the atmosphere around them.

The overall internal air quality (IAQ) is related to the volumetric flow rate of air entering the conditioned zone, the concentration of pollutants in the air entering the conditioned space *C* (in parts per million by volume or ppmv), the rate of generation of pollutants inside the conditioned space *0* (in ml/s). Therefore, the generalized lumped transient equation describing the pollutants concentration inside the conditioned space may be written as

$$V\frac{dC}{dt} = \dot{V}_a\left(C_s - C\right) + L + \left(\frac{ACH \times V}{3600}\right)\left(C_\infty - C\right) \qquad (4.2.6)$$

Note that equation (4.2.6) was written neglecting the change of density of air due to temperature; i.e., in writing equation (4.2.6), the density of air is assumed to be constant meaning that the mass balance inside the conditioned zone (the considered control volume) is assumed to be equivalent to a volumetric balance applied on the same control volume.

The indoor air quality equations are used to determine the concentration of pollutants (such as carbon dioxide, volatile organic compounds, etc…) inside the indoor air due to the pollutant generation. According to the concentration of pollutants, the minimum amount of fresh air entered into the conditioned space may be determined. Thus, the main aim of using equation (4.2.6) is to determine the minimum amount of fresh air entering the space by comparing the existing concentration of pollutants to the maximum specified allowable concentration inside the space in accordance with air conditioning standards.

4.2.1.4. Evaluating the wall internal temperature

The wall internal temperature is an important parameter in the thermal analysis, referring to the numerical wall model stated in another text, the internal wall temperature may be evaluated by including equivalent internal and external overall heat transfer coefficients and temperature values (that include the convection and radiation).

The external overall heat transfer coefficient depends on the temperature difference between the exterior surface and the outside air and the wind speed at standard conditions. Refer to the section entitled: *Evaluating the external heat transfer coefficient* found on page 18.

The internal heat transfer coefficient depends on the temperature difference between the internal wall surface temperature and the internal air temperature. For vertical walls, the convective heat transfer coefficient may be calculated using equation (4.2.7).

$$h_{conv} = 1.49 \times (\Delta T)^{0.345} \qquad (4.2.7)$$

For the ceiling, refer to the chilled ceiling model described in a later section. On the other hand the convective heat transfer for the floor is considered to be $h = 2.1$ W/m^2-K.

Evaluating the View Factors Matrix

The view factor F_{ij} between two surfaces *i* and *j* (as shown in Fig.4.4) is defined as the fraction of radiation leaving a surface *i* that is intercept by a surface *j*; i.e. the view factor is a fraction that is less than 1 representing the amount of radiation exchange between surfaces *i* and *j* due to the fact that it is not a necessary condition that

surface *j* enclosures surface *i* completely or vice versa. Mathematically, the most general equation for the view factor is

$$F_{ij} = \frac{1}{A_i}\int_{A_i}\int_{A_j} \frac{\cos\theta_i \times \cos\theta_j}{\pi R^2} dA_i dA_j \tag{4.2.8}$$

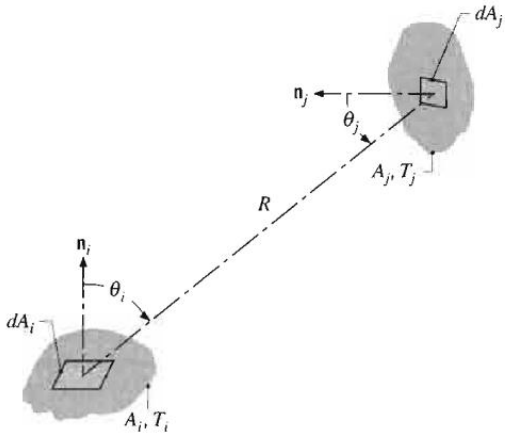

Fig.4.4: View Factors between Two Surfaces *i* and *j*

It is not convenient to use equation (4.2.8) to compute the view factors between the different walls in a simple room setup (a room with 6 surfaces) since it contains a double area integral. However, this area integral was solved analytically for different configurations:

For perpendicular intersecting surfaces with a common surface, the equation is:

$$W = {}^{Y}\!/_{X}, \quad H = {}^{Z}\!/_{X}$$

$$F_{ij} = \frac{1}{\pi W}\left(\begin{array}{l} W\tan^{-1}\left(\frac{1}{W}\right) + H\tan^{-1}\left(\frac{1}{H}\right) - \left(\sqrt{H^2+W^2}\right)\tan^{-1}\left(\frac{1}{\sqrt{H^2+W^2}}\right) \\ + 0.25\times\ln\left\{ \frac{\left(1+W^2\right)\left(1+H^2\right)}{1+W^2+H^2}\left[\frac{W^2\left(1+W^2+H^2\right)}{\left(1+W^2\right)\left(W^2+H^2\right)}\right]^{W^2}\left[\frac{H^2\left(1+W^2+H^2\right)}{\left(1+H^2\right)\left(W^2+H^2\right)}\right]^{H^2} \right\} \end{array} \right)$$

(4.2.9)

For parallel aligned surfaces, the equation is:

$$\bar{X} = X/L, \quad \bar{Y} = Y/L$$

$$F_{ij} = \frac{2}{\pi \bar{X} \bar{Y}} \left\{ \begin{array}{l} \ln\left[\sqrt{\frac{\left(1+\bar{X}^2\right)\left(1+\bar{Y}^2\right)}{1+\bar{X}^2+\bar{Y}^2}} \right] + \bar{X}\sqrt{1+\bar{Y}^2}\,\tan^{-1}\left(\frac{\bar{X}}{\sqrt{1+\bar{Y}^2}} \right) \\ +\bar{Y}\sqrt{1+\bar{X}^2}\,\tan^{-1}\left(\frac{\bar{Y}}{\sqrt{1+\bar{X}^2}} \right) - \bar{X}\,\tan^{-1}\bar{X} - \bar{Y}\,\tan^{-1}\bar{Y} \end{array} \right\} \qquad (4.2.10)$$

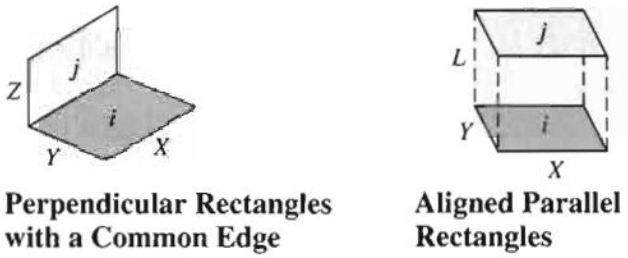

Fig.4.5: View Factor Configurations

Evaluating the Radiative Heat Transfer Rate between the internal Wall Surfaces

Assuming that all internal wall surfaces are grey surfaces, the radiation exchange between the internal walls could be modeled by using a radiation exchange network. A thermal network for a zone including six different surfaces is shown in Fig.4.6(Underwood and Yik 2004).

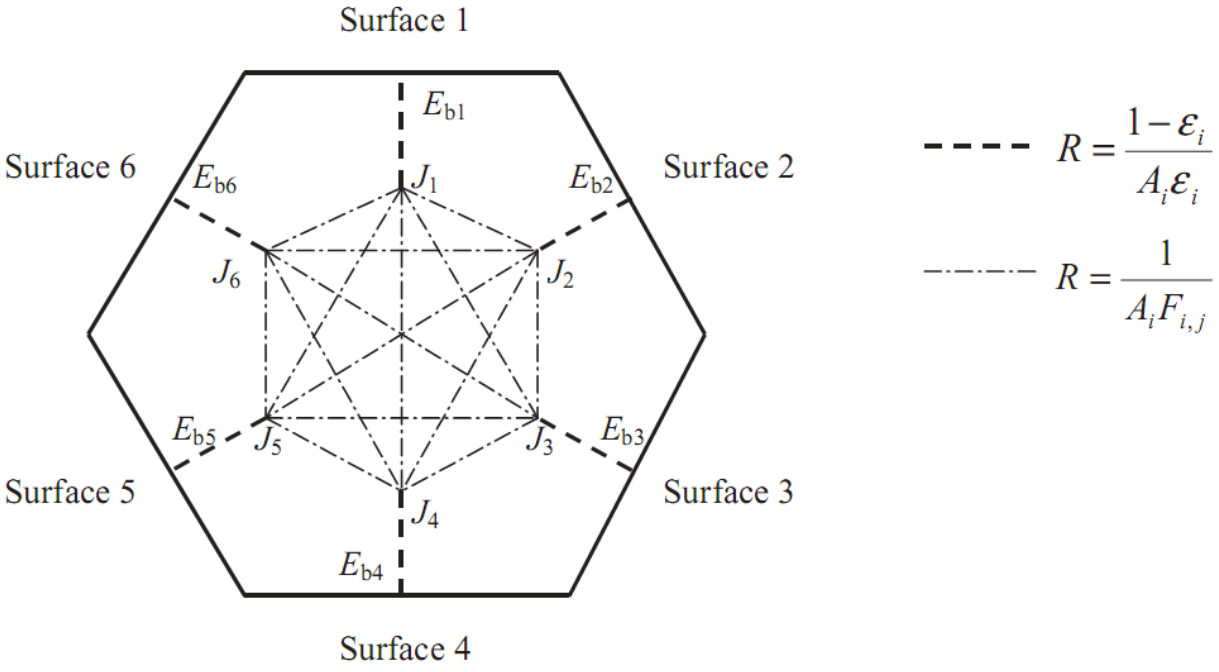

Fig.4.6: Radiation Thermal Network for a Zone Including Six Surfaces

From the definition of the radiosity, the net rate of radiation of exchange of a grey surface *i* may be written in terms of the emissive power, the radiosity and the surface emissivity as

$$q_{wall,rad,i} = \frac{\varepsilon_i \times A_i}{1-\varepsilon_i}\left(E_{b,i} - J_i\right) \qquad (4.2.11)$$

The terms in equation (4.2.11) are:

ε_i The emissivity of the material

$E_{b,i}$ The emissive power of a black body at temperature $T_{w,i}$, equal to $\sigma {T_{w,i}}^4$

J_i The radiosity of the surface at a certain time

For a certain wall *i*, the radiation network analysis results in the following equation

$$\frac{\varepsilon_i A_i}{1-\varepsilon_i}\left(E_{b,i}-J_i\right)=\sum_{j=1}^{N}A_i F_{ij}\left(J_i-J_j\right) \tag{4.2.12}$$

Simplifying equation (4.2.12) results in the equation

$$\left(\frac{\varepsilon_i}{1-\varepsilon_i}\right)\left(E_{b,i}-J_i\right)+\sum_{j=1}^{N}F_{ij}\left(J_j-J_i\right)=0 \tag{4.2.13}$$

To write equation (4.2.13) in matrix format, the equation is rewritten as

$$J_i-\left(1-\varepsilon_i\right)\sum_{j=1}^{N}F_{ij}J_j=\varepsilon_i E_{b,i} \tag{4.2.14}$$

The matrix form of the equation is

$$\mathbf{A}\times\mathbf{J}=\mathbf{C} \tag{4.2.15}$$

Thus in indicial notation, the coefficient and constant matrices in equation (4.2.15)may be written as

$$a_{ij}=\delta_{ij}-\left(1-\delta_{ij}\right)\left(1-\varepsilon_i\right)F_{ij} \tag{4.2.16}$$

$$c_i=\varepsilon_i\sigma T_{w,i}{}^4 \tag{4.2.17}$$

In equation (4.2.16), $\delta_{ij}$is the Kronecker delta defined such that $\delta_{ij}=1$ when $i=j$, otherwise $\delta_{ij}=0$.

Calculating the Equivalent Internal Air Temperature and Convection Coefficient

Applying an energy balance on the internal wall surface equation (4.2.18)is obtained

$$q_{wall,net,i} = q_{wall,conv,i} + q_{wall,rad,i} - q_{\text{int},rad,i} \tag{4.2.18}$$

Noting that since the surface does not have any varying area elements, the sum and equivalence of heat transfer rates is equivalent to the sum and equivalence of the different heat fluxes.

The net radiation leaving the internal surface of the wall may be written in terms of the equivalent overall heat transfer rate and equivalent temperature, thus equation (4.2.18) may be written in the form

$$h_{eq}\left(T_{w,i,0} - T_{eq}\right) = h_{conv}\left(T_{w,i,0} - T_{a,\text{int}}\right) + \frac{\varepsilon_i}{1-\varepsilon_i}\left(E_{b,i} - J_i\right) - \frac{q_{\text{int},rad,i}}{A_{w,i}} \tag{4.2.19}$$

Noting that $E_{b,i} = \sigma {T_{w,i}}^4$, equation (4.2.19) may be written as

$$h_{eq}\left(T_{w,i,0} - T_{eq}\right) = \left(h_{conv} + \frac{\varepsilon_i \sigma {T_{w,i,0}}^3}{1-\varepsilon_i}\right)T_{w,i,0} - h_{conv}T_{a,\text{int}} - \frac{\varepsilon_i J_i}{1-\varepsilon_i} - \frac{q_{\text{int},rad,i}}{A_{w,i}} \tag{4.2.20}$$

Equating the respective terms in equation (4.2.20), the equivalent wall internal temperature and convection rate are expressed in equations (4.2.21) and (4.2.22).

$$h_{eq,i} = h_{conv} + \frac{\varepsilon_i \sigma {T_{w,i,0}}^3}{1-\varepsilon_i} \tag{4.2.21}$$

$$T_{eq,i} = \frac{h_{conv} T_{a,\text{int}} + \frac{\varepsilon_i J_i}{1-\varepsilon_i} + \frac{q_{\text{int},rad,i}}{A_{w,i}}}{h_{conv} + \frac{\varepsilon_i \sigma T_{w,i,0}{}^3}{1-\varepsilon_i}} \tag{4.2.22}$$

4.2.1.5. Steady State Analysis

For steady state analysis, the energy balance applied on the space inside the room shown in equation (4.2.3)may be written as shown in equation(4.2.23).

$$\begin{aligned} &\sum_{i=1}^{N} h_{conv} A_i \left(T_{wall,i,0} - T_a\right) + q_{\text{int},sens} - \dot{m}_a c_{p,a} \left(T_a - T_{a,in}\right) \\ &\quad - ACH \left(\frac{\rho \forall}{3600}\right) c_{p,a} \left(T_a - T_{a,\infty}\right) = 0 \end{aligned} \tag{4.2.23}$$

Rearranging the terms in equation(4.2.23), the following equation is obtained

$$\begin{aligned} &\left[\sum_{i=1}^{N} h_{conv} A_i + \dot{m}_a c_{p,a} + ACH \left(\frac{\rho \forall}{3600}\right) c_{p,a}\right] T_a = \\ &\quad \sum_{i=1}^{N} h_{conv} A_i T_{wall,i,0} + q_{\text{int},sens} + \dot{m}_a c_{p,a} T_{a,in} + ACH \left(\frac{\rho \forall}{3600}\right) c_{p,a} T_{a,\infty} \end{aligned} \tag{4.2.24}$$

Nevertheless, the temperatures of the internal surfaces of the different walls are related to the internal air temperature of the room implying that the number of unknowns is greater than the number of equations. Thus an additional number of equations shall be written to solve for the internal wall temperatures. These equations are obtained by noting that at steady state, the temperature difference to heat transfer relation is represented by using linear resistance values, thus for each wall, the internal wall temperature may be written as

$$T_{wall,i,0} = T_{ext} - \left[\frac{\frac{1}{h_{ext} A_i} + R_{cond}}{\frac{1}{h_{ext} A_i} + R_{cond} + \frac{1}{h_{eq} A_i}} \right] \left(T_{ext,i} - T_{eq,i} \right) \quad (4.2.25)$$

The external wall air temperature is equal to the sol-air temperature for an external wall or to the unconditioned space temperature for an internal partition. The internal equivalent temperature and heat transfer rate are calculated by using equations (4.2.21) and (4.2.22) respectively.

Note that equation (4.2.25) could be written in a wall area independent fashion, by defining the heat flux thermal resistance $R'' = R \times A = {}^{L}/_{k}$

$$T_{wall,i,0} = T_{ext} - \left[\frac{\frac{1}{h_{ext}} + R''_{cond}}{\frac{1}{h_{ext}} + R''_{cond} + \frac{1}{h_{eq}}} \right] \left(T_{ext,i} - T_{eq,i} \right) \quad (4.2.26)$$

The form in equation (4.2.26) is preferable since the contact heat flux resistance between the different materials of a multilayered wall may be added easily.

Therefore, there are three simultaneous sets of equations to be solved, one set is to find the radiosity of a surface, the second set is to calculate the equivalent interacting temperature and overall heat transfer coefficient, an equation to calculate the air temperature, and a third set to calculate the internal wall temperatures. To be able to solve all sets of equations, a procedure has to be followed.

The first step is to assume the unknown wall temperatures and calculate the corresponding internal air temperature based on equation (4.2.24).

The wall temperatures are used in the system of equations (4.2.15) to solve for the radiosity of a certain surface; note that the system of equations used to solve for the radiosity contains an equation for each internal surface (surfaces of known and unknown temperatures).

The radiosity values along with the internal air temperature are used to calculate the corresponding equivalent internal air side overall heat transfer coefficient h_{eq} and equivalent temperature T_{eq} by using equations (4.2.21) and (4.2.22) respectively. These equations are applied on each internal surface.

After calculating the overall equivalent internal air side heat transfer coefficient and equivalent temperature, equation (4.2.26) is applied on surfaces with unknown (not fixed) internal surface temperatures to update the calculated wall temperature.

The procedure is repeated until convergence is reached; for this text, convergence is considered to be reached if the difference in the norm of the wall temperatures between two successive iterations is less than 0.001 K. The procedure is shown in the flowchart shown in Fig.4.7.

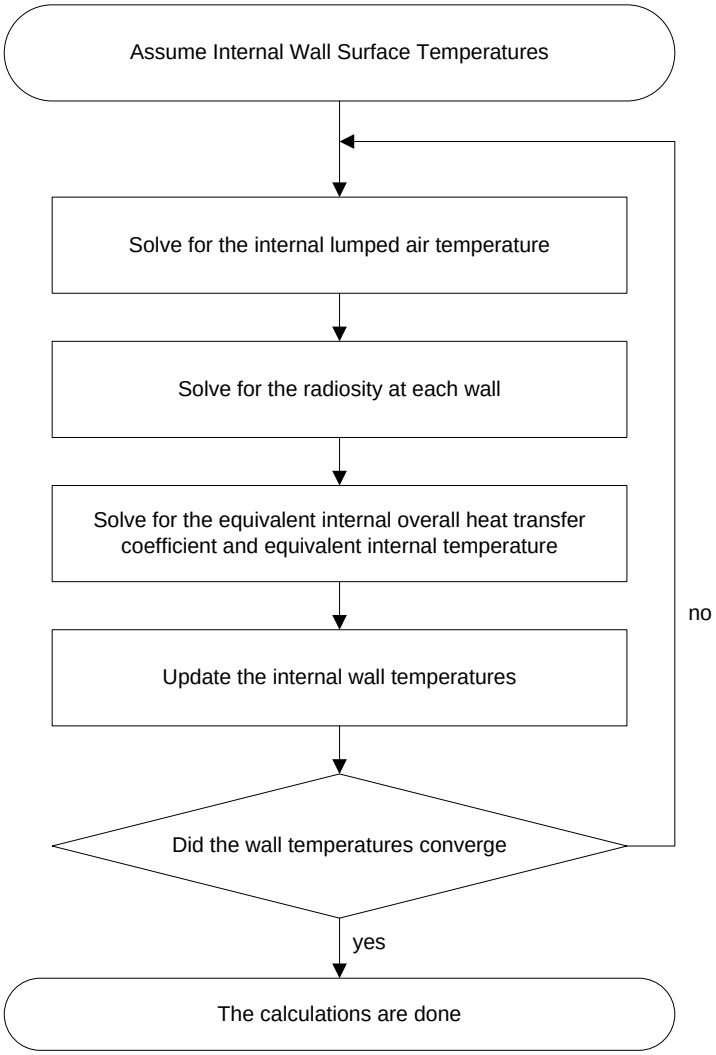

Fig.4.7:Steady State Solution Procedure

For steady state calculations the lumped moisture balance inside the cooled space may be written as

$$\left[\dot{m}_a + ACH\left(\frac{\rho\forall}{3600}\right)\right] w_a = \dot{m}_a \times w_{a,s} + ACH\left(\frac{\rho\forall}{3600}\right) \times w_{a,\infty} + \left(\sum \dot{m}_{w,\text{int}} + \frac{q_{\text{int},lat}}{h_{fg}}\right) \quad (4.2.27)$$

In a similar formulation, the equation used to determine the carbon dioxide concentration inside the space is given by the equation

$$\left[\dot{V}_a + \frac{ACH \times V}{3600}\right] C_c = \dot{V}_a \times C_{c,s} + \left(\frac{ACH \times V}{3600}\right) \times C_{c,\infty} + L_c \qquad (4.2.28)$$

4.2.1.6. Transient Analysis

To be able to perform transient analysis, equation (4.2.3) is discritized in an implicit form to solve it by using backward Euler technique, thus the discritized equation may be written as

$$m_a c_{p,a}\left(\frac{T_a^{k+1} - T_a^k}{\Delta t}\right) = \sum_{j=1}^{N} h_{conv} A_j \left(T_{wall,j,0}^{k+1} - T_a^{k+1}\right) + q_{\text{int},sens} - \dot{m}_a c_{p,a}\left(T_a^{k+1} - T_{a,in}^{k+1}\right) - ACH\left(\frac{m_a}{3600}\right) c_{p,a}\left(T_a^{k+1} - T_{a,\infty}^{k+1}\right) \qquad (4.2.29)$$

Solving for the air temperature at the next time step

$$\left[\frac{m_a c_{p,a}}{\Delta t} + \sum_{j=1}^{N} h_{conv} A_j + \dot{m}_a c_{p,a} + ACH\left(\frac{m_a c_{p,a}}{3600}\right)\right] T_a^{k+1} = \sum_{j=1}^{N} h_{conv} A_j \left(T_{wall,j,0}^{k+1}\right) + q_{\text{int},sens} - \dot{m}_a c_{p,a}\left(T_{a,in}^{k+1}\right) - ACH\left(\frac{m_a c_{p,a}}{3600}\right)\left(T_{a,\infty}^{k+1}\right) + \left(\frac{m_a c_{p,a}}{\Delta t}\right)\left(T_a^k\right) \qquad (4.2.30)$$

The discretized numerical wall model is used to solve the equations (refer to the discretized wall model section) to solve for the inner wall surface temperature. The model uses mixed boundary conditions meaning that it uses a convective heat transfer value accompanied with the temperature of the fluid of contact. For the outer surface, the convective heat transfer coefficient h_{ext} and sol-air temperature are specified, the inner equivalent overall heat transfer coefficient and equivalent temperature are determined by using equations (4.2.21) and (4.2.22) respectively. The procedure for

solving the transient equation at each time step is very similar to that used for the steady state calculation

The first step is to assume the unknown wall temperatures and calculate the corresponding internal air temperature based on equation (4.2.24).

The wall temperatures are used in the system of equations (4.2.15) to solve for the radiosity of a certain surface; note that the system of equations used to solve for the radiosity contains an equation for each internal surface (surfaces of known and unknown temperatures).

The radiosity values along with the internal air temperature are used to calculate the corresponding equivalent internal air side overall heat transfer coefficient h_{eq} and equivalent temperature T_{eq} by using equations (4.2.21) and (4.2.22) respectively. These equations are applied on each internal surface.

After calculating the overall equivalent internal air side heat transfer coefficient and equivalent temperature, the discretized transient wall model is applied on surfaces with unknown (not fixed) internal surface temperatures to update the calculated wall temperature.

The procedure is repeated until convergence is reached; for this text, convergence is considered to be reached if the difference in the norm of the wall temperatures between two successive iterations is less than 0.001 K. The procedure is shown in the flowchart shown in Fig.4.7 (same as that used in the steady state section).

The moisture (or latent load) transient equation (equation (4.2.5)) may be written as

$$\left[\dot{m}_a + ACH\left(\frac{\rho\forall}{3600}\right) + \frac{m_a}{\Delta t}\right] w_a^{k+1} = \dot{m}_a \times w_{a,s}^{k+1} + \left(\sum \dot{m}_{w,\text{int}} + \frac{q_{\text{int},lat}}{h_{fg}}\right) + \frac{m_a}{\Delta t} \times w_a^k + ACH\left(\frac{\rho\forall}{3600}\right) \times w_{a,\infty}^{k+1} \quad (4.2.31)$$

The contaminant concentration equation may be written as

$$\left[\dot{\forall}_a + \frac{ACH \times \forall}{3600} + \frac{\forall}{\Delta t}\right] C_c^{k+1} = \dot{\forall}_a \times C_{c,s}^{k+1} + \left(\frac{ACH \times \forall}{3600}\right) \times C_{c,\infty}^{k+1} + L_c + \frac{\forall}{\Delta t} \times C_c^k \quad (4.2.32)$$

4.2.2. Dual Zone Room Balance

The chilled ceiling displacement ventilation dual zone air conditioned model provides a greater accuracy than the single zone model. The room is divided into two different zones separated by the stratification height formed due to buoyancy effects inside the room induce by air heated from the internal load elements.

4.2.2.1. Calculation of the Stratification Height

The stratification height is defined to be the height that separates between two different zones in a displacement ventilation system: occupied and contaminated zones; i.e. the occupied zone is the zone where the thermal and air quality standards shall be maintained. Adding the chilled ceiling to the space results (in addition to radiation exchange with the persons inside the room) in cooling the contaminated zone by convection effects, the proposed dual zone model covers this effect. Mathematically, the stratification height is defined to be the height where the transported mass flow rate resulting from the plume is equal to the supply air mass flow rate. To be able to

determine the stratification height, the internal air flow rate due to the plumes shall be determined.

Assuming that the walls are of uniform temperature, the temperature difference would induce either an upward flow (plume) if the wall is warmer than indoor air or a downward flow (downdraught) if the wall is cooler than indoor air. The corresponding volumetric flow rates are shown in equations (4.2.33)and (4.2.34) respectively.

$$Q_u = 2.8\times10^{-3}\left|\Delta T\right|^{2/5} z^{6/5} l \qquad (4.2.33)$$

$$Q_d = 2.8\times10^{-3}\left|\Delta T\right|^{2/5} \left(Z - z\right)^{6/5} l \qquad (4.2.34)$$

The parameters in equations (4.2.33)and (4.2.34) are

ΔT	Temperature difference between the wall and lumped indoor air
z	Position from the ground
Z	Height of the wall
l	Horizontal width of the wall

The plume generated from a point heat source with a heat transfer rate q may be determined by solving equations (4.2.35), (4.2.36) and (4.2.37) for a zone with internal air having a temperature gradient

$$A_1 = 2.86\times Z\left(\frac{dT_a}{dz}\right)^{3/8} q^{-1/4} \qquad (4.2.35)$$

$$B_1 = 0.004 + 0.039A_1 + 0.38A_1^{\,2} - 0.062A_1^{\,3} \qquad (4.2.36)$$

$$Q_{plume} = 0.00238\times q^{3/4}\left(\frac{dT_a}{dz}\right)^{-5/8}\times B_1 \qquad (4.2.37)$$

At the stratification height, the flow of air resulting from the different plumes is equal to the flow of air entering the room. Since infiltration occurs at several locations inside the room, the overall flow rate due to infiltration may be neglected. Assuming that air density variation inside the room is negligible, it is safe to write the equation determining the stratification height in terms of the volumetric flow rate Q, thus the equation used to determine the stratification height is

$$Q_s = NQ_p + \sum_{k=1}^{n} Q_{u,k} - \sum_{k=1}^{m} Q_{d,k} \qquad (4.2.38)$$

The parameters in equation (4.2.38) are

Q_s	The supply air volumetric flow rate
Q_p	Air volumetric flow rate of air due to the plume
$Q_{u,k}$	Air volumetric flow rate of the plume along the *k*-th warm wall
$Q_{d,k}$	Air volumetric flow rate of the downdraught along the *k*-th cool wall
N	The number of point sources inside the room
n	The number of warm walls
m	The number of cool walls

4.2.2.2. General Sensible Energy Balances

The sensible energy balance for the lower occupied zone may be written after applying the first law of thermodynamics as

$$m_{a,1}c_{p,a}\frac{dT_{a,1}}{dt} = \sum_{j=1}^{n} h_{conv}A_{j,1}\left(T_{wall,j,0} - T_{a,1}\right) + q_{elec} + q_{people,sens} - \dot{m}_a c_{p,a}\left(T_{a,1} - T_{a,in}\right) - ACH\left(\frac{\rho V_1}{3600}\right)c_{p,a}\left(T_{a,1} - T_{a,\infty}\right) \qquad (4.2.39)$$

In equation (4.2.39), it is assumed that the infiltration rate is uniform over the volume of the whole room. Therefore, the number of changes per hour is multiplied by

the volume of the lower part. It is worth to note that in the terms that include convection with the walls, the wall temperature obtained from the lumped energy balance is used and the area is the wall area that is included in the first zone. The ceiling is not included in this balance.

For the upper contaminated zone, the sensible energy balance may be written as

$$m_{a,2}c_{p,a}\frac{dT_{a,2}}{dt}=\sum_{j=1}^{m}h_{conv}A_{j,2}\left(T_{wall,j,0}-T_{a,2}\right)+q_{light,conv}-\dot{m}_a c_{p,a}\left(T_{a,2}-T_{a,1}\right)$$
$$-ACH\left(\frac{\rho\forall_2}{3600}\right)c_{p,a}\left(T_{a,2}-T_{a,\infty}\right) \qquad (4.2.40)$$

The temperature gradient inside the room is defined in equation (4.2.41) as the difference in temperature between both zones divided by the difference in height from the center of the first zone to the center of the second zone that is equal of half the overall room length.

$$\frac{dT}{dz}=\frac{T_{a,2}-T_{a,1}}{z_2-z_1}=2\times\frac{T_{a,2}-T_{a,1}}{Z} \qquad (4.2.41)$$

Note that while defining the temperature gradient in equation (4.2.41), it is assumed that the temperature variation inside a space cooled by using the chilled ceiling displacement ventilation system is linear that is somehow accurate within the working range (between the centers of both zones).

4.2.2.3. Steady State Room Zonal Sensible Energy Balance

For steady state analysis, the energy balances shown in equations (4.2.39) and (4.2.41) are written as

$$\left[\sum_{i=1}^{n} h_{conv} A_{i,1} + \dot{m}_a c_{p,a} + ACH\left(\frac{\rho \forall_1}{3600}\right) c_{p,a}\right] T_{a,1} =$$
$$\sum_{i=1}^{n} h_{conv} A_{i,1} T_{wall,i,0} + q_{elec} + q_{people,sens} + \dot{m}_a c_{p,a} T_{a,in} + ACH\left(\frac{\rho \forall_1}{3600}\right) c_{p,a} T_{a,\infty} \quad (4.2.42)$$

$$\left[\sum_{i=1}^{m} h_{conv} A_{i,2} + \dot{m}_a c_{p,a} + ACH\left(\frac{\rho \forall}{3600}\right) c_{p,a}\right] T_{a,2} =$$
$$\sum_{i=1}^{m} h_{conv} A_{i,2} T_{wall,i,0} + q_{light,conv} + \dot{m}_a c_{p,a} T_{a,1} + ACH\left(\frac{\rho \forall_1}{3600}\right) c_{p,a} T_{a,\infty} \quad (4.2.43)$$

4.2.2.4. Transient Room Zonal Sensible Energy Balance

Discretizing the energy balances shown in equations (4.2.39) and (4.2.41) in an implicit manner, the discretized equations are written as

$$m_{a,1} c_{p,a}\left(\frac{T_{a,1}^{k+1} - T_{a,1}^{k}}{\Delta t}\right) = \sum_{j=1}^{n} h_{conv} A_{j,1}\left(T_{wall,j,0}^{k+1} - T_{a,1}^{k+1}\right) + q_{elec} + q_{people,sens}$$
$$-\dot{m}_a c_{p,a}\left(T_{a,1}^{k+1} - T_{a,in}^{k+1}\right) - ACH\left(\frac{\rho \forall_1}{3600}\right) c_{p,a}\left(T_{a,1}^{k+1} - T_{a,\infty}^{k+1}\right) \quad (4.2.44)$$

$$m_{a,2} c_{p,a}\left(\frac{T_{a,2}^{k+1} - T_{a,2}^{k}}{\Delta t}\right) = \sum_{j=1}^{m} h_{conv} A_{j,2}\left(T_{wall,j,0}^{k+1} - T_{a,2}^{k+1}\right) + q_{light,conv} - \dot{m}_a c_{p,a}\left(T_{a,2}^{k+1} - T_{a,1}^{k+1}\right)$$
$$-ACH\left(\frac{\rho \forall_2}{3600}\right) c_{p,a}\left(T_{a,2}^{k+1} - T_{a,\infty}^{k+1}\right) \quad (4.2.45)$$

Solving for the corresponding air temperature

$$\left[\frac{m_{a,1}c_{p,a}}{\Delta t}+\sum_{i=1}^{n}h_{conv}A_{i,1}+\dot{m}_a c_{p,a}+ACH\left(\frac{\rho\forall_1}{3600}\right)c_{p,a}\right]T_{a,1}^{k+1}=\sum_{i=1}^{n}h_{conv}A_{i,1}T_{wall,i,0}^{k+1}+$$

$$q_{elec}+q_{people,sens}+\dot{m}_a c_{p,a}T_{a,in}^{k+1}+ACH\left(\frac{\rho\forall_1}{3600}\right)c_{p,a}T_{a,\infty}^{k+1}+\left(\frac{m_a c_{p,a}}{\Delta t}\right)\left(T_{a,1}^{k}\right) \quad (4.2.46)$$

$$\left[\frac{m_{a,2}c_{p,a}}{\Delta t}+\sum_{i=1}^{m}h_{conv}A_{i,2}+\dot{m}_a c_{p,a}+ACH\left(\frac{\rho\forall_2}{3600}\right)c_{p,a}\right]T_{a,2}^{k+1}=\sum_{i=1}^{m}h_{conv}A_{i,2}T_{wall,i,0}^{k+1}$$

$$+q_{light,conv}+\dot{m}_a c_{p,a}T_{a,1}^{k+1}+ACH\left(\frac{\rho\forall_2}{3600}\right)c_{p,a}T_{a,\infty}^{k+1}+\left(\frac{m_a c_{p,a}}{\Delta t}\right)\left(T_{a,2}^{k}\right) \quad (4.2.47)$$

4.3. Cooling Coil Model

The cooling coil is a common method used to cool air which may be used to cool different equipment such as car radiators, etc… or in HVAC (Heating, ventilation and air-conditioning) applications. Nevertheless the cooled air may condense inside the cooling coil unit which results from a mass transfer between water and air in conjunction with heat transfer resulting in an added complexity to the model. An additional complexity to the model is the calculation of the air-side heat coefficient at the wet and dry fins.

The model in this text considers the fan-coil unit as a single lumped unit where a model for the whole fan-coil unit shall be developed and analyzed. This model shall be used to estimate the performance of the fan-coil unit and calculate the exit air condition, exit water temperature, water condensate rate, heat transfer rate and pressure

drop in the cooling coil if the inlet air condition, mass flow rate of air and water, inlet water temperature and coil dimensions are given.

The lumped coil method is a robust method that may be integrated in systems modeling and may be used in optimization routines.

4.3.1. Coil Types

Coil are classified into four categories according to the construction, cooling liquid and usage, the four types are: Water Cooling Coils, Direct Expansion Coils, Water Heating Coils, and Steam Heating Coils. It is noted that the heat transport fluid in water heating and cooling coils is water, on the other hand in direct expansion coils; the heat transport fluid consists of a type of the various refrigerants used currently in the market.

4.3.1.1. Water Cooling Coil

A water cooling coil uses chilled water as the coolant inside the tubes. The chilled water cools or cools and dehumidifies the moist air that flows over the external surface of the tubes and fins, as shown in Fig.4.10a. To maintain a higher rate of heat transfer, the air and water normally follow a counter-flow arrangement; i.e., coldest air meets the coldest water and the warmest air meets the warmest water.

The water tubes are usually copper tubes of ½- to ¾-in. (13- to 16-mm) diameter with a thickness of 0.01 to 0.02 in. (0.25 to 0.5 mm). They are spaced at a center-to-center distance of 0.75 to 1.25 in. (19 to 31 mm) longitudinally and 1 to 1.5 in.

(25 to 38 mm) transversely, nominal spacing is 1.083 longitudinally and 1.25 transversally. The tubes may be arranged along the airflows in 2, 3, 4, 6, or 8 rows, in either staggered or aligned form. The staggered arrangement provides better heat transfer and a higher air pressure drop. Chilled water coils are commonly rated at a pressure of 175 to 300 psig (1205 to 2070 kPag). Figure 15.26 shows the structure of a water cooling coil and a DX coil.

4.3.1.2. Direct-Expansion (DX) Coil

In a direct-expansion coil, the refrigerant (usually HCFC-22, HFC-134a, HFC-404A, HFC-410A, HFC-407A, or HFC-407C) is evaporated and expanded directly inside the tubes to cool and dehumidify the air flowing over it, and condensation occurs on the outer surface of the DX coil, as shown in Fig.4.10*b*. This is why it is called a DX coil or wet coil. A DX coil acts as the evaporator in a refrigerating system. In a DX coil, coolant or the refrigerant is fed into a distributor and is evenly distributed to various tube circuits, which are made of copper tubes, typically 0.5 in. (13 mm) in diameter. Refrigerant distribution and loading to various circuits are critical to the performance of a DX coil. After evaporation, the vapor refrigerant is discharged from the header to the suction line.

4.3.1.3. Water Heating Coil

The water heating coil shown in Fig.4.10*c* is similar in construction to the water cooling coil. There are two main differences between them. Hot water, instead of chilled water, is used as the heating medium in a water heating coil. Also, there are

fewer rows in the water heating coil than in the water cooling coil. Generally, only two-, three-, or four-row water heating coils are available on the market. Water heating coils are rated at pressures of 175 to 300 psig (1205 to 2070 kPag) at temperatures up to 250°F (120°C).

4.3.1.4. Steam Heating Coil

Steam heating coils use the latent heat of condensation released by steam inside the tubes to heat outside and re-circulating air, as shown in Fig.4.10. In a standard steam heating-coil, steam enters at one end of the coil and condensate comes out the other end. For more even distribution of steam, a baffle plate is often installed just after the inlet. In a steam heating coil, it is important that the coil core inside the casing expand and contract freely. The coil core is also pitched toward the return connection to facilitate drainage of the condensate. Steam heating coils usually have a rating of 100 to 200 psig (690 to 1380 kPag) at 400°F (205°C). Steam heating coil tubes are usually made of copper, steel, or stainless steel.

The analysis used in this text applies to water heating and cooling coils; it does not apply to direct expansion or steam coils since there may be a change of state in the heat transport fluid inside the coil.

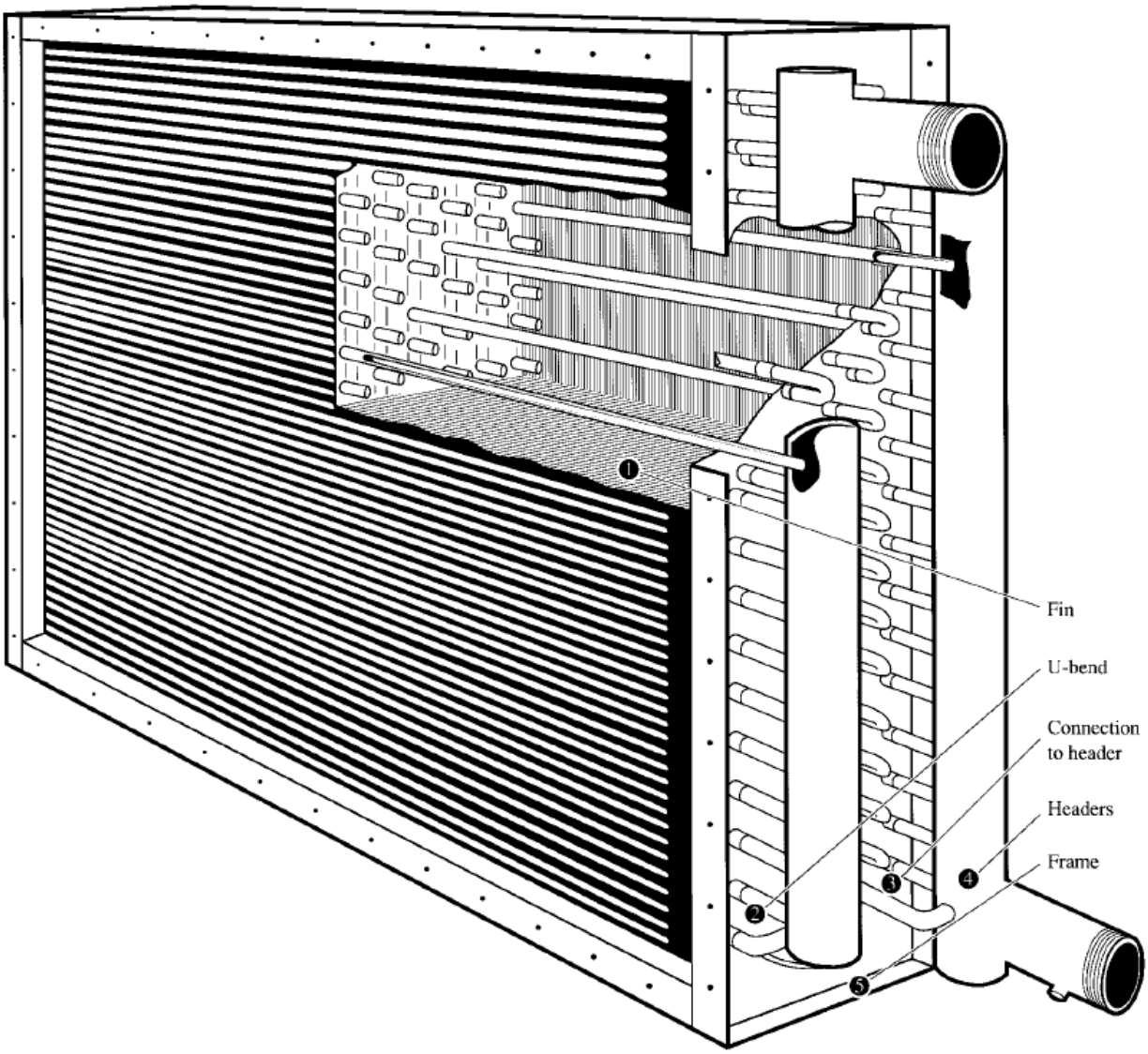

Fig.4.8: Structure of a water cooling coil

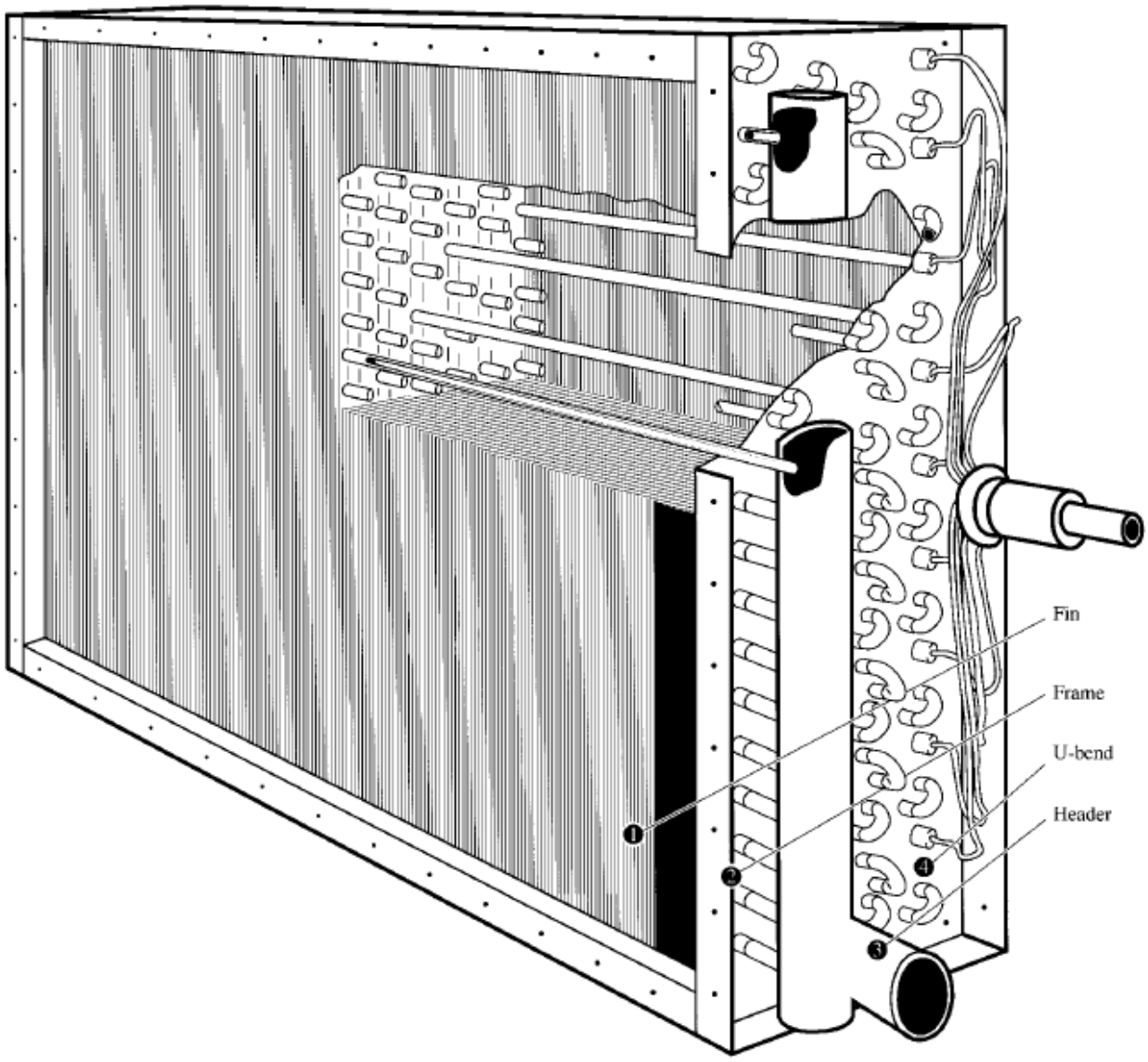

Fig.4.9: Structure of a DX cooling coil

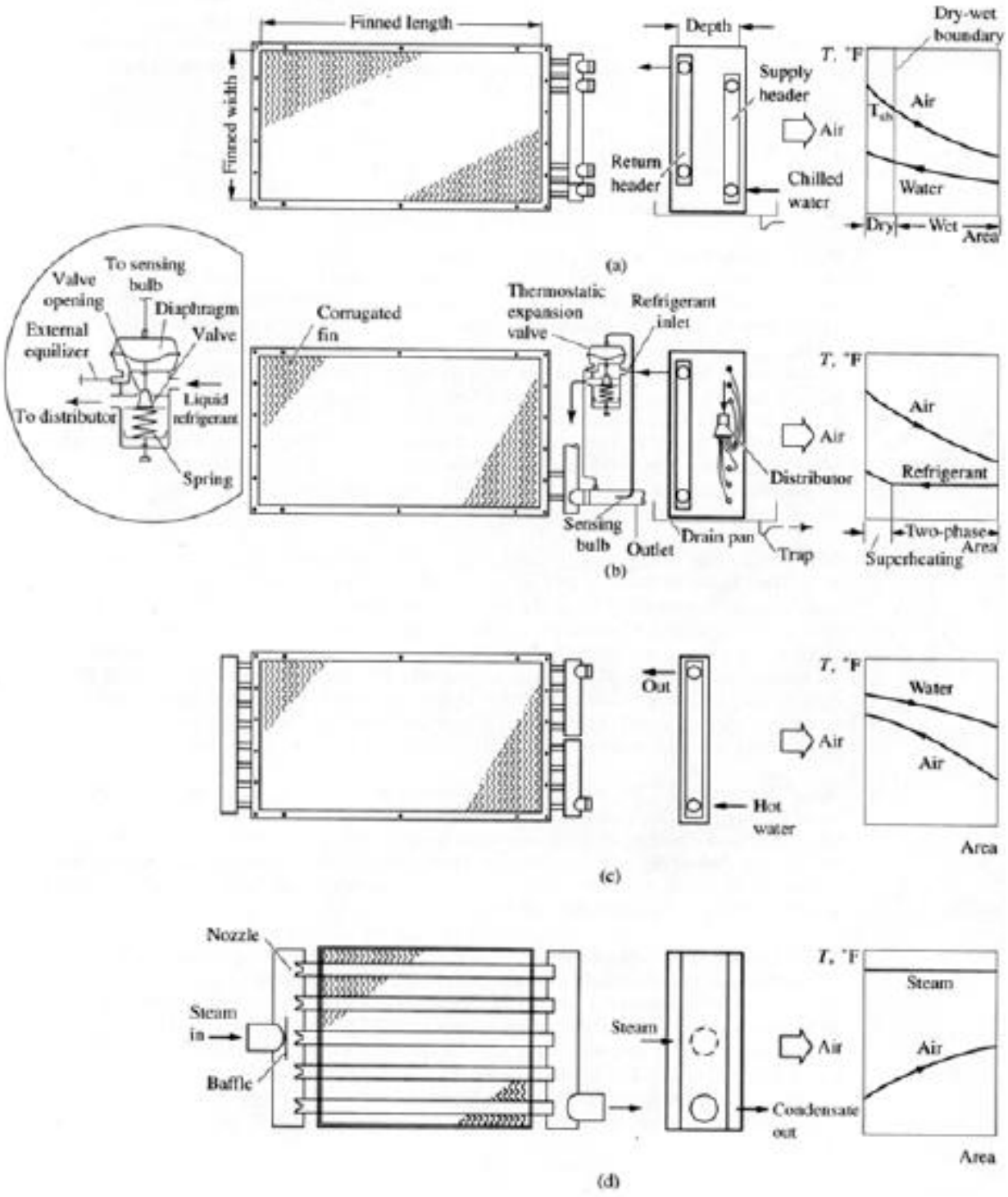

Fig.4.10: Types of coils (a) water cooling; (b) Direct Expansion; (c) Water heating; (d) Steam heating

4.3.2. Fins

To enhance the heat transfer between the refrigerant or heat transport medium and air passing through the coil, the outer area of the coil shall be extended. The outer area of the coil is extended by using fins.

Fins are extended surfaces that are often called the coil's secondary surface (the outer surface of the tubes is called the primary surface of the coil). Fins are usually made of aluminum, with a fin thickness F_t of 0.005 to 0.008 in. (0.13 to 0.2 mm). They can also be directly extruded, or shaved, from the parent tubes. Fins may be also made of copper, steel, or stainless-steel.

Three types of fins are widely used today:

- Continuous plate fins and corrugated plate fins. Plate fins are usually made of aluminum.
- Smooth spiral and crimped spiral fins, used in many commercial and industrial applications. Smooth spiral fins may be extruded from the parent tubes.
- Spine pipes which is made by shaving the spines and lifting them from the parent tubes.

The fins are illustrated in the figure shown on the following page.

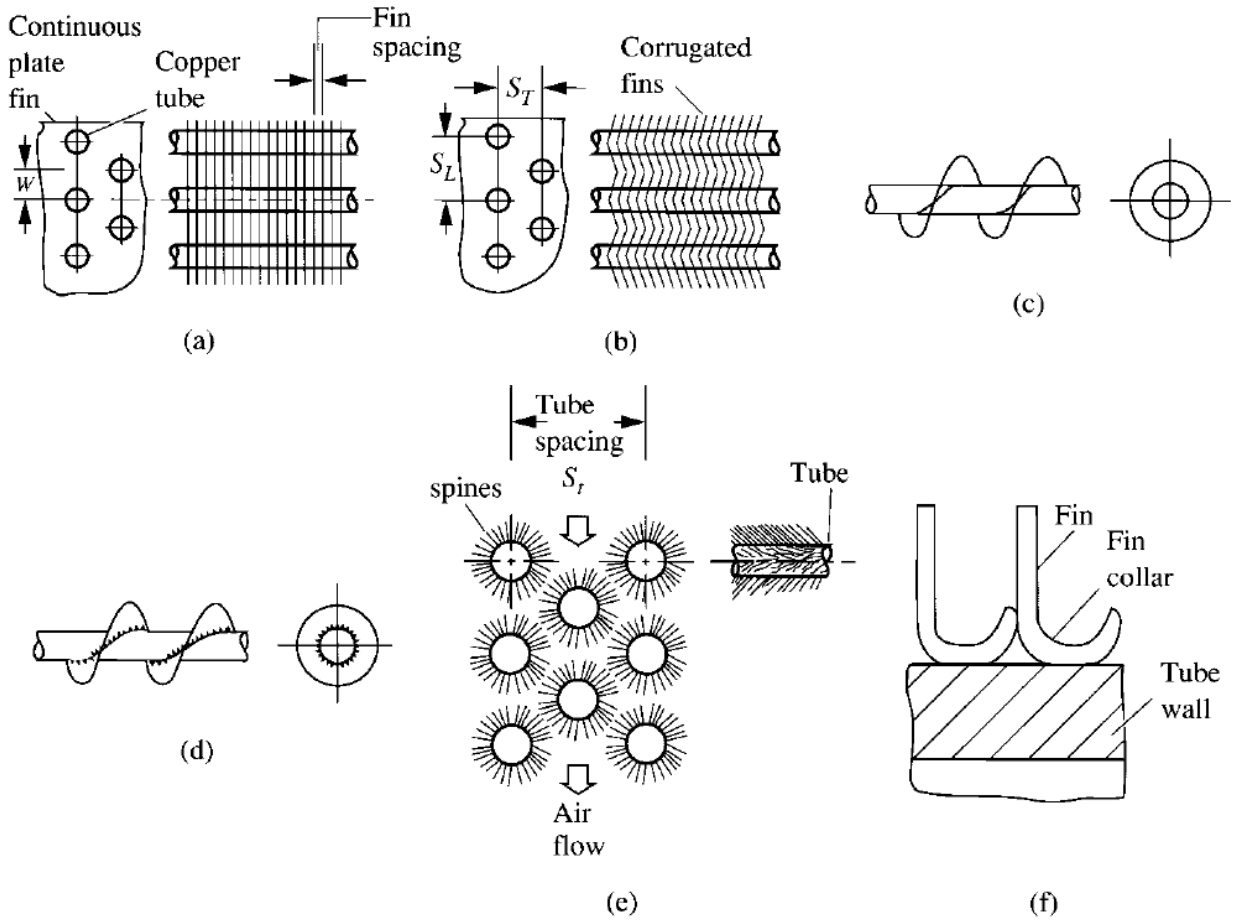

Fig.4.11: Types of fins (a) continuous fin plate; (b) corrugated fin plates; (c) smooth spiral fins; (d) crimped spiral fins; (e) spine pipe; and (f) fin collar and tube bonding

4.3.3. Water Circuits

In water cooling or water heating coils, tube feeds or water circuits determine the number of water flow passages. The greater the finned width, the greater the number of tube feeds and thus the greater the number of flow passages. For two finned-tube coils of the same finned width, a difference in the number of tube feeds or water circuits means that the water flow rate, in gpm (L/s), number of passes, and pressure drop of the chilled water, in ft WC (Pa), inside the two coils are different. One pass means that water flows through the coil's finned length once.

The number of serpentines (¼, ½, ¾, 1, 1½, or 2) of a water cooling or water heating coil indicates its water flow arrangement. As the number of serpentines becomes larger, the total cross-sectional area of the water circuits increases along with the water volumetric flow rate. Fig.4.12 shows five water cooling coils, each specified by the number of serpentines, water circuits, passes, and rows, all made by the same manufacturer. In Fig.4.12, serpentine means that at the first row, there are eight tubes across the finned width, but only four of them are tube feeds that are connected to the return header. For a full serpentine coil, all eight tubes in the first row are tube feeds and connect to the return header.

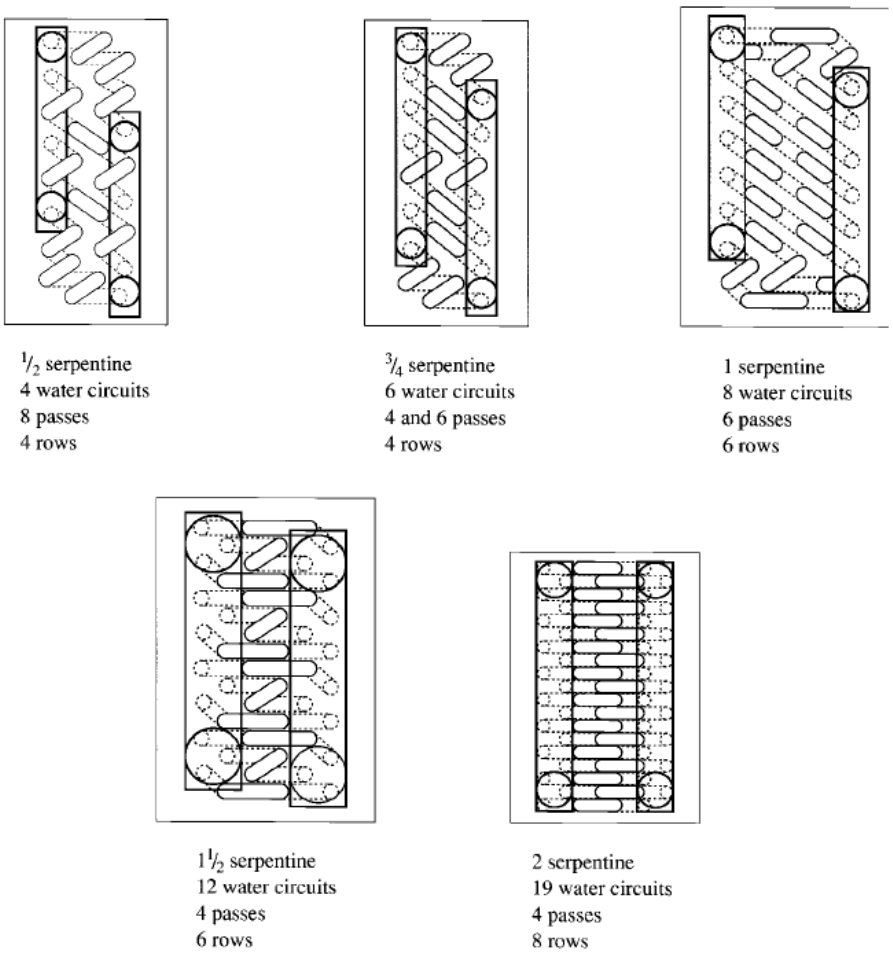

Fig.4.12: Water Circuits for Water Cooling Coils

4.3.4. The Cooling Coil Model

The model presented in this text is a simple steady state lumped model for a cooling coil, this model is robust and practical in the sense that it could be used as sub model for HVAC systems, and it could be used in selection and optimization routines.

The coil model is based on performing energy balances on the whole lumped coil at steady state using the heat exchange effectiveness NTU method. The effectiveness NTU method is a suitable method in the sense that it is a simulation method that requires only the input parameters of the coil; i.e. the air inlet temperature/enthalpy and water inlet temperature are required to calculate the water exit temperature and air exit psychrometric state. Therefore, by using the effectiveness NTU method, there is no need to iterate for the air and water exit conditions (if the coil is dry).

4.3.4.1. The model inputs

The model takes as inputs the psychrometric state of wet air entering the coil (such as the dry and wet bulb temperatures of air), the temperature of water entering the coil, the mass flow rates of air and water entering the coil and dimensional variables of the coil to determine the outlet psychrometric state of air, the outlet water temperatures and the pressure drop of air and water.

The dimensional variables include the number of rows, pipe inner and outer diameters, the longitudinal and transverse pitches, finned height, finned length, fin thickness, number of fines per inch. The number of feeds or serpentine is also

considered to be inputs to the model. Moreover material properties are inserted into the model such as the thermal conductivity of the fin which depends on the fins materials.

4.3.4.2. The model procedure

In principle, the program determines the type of the lumped coil to evaluate the output parameters using an analysis that is selected based on the type of the coil. A flowchart representing the procedure of the model is shown on the next page.

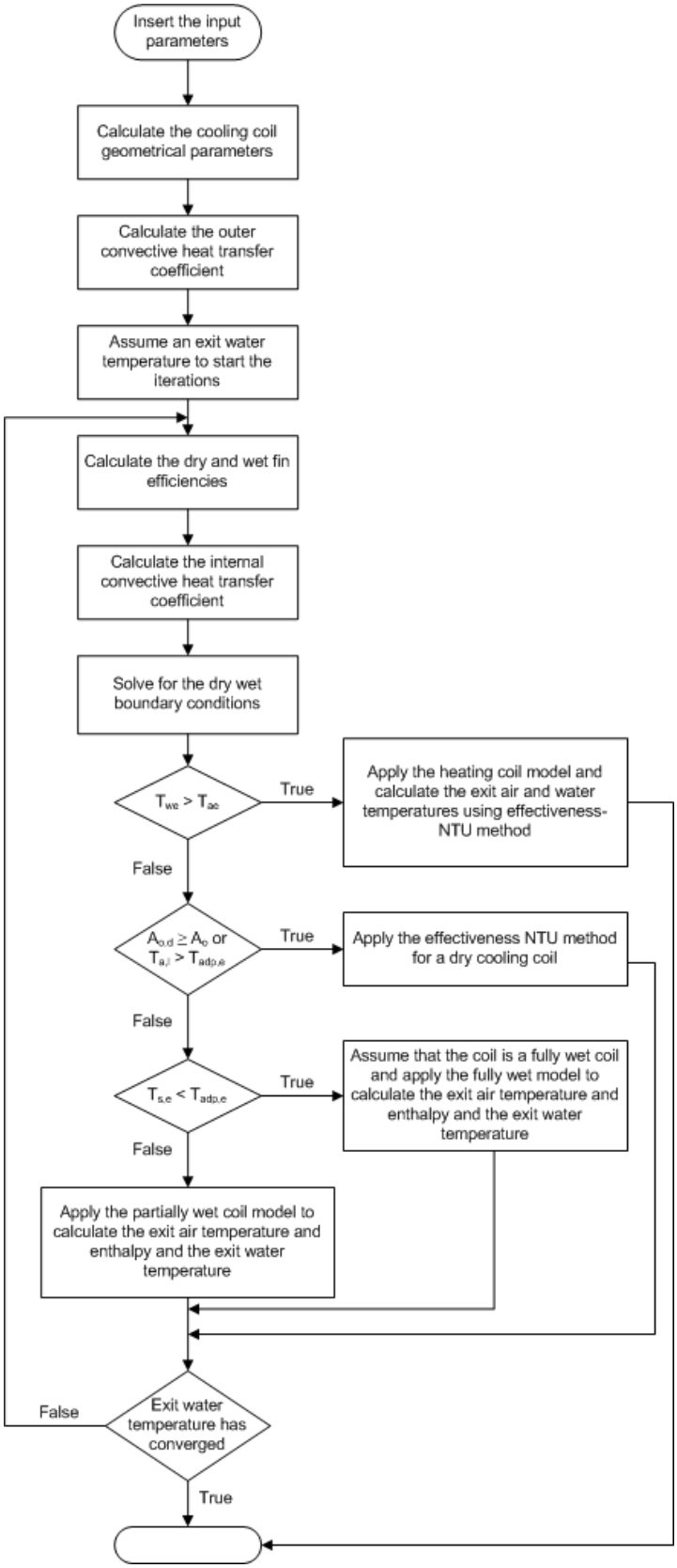

Fig.4.13: The cooling coil model program flow chart

4.3.5. Finned-Tube coil Geometric Construction Parameters

In the analysis and performance calculation of water-cooling, water-heating, steam heating or direct expansion coils, the outer to inner surface area ratio A_o/A_i, fin spacing, and tube spacing are the optimal parameters needed to determine the coil performance. Note that A_o indicates the total outer surface area of the coil and A_i represents the inner surface area of the coil. The following coil construction parameters have been adopted by many manufacturers to optimize the rate of heat transfer, air-side pressure drop, and manufacturing cost:

Longitudinal tube spacing S_L	1.083 in. (27.5 mm)
Transverse tube spacing S_T	1.25 in. (31.8 mm)
Outside nominal diameter of copper tube D_o	0.5 in. (23 mm)
Aluminum fin thickness F_t	0.006 in. (0.15 mm)

The following table lists the construction parameters for smooth fins based on the given coil construction parameters.

Table 4.2: Cooling coil geometric parameters

Fin Spacing		A_o/A_p	A_o/A_i	A_f/A_o	F_s	S_f/F_t
Fins/in	in					
8	0.125	7.85	7.95	0.873	9.91	20.8
10	0.1	9.68	9.68	0.896	12.07	16.7
12	0.0833	11.54	11.4	0.913	14.21	13.9
14	0.0714	13.46	13.17	0.925	16.37	11.9
15	0.0667	14.47	14.03	0.928	17.48	11.1

If the cooling coil construction parameters do not match the foregoing cooling coil construction parameters, it is recommended in this text to use the following equations to generate the appropriate coil ratios for a single row:

$$A_f = S_L \times S_T \times FPI \tag{4.3.1}$$

$$A_p = \pi D_o \times \left(1 - FPI \times F_t\right) \tag{4.3.2}$$

$$A_o = A_f + A_p \tag{4.3.3}$$

$$A_i = \pi D_i \tag{4.3.4}$$

$$F_s = \frac{A_o}{S_T} \tag{4.3.5}$$

To generate the values found in the foregoing table, divide the appropriate ratios from the values found from equations (4.3.1) to (4.3.5).

4.3.6. Calculation of the Coil Geometric Parameters

To be able to proceed in the cooling coil analysis several geometric parameters shall be calculated, these parameters are crucial in the determination of the finned surface efficiency which is an important parameter in determining the overall U value of the coil and the air U value of the coil.

The face area of the coil is calculated by the equation

$$A_a = F_L \times F_W \tag{4.3.6}$$

The total outer area of the coil is calculated by using the following equation:

$$A_o = F_s \times A_a \times N_r \tag{4.3.7}$$

The inner area of the coil is found by using the ratio $B = A_o / A_i$ by using the following equation:

$$A_i = \frac{A_o}{A_o / A_i} = \frac{A_o}{B} \tag{4.3.8}$$

The number of feeds is related to the serpentine by the following equation:

$$N_{feeds} = \text{serpentine} \times N_{\text{tubes in a row}} \tag{4.3.9}$$

4.3.7. Effect of the Number of Feeds on the coil

The number of feeds is a substantial parameter in the performance of cooling coils. As the number of feeds increase, the mass flow rate of water in each tube decreases results in greater temperature change in water; as the number of feeds decreases, the mass flow rate increases and the temperature change of water also decreases. The temperature change of water affects the temperature change of air affecting the performance of the coil.

Mathematically the number of feeds is related to the mass flow rate of water by the following equation:

$$\dot{m}_w = \frac{\dot{m}_{w,coil\,total}}{N_{feeds}} \tag{4.3.10}$$

4.3.8. Lumped Cooling Coil Analysis

In this section, a lumped heat transfer model is developed to model the cooling coil; the model is based on the efficiency, NTU (Number of Transfer Units) method.

The lumped model is based on the equations:

4.3.8.1. Sensible or heating coil

For a sensible coil, the coil effectiveness is defined as:

$$\varepsilon_{dry} = \frac{C_a\left(T_{a,e} - T_{a,l}\right)}{C_{\min}\left(T_{a,e} - T_{w,e}\right)} = \frac{C_w\left(T_{w,l} - T_{w,e}\right)}{C_{\min}\left(T_{a,e} - T_{w,e}\right)} \tag{4.3.11}$$

The effectiveness of the coil is calculated from the Number of Transfer Units (NTU) inside the coil by using the following equation:

$$\varepsilon_{dry} = \frac{1 - \exp\left[-NTU\left(1 - C_r\right)\right]}{1 - C_r \times \exp\left[-NTU\left(1 - C_r\right)\right]} \tag{4.3.12}$$

Note that the number of transfer units is calculated from the U-value by using the equation

$$NTU = \frac{U \times A}{C_{\min}} \tag{4.3.13}$$

After applying an energy balance on the coil, the exit air and water temperature may be calculated after discriminating the difference between a sensible cooling coil and a water heating coil.

Sensible cooling coil

$$T_{a,l} = T_{a,e} - \varepsilon_{dry}\left(T_{a,e} - T_{w,e}\right) \tag{4.3.14}$$

$$T_{w,l} = T_{w,e} + C_r\left(T_{a,e} - T_{a,l}\right) \tag{4.3.15}$$

Water heating coil

$$T_{a,l} = T_{a,e} + \varepsilon_{dry}\left(T_{a,e} - T_{w,e}\right) \tag{4.3.16}$$

$$T_{w,l} = T_{w,e} - C_r \left(T_{a,e} - T_{a,l} \right) \tag{4.3.17}$$

4.3.8.2. Fully wet coil

The number of transfer units of air may be defined as

$$NTU_a = \frac{U_a A_o}{C_a} \tag{4.3.18}$$

The number of transfer units of water may be defined as

$$NTU_w = \frac{U_w A_i}{C_w} \tag{4.3.19}$$

Neglecting the tube thickness, the number of transfer units for a wet coil may be calculated as

$$NTU_{wet} = \frac{NTU_a}{1 + C_{r,wet} \left(NTU_a / NTU_w \right)} \tag{4.3.20}$$

As for dry cooling coils, the effectiveness-NTU method may be applied for a wet cooling coil after replacing the air temperature inside the coil with the enthalpy; i.e., the effectiveness coil equations yield

$$i_{a,l} = i_{a,e} - \varepsilon_{wet} \left(i_{a,e} - i_{s,w,e} \right) \tag{4.3.21}$$

Note that $i_{s,w,e}$ is the saturated enthalpy calculated at the saturated water temperature.

The exit water temperature is calculated by using the following equation

$$T_{w,l} = T_{w,e} + \frac{\dot{m}_a}{\dot{m}_w c_{p,w}} \left(i_{a,e} - i_{a,l} \right) \tag{4.3.22}$$

The effectiveness is calculated as

$$\varepsilon_{wet} = \frac{1 - \exp\left[-NTU \left(1 - C_{r,wet} \right) \right]}{1 - C_{r,wet} \times \exp\left[-NTU \left(1 - C_{r,wet} \right) \right]} \tag{4.3.23}$$

The wet flow ratio is calculated by using the following equation

$$C_{r,wet} = \frac{\dot{m}_a \times m''}{\dot{m}_w \times c_{p,w}} \tag{4.3.24}$$

The exit air temperature is calculated by using the following equation

$$T_{a,l} = T_{s,e} + \left(T_{a,e} - T_{s,e} \right) \exp\left(-NTU_a \right) \tag{4.3.25}$$

From the exit air enthalpy and exit air temperature, the exit psychrometric state of air is calculated.

The effective surface temperature is determined from its corresponding saturated enthalpy; the saturated enthalpy is calculated from the following equations

$$i_{s,s,e} = i_{a,e} + \frac{i_{a,l} - i_{a,e}}{1 - \exp\left(-NTU_a \right)} \tag{4.3.26}$$

4.3.8.3. Dry-wet coil

A dry-wet coil is separated into two lumped coils, a dry coil and a wet coil. To be able to determine the dry-wet boundary, the dry coil area and the boundary air and water temperatures were calculated. To calculate the enthalpy of air at the boundary, it is noticed that at the boundary, the dew-point temperature of moist air at the boundary is equal to the dew point of air at the inlet of the coil. Therefore, the enthalpy of wet-air at the boundary may be calculated from the knowledge of the dew point temperature (equal to the dew point temperature of the entering air) and the air dry bulb temperature calculated at the boundary. An alternative method is to apply an energy balance on the dry-coil part to calculate the enthalpy. This energy balance results in the equation

$$i_{ab} = i_{a,e} - \varepsilon_{dry} \times c_{pa} \left(T_{a,e} - T_{wb} \right) \tag{4.3.27}$$

In equation (4.3.27) the air enthalpy at the boundary is calculated from the air inlet temperature $T_{a,e}$, the air inlet enthalpy $i_{a,e}$, and the water boundary temperature T_{wb}. It is worth to note that the psychrometric calculation and energy balance methods yield the same results.

The heat transfer rate in the dry part of the dry wet coil is calculated from the equation

$$Q_{cs} = \dot{m}_a c_{p,a} \left(T_{a,e} - T_{ab} \right) \tag{4.3.28}$$

After calculating the boundary air enthalpy a fully wet coil model is considered where the inlet air temperature is equal to the boundary air temperature and the inlet air enthalpy is equal to the boundary air enthalpy. The heat transfer rate in the wet part of the coil is calculated from the boundary air enthalpy and the enthalpy of saturated air

evaluated at the entering water temperature, thus the heat transfer rate of the wet part of the coil is

$$Q_{cw} = \varepsilon_{wet} \times \dot{m}_a \left(i_{ab} - i_{sat@T_{w,e}} \right) \tag{4.3.29}$$

Therefore, the exit enthalpy of the dry-wet coil is calculated by using the following equation

$$i_{a,l} = i_{a,e} - \frac{Q_{cs} + Q_{cw}}{\rho_a \times \dot{m}_a} \tag{4.3.30}$$

The saturated air surface enthalpy is calculated from the equation

$$i_{s,s,e} = i_{ab} + \frac{i_{a,l} - i_{ab}}{1 - \exp\left(-NTU_a\right)} \tag{4.3.31}$$

The surface air temperature is evaluated from the saturated air surface enthalpy. The coil exit air temperature is evaluated by using the equation

$$T_{a,l} = T_{s,e} + \left(T_{ab} - T_{s,e}\right)\exp\left(-NTU_a\right) \tag{4.3.32}$$

4.3.9. Calculating the Heat Transfer Coefficients

To be able to calculate the overall coil efficiency for dry and wet coils, the Number of transfer units has to be estimated; to calculate the number of transfer units, the overall heat transfer coefficient has to be calculated.

The overall heat transfer coefficient is calculated by using the equation

$$\frac{1}{UA} = \frac{1}{\eta_s h_o A_o} + \frac{\ln\left(D_o / D_i\right)}{2\pi k_{tube} L} + \frac{1}{h_i A_i} \tag{4.3.33}$$

If conduction heat transfer is neglected, then the overall heat transfer coefficient may be calculated as

$$\frac{1}{UA} = \frac{1}{\eta_s h_o A_o} + \frac{1}{h_i A_i} \tag{4.3.34}$$

In a second formulation using the ratio $B = A_o / A_i$ the U-value based on the outer area of the coil is

$$U_o = \frac{1}{\frac{1}{\eta_s h_o} + \frac{B}{h_i}} \tag{4.3.35}$$

In a similar analysis, the U-value based on the inner area of the coil tubes is

$$U_i = \frac{1}{\frac{1}{\eta_s h_o B} + \frac{1}{h_i}} \tag{4.3.36}$$

The heat transfer coefficient of air is calculated from the equation

$$U_a = \eta_s h_o \tag{4.3.37}$$

The heat transfer coefficient of water is equal to the internal convective heat transfer coefficient of water.

To be able to calculate the heat transfer coefficients, the internal and external heat transfer coefficients are to be calculated. The calculation of the internal and external heat transfer coefficients is described in the next two sub-sections.

4.3.9.1. Calculation of the Internal Convective Heat Transfer Coefficient

To be able to calculate the overall heat transfer coefficient and the Number of transfer units, the inner convective heat coefficient shall be calculated. To calculate the inner heat transfer coefficient the Nussult number of the flow shall be calculated. The Reynolds number of the flow is found by using the following equation:

$$\mathrm{Re}_D = \frac{\rho V_w D_i}{\mu_w} = \frac{4\dot{m}_w}{\pi D_i \mu_w} \tag{4.3.38}$$

Based on the Reynolds Number, the Nussult number is calculated by using the following procedure:

If the flow is laminar (Re < 2300), then the Sieder and Tate Correlation shall be used, thus the Nussult Number may be calculated from the following equation

$$Nu_D = 0.027\,\mathrm{Re}_D{}^{0.8}\,\mathrm{Pr}^{1/3}\left(\frac{\mu}{\mu_s}\right)^{0.14} \tag{4.3.39}$$

Note that all properties are calculated at the fluid mean temperature, except μ_s which is calculated at the tube surface temperature.

If the flow is in the transition region (Re ≥ 2300 and Re ≤ 10000), then Gnielinski's correlation shall be used, thus the Nussult Number may be calculated from the following equation

$$Nu_D = \frac{(f/8)(\mathrm{Re}_D - 1000)\,\mathrm{Pr}}{1 + 12.7\left(\sqrt{f/8}\right)\left(\mathrm{Pr}^{2/3} - 1\right)} \tag{4.3.40}$$

Note that all parameters are calculated at the fluid mean temperature, and the friction factor *f* is calculated from the following equation for smooth pipes

$$f = \left(0.79 \times \ln\left(\mathrm{Re}_D\right) - 1.64\right)^{-2} \qquad (4.3.41)$$

If the flow is turbulent (Re > 10000), the Dittus-Boelter correlation shall be used, thus the Nussult Number may be calculated from the following equation

$Nu_D = 0.023\,\mathrm{Re}_D^{\,0.8}\,\mathrm{Pr}^{0.4}$ for water cooling coils

$Nu_D = 0.023\,\mathrm{Re}_D^{\,0.8}\,\mathrm{Pr}^{0.3}$ for water heating coils

Note that all parameters are calculated at the fluid mean temperature.

4.3.9.2. Calculation of the External Convective Heat Transfer Coefficient

For the convective heat transfer coefficient on the air side, the correlation used is dependent on the Colburn *j* factor (McQuiston 1978):

$$j = 0.00125 + 0.27 \times JP$$

$$JP = \mathrm{Re}_D^{-0.4}\left[\frac{A_o}{A_p}\right]^{-0.15}$$

The correlation of Webb and his co-workers may also be used (N., Youn and Webb 1999):

$$\frac{j_{N=1,2}}{j_{N=3}} = 1.043\left[\mathrm{Re}_D^{-0.14}\left(\frac{S_l}{S_t}\right)^{-0.564}\left(\frac{s}{D}\right)^{-0.123}\left(\frac{S_t}{D}\right)^{1.17}\right]^{(3-N)}$$

$$j_{N\geq 3} = 0.163\left[\mathrm{Re}_D^{-0.369}\left(\frac{S_l}{S_t}\right)^{-0.106}\left(\frac{s}{D}\right)^{0.0138}\left(\frac{S_t}{D}\right)^{1.13}\right]$$

The external heat transfer coefficient depends on the Colburn *j* factor by using the following relation:

$$j = \left(\frac{h_o}{G_c c_{pa}} \right) \mathrm{Pr}^{2/3} \tag{4.3.42}$$

Note that the Reynolds number and the Colburn factor j both depend on the factor G_c which is a parameter that represents the air flow in the coil. The Reynolds number is found from the equation

$$\mathrm{Re}_D = \frac{G_c D_c}{\mu_a} \tag{4.3.43}$$

The parameter G_c is found from the equation

$$G_c = \rho_a v_{\min} \tag{4.3.44}$$

Where $v_{\min}$, is that velocity of air in the minimum area found inside the coil, note that this is actually the maximum velocity that would be found inside the coil and NOT the minimum velocity; this velocity is found by using the expression

$$v_{\min} = \frac{v_{face}}{A_{\min}/A_a} = \frac{\dot{m}_{face}}{\rho_a A_a \left(A_{\min}/A_a \right)} = \frac{\dot{V}_{face}}{\rho_a \left(A_{\min}/A_a \right)} \tag{4.3.45}$$

It is recommended to calculate the minimum flow area ratio by using the following equation

$$\frac{A_{\min}}{A_a} = S_T - D_o \times 1.1 - FPI \times F_t \times S_T \tag{4.3.46}$$

Nevertheless, a roundabout value of 0.58 may be used to estimate the minimum flow area.

4.3.10. Determination of the Fin and Surface Efficiencies

The determination of the fin and surface efficiencies for wet, dry and partially wet fins is an important part of the analysis. Therefore this determination shall be described in a separate section. In the methods described by (Wang and Hihara 2002), (Vardhan and Dhar 1998) and the method used in this text mass transfer is accounted in the convective heat transfer coefficient and surface efficiencies.

To determine the fin efficiency, an appropriate fin profile shall be determined. Threlkeld proposed to transform the plate fins of the cooling coil unit to annular fins that surround every tube in the cooling coil where the thickness of the annular coils is equal to the thickness of the original plate finned coil (Kuehn, Ramsey and Threlkeld 1998). Nevertheless, the inner radius of the annular fin is equal to the outer radius of the cooling refrigerant tube. The outer radius of the fin is found by applying the following equation:

$$r_2 = \sqrt{\frac{S_L S_T}{\pi}}$$

After transforming the plate fins to annular fins, the fin efficiency shall be determined. For annular fins Incorpera and Dewitt recommend the following expression to calculate the annular fin efficiency (Incropera and Dewitt 2005):

$$\eta_f = C_2 \frac{K_1(mr_1) I_1(mr_{2c}) - I_1(mr_1) K_1(mr_{2c})}{I_0(mr_1) K_1(mr_{2c}) + K_0(mr_1) I_1(mr_{2c})} \tag{4.3.47}$$

$$C_2 = \frac{2r_1}{m\left(r_{2c}^2 - r_1^2\right)} \qquad r_{2c} = r_2 + \frac{F_t}{2} \tag{4.3.48}$$

If a plate fine is assumed (instead of a circular fin); the expression of the fin efficiency is formulated to be:

$$\eta_f = \frac{\tanh\left(mr_2\right)\cos\left(0.1\times mr_2\right)}{mr_2} \tag{4.3.49}$$

Note that r_2 is defined in the previous equations; the factor m is defined by the following equations:

If the surface is dry: $m = \sqrt{\frac{2h_{a,dry}}{kF_t}}$

If the surface is wet: $m = \sqrt{\frac{2h_{a,dry}C_{wet}}{kF_t}}$ $\qquad$ $C_{wet} = \frac{di/dT_{aw}}{c_{p,ma}}$

The derivative of the enthalpy versus the wet bulb temperature is evaluated at a wet bulb temperature equal to the average fin temperature t_{avf}. Assuming that the lines of the enthalpy and wet bulb temperature are parallel on the psychrometric chart, a relation was obtained for the enthalpy versus the wet bulb temperature:

$$m'' = \frac{di}{dt_{aw}} = 3.5625\times10^{-7}\times t_{avf}^4 + 3.646\times10^{-5}\times t_{avf}^3 + 0.0006939\times t_{avf}^2 + 0.5472\times t_{avf} + 1.667$$

The surface efficiency is defined to be:

$$\eta_s = 1 - \frac{A_f}{A_o}\left(1-\mu_f\right) \tag{4.3.50}$$

It is worth to note that (Zhou, Braun and Zeng September 2007) recommend applying a correction factor on the wet fin efficiency expression. The heat transfer fin efficiency correction factor is defined as

$$C_F = \frac{1}{m''}\left(\frac{h_{s,sat} - h_a}{T_s - T_a}\right) \tag{4.3.51}$$

The inlet or average air temperature may be used in equation (4.3.51) to calculate the heat transfer fin efficiency correction factor. The corrected wet fin efficiency is calculated as

$$\eta_{f,corr} = 1 - C_F\left(1 - \eta_f\right) \tag{4.3.52}$$

4.3.11. Calculation of the Dry-Wet boundary

In dry-wet coils, the calculation of the dry-wet boundary is essential for calculating the dry and wet portions of the coil so that each portion may be treated in a lumped manner; i.e. the coil is lumped into two different parts, a dry part and a wet part.

If the thermal resistance of the metal tube, fouling effects and heat released by the condensate are reduced; and applying the first law of thermodynamics noting that at the dry-wet boundary the surface temperature of the tube is equal to the dew-point temperature of the air entering the coil, the following equation is obtained:

$$h_{wet}\eta_s A_o\left(T_{ab} - T_{sb}\right) = h_i\left(\frac{A_o}{B}\right)\left(T_{sb} - T_{wb}\right) \tag{4.3.53}$$

Note that the terms found in equation (4.3.53) are:

T_{sb} : outer-surface temperature of tubes at dry-wet boundary (equal to dew-point temperature of entering air)

T_{ab} : Temperature of air at the dry-wet boundary

T_{wb} : Temperature of water at the dry-wet boundary

To calculate Tab and Twb, a second equation shall be used:

$$\dot{m}_a c_{p,a}\left(T_{a,e}-T_{ab}\right)=\dot{m}_w c_{p,w}\left(T_{w,l}-T_{wb}\right) \tag{4.3.54}$$

Assuming the leaving water temperature, the above system of equations (equations (4.3.53) and (4.3.54)) are solved analytically to yield the following results:

$$T_{ab}=\frac{\left(\frac{h_i}{B}+h_{wet}\eta_s\right)T_{sb}-\frac{h_i}{B}T_{wl}+\left(\frac{\dot{m}_a c_{p,a}}{\dot{m}_w c_{p,w}}\right)T_{ae}\left(\frac{h_i}{B}\right)}{h_{wet}\eta_s+\left(\frac{\dot{m}_a c_{p,a}}{\dot{m}_w c_{p,w}}\right)\left(\frac{h_i}{B}\right)} \tag{4.3.55}$$

$$T_{wb}=T_{wl}-\left(\frac{\dot{m}_a c_{p,a}}{\dot{m}_w c_{p,w}}\right)\left(T_{a,e}-T_{ab}\right) \tag{4.3.56}$$

The sensible cooling capacity of the dry part of the dry-wet coil is calculated from the equation

$$Q_{cs}=\dot{m}_a c_{p,a}\left(T_{a,e}-T_{ab}\right) \tag{4.3.57}$$

The average air stream and water flow temperatures in the dry part of the cooling coil are calculated by using the following equations

$$T_{ad,m}=\frac{T_{a,e}+T_{a,b}}{2} \tag{4.3.58}$$

$$T_{wd,m}=\frac{T_{w,l}+T_{w,b}}{2} \tag{4.3.59}$$

Therefore, the outer surface area of the dry part is calculated as:

$$A_{o,d} = \frac{Q_{cs}}{U_o\left(T_{ad,m} - T_{wd,m}\right)} \qquad (4.3.60)$$

Thus the outer area of the dry part of the coil is calculated and the coil may be divided into two lumped systems: a dry coil and a wet coil succeeding the dry coil.

4.3.12. Generalized Transient Cooling Coil Equations

The cooling coil can be modeled as a simple counter flow heat exchanger where the air and water streams flow in opposite directions as shown inFig.4.14. There are four different zones that are to be taken into consideration: the zone that includes the air stream, a zone that includes the extended surface consisting of fins, the tube walls and the water zone.

In the simulation model each zone will be represented by its corresponding differential equation that is coupled with other zones to solve for the corresponding air and water temperature.

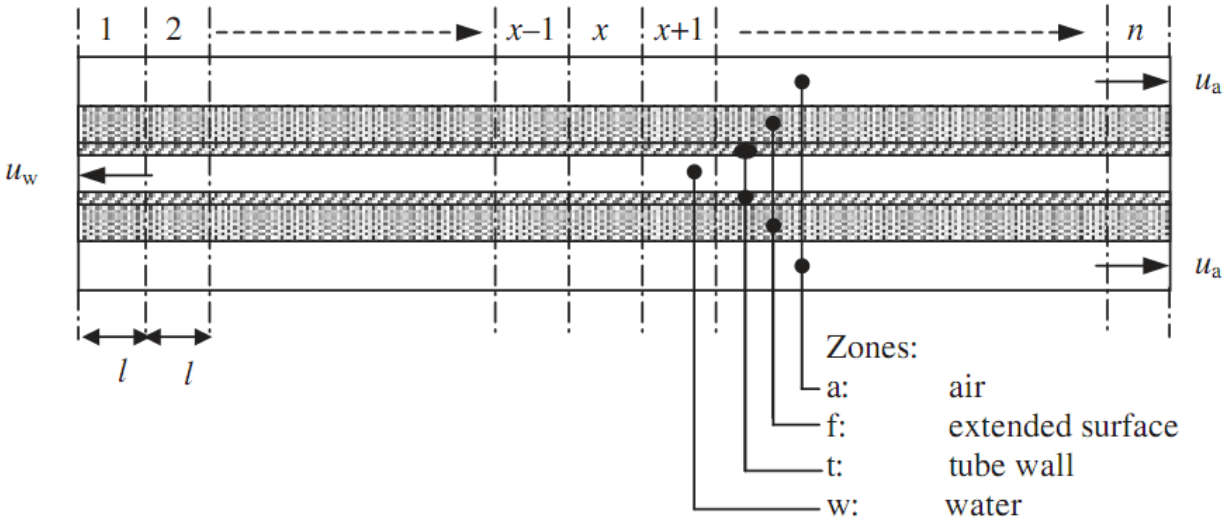

Fig.4.14: A counter flow model for cooling coil

At the air node for an element of length Δx:

$$\rho_a A_{af} \Delta x \frac{\partial h_a}{\partial t} = -\dot{m}_a \Delta x \frac{\partial h_a}{\partial x} - M_a D_o \Delta x \left(h_a - h_{a,s@T_f} \right) \tag{4.3.61}$$

Replacing the enthalpy in equation (4.3.61)by the equivalent temperature and humidity ratio using the psychrometric relation $h_a = c_{p,a} T_a + w_a h_{fg}$

$$c_{p,a} \frac{\partial T_a}{\partial t} + h_{fg} \frac{\partial w_a}{\partial t} = -u_a c_{p,a} \frac{\partial T_a}{\partial t} - u_a h_{fg} \frac{\partial w_a}{\partial x} - \frac{M_a D_o}{\rho_a A_{af}} \left[c_{p,a} \left(T_a - T_f \right) + h_{fg} \left(w_a - w_{a,s@T_f} \right) \right] \tag{4.3.62}$$

The heat and mass transfer are related by the Lewis relation

$$M_a = \eta_f \frac{h_o}{c_{p,a} Le^{2/3}} \tag{4.3.63}$$

Equation (4.3.62) can be separated into sensible and latent components represented by the temperature and humidity ratio of air in the cooling coil, these components are expressed in equations (4.3.64) and (4.3.65)

For the sensible heat transfer from air:

$$\frac{\partial T_a}{\partial t} = -u_a \frac{\partial T_a}{\partial x} - \frac{M_a D_o}{\rho_a c_{p,a} A_{af}} \left(T_a - T_f \right) \tag{4.3.64}$$

For the latent heat transfer from air

$$\rho_a A_{af} \Delta x \frac{\partial w_a}{\partial t} = -\rho_a u_a A_{af} \Delta x \frac{\partial w_a}{\partial x} - M_a D_o \Delta x \left(w_a - w_{a,s@T_f} \right) \tag{4.3.65}$$

$$\frac{\partial w_a}{\partial t} = -u_a \frac{\partial w_a}{\partial x} - \frac{M_a D_o}{\rho_a A_{af}} \left(w_a - w_{a,s@T_f} \right) \tag{4.3.66}$$

The other zones are expressed in equations

For the heat transfer to water

$$\rho_w A_{wf} c_{p,w} \Delta x \frac{\partial T_w}{\partial x} = \rho_w u_w A_{wf} c_{p,w} \Delta x \frac{\partial T_w}{\partial x} - h_i D_i \Delta x \left(T_w - T_t\right) \tag{4.3.67}$$

Simplifying equation (4.3.67)

$$\frac{\partial T_w}{\partial x} = u_w \frac{\partial T_w}{\partial x} - \frac{h_i D_i}{\rho_w c_{p,w} A_{wf}} \left(T_w - T_t\right) \tag{4.3.68}$$

For the inner tube material

$$\rho_r c_{p,t} D_i x_t \Delta x \frac{\partial T_t}{\partial x} = -h_i D_i \Delta x \left(T_t - T_w\right) - \frac{D_i \Delta x}{R_{tf}} \left(T_t - T_f\right) \tag{4.3.69}$$

Simplifying equation (4.3.69)

$$\frac{\partial T_t}{\partial x} = -\frac{h_i}{\rho_r c_{p,t} x_t} \left(T_t - T_w\right) - \frac{\left(T_t - T_f\right)}{\rho_r c_{p,t} x_t R_{tf}} \tag{4.3.70}$$

For the outer fin surface material

$$\rho_f c_{p,f} D_o x_f \Delta x \frac{\partial T_f}{\partial t} = -M_a D_o \Delta x \left(h_{a,s@T_f} - h_a\right) - \frac{D_i \Delta x}{R_{tf}} \left(T_f - T_t\right) \tag{4.3.71}$$

Simplifying equation (4.3.71) and inserting the psyhrometric relation between the enthalpy, temperature and relative humidity, equation (4.3.72) is obtained

$$\frac{\partial T_f}{\partial t} = -\frac{M_a}{\rho_f c_{p,f} x_f} \left[c_{p,a} \left(T_f - T_a\right) + h_{fg} \left(w_{a,s@T_f} - w_a\right) \right] - \frac{D_i}{\rho_f c_{p,f} D_o x_f R_{tf}} \left(T_f - T_t\right) \tag{4.3.72}$$

For a sensible coil latent heat transfer and mass transfer are neglected, thus the equations for a sensible coil are:

$$\frac{\partial T_a}{\partial t} = -u_a \frac{\partial T_a}{\partial x} - \frac{\eta_s h_o D_o}{\rho_a c_{p,a} A_{af}} \left(T_a - T_f \right) \tag{4.3.73}$$

$$\frac{\partial T_f}{\partial t} = -\frac{h_o}{\rho_f c_{p,f} d_f} \left(T_f - T_a \right) - \frac{D_i}{\rho_f c_{p,f} D_o x_f R_{tf}} \left(T_f - T_t \right) \tag{4.3.74}$$

4.4. Chilled Ceiling Model

The aim of a model for the chilled ceiling is to calculate the panel temperature and the temperature of water leaving the chilled ceiling from the inlet water temperature and mass flow rate and the chilled ceiling dimensions. The dimensions required for the chilled ceiling and the length and width of the ceiling to calculate the panel area; moreover, the diameter of the chilled ceiling tubes along with the pitch between the different tubes.

In principle chilled panels respond transiently to a change in room loads. However, the response time constant in a metal of chilled panels is very short (<5min). This justifies developing a steady-state radiant panel model which may be sufficient for engineering calculations and hourly analysis procedures (Jeong and Mumma 2004). (Conroy and Mumma 2001)derived an analytical model for top insulated metal Chilled ceiling with parallel tubes, which was based on the basic derivation by (Hottel and Whillier 1958). Natural convection and steady state conditions were assumed as well as a perfect insulation on the top part of the chilled ceiling. The derived model calculated

the cooling capacity of the Chilled ceiling (q_o) by finding the unknown mean panel surface temperature (T_{pm}) in an iterative process for given boundary conditions.

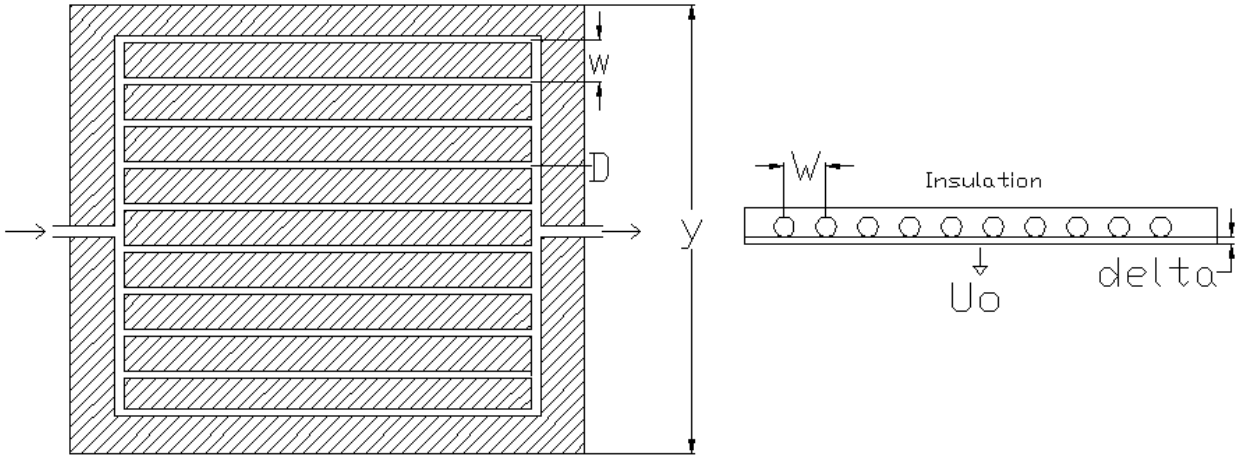

Figure 4.1: Cross-sectional geometry of top insulated metal chilled ceiling

The sensible heat absorbed by the chilled ceiling by conducted through the metal located at the ceiling and is convection by the flowing water inside the tubes embedded in the chilled ceiling. The temperature distribution between the tubes is derived by applying energy equation on a fin element and by assuming negligible temperature gradient in the direction of the flow; i.e. the metallic plate is considered to have a uniform temperature since it is assumed to be constructed of a highly conductive material. The sensible heat gain by the panel includes radiant energy from the persons and surfaces present inside the room and the heat gain by natural convection from the air layer just below the panel.

The nomenclature used in this section is shown below

A_p : Panel Area [m^2]
AUST : Area-weighted average temperature [°C]
b_w : Bond width [m]
w : Distance between the tubes [m]
D_o : Tube outer diameter [m]
F : Fin effectiveness
T_b : Temperature at the base [°C]
T_a : Temperature of air adjacent to the panel
F' : Panel efficiency factor
U_o : Overall heat transfer coefficient [W/m^2K]
h_i : Inside convective heat transfer coefficient [W/m^2K]
D_i : Tube inner diameter [m]
n : Number of tubes
F : Fin effectiveness

The total sensible heat gain by the panel per unit length (q') is expressed by equation (4.4.1)

$$q' = -\left[(w - D_o)F + D_o\right] \times U_o \times (T_b - T_a) \tag{4.4.1}$$

The boundary conditions considered are: the heat flux is zero midway between the tubes and the fin temperature immediately below the tubes is the fin base temperature (T_b).

The fin effectiveness is calculated from the overall U value U_0 by using the following equations (Incropera and Dewitt 2005):

$$F = \frac{\tanh\left(m(w - D_0)/2\right)}{m(w - D_0)/2} \tag{4.4.2}$$

Where the parameter *m* is determined from the following equation

$$m = \sqrt{\frac{U_0}{k \times \delta}} \tag{4.4.3}$$

The panel efficiency factor (F') is the ratio of overall heat transfer coefficient between the fluid flowing inside the tubes and the room to overall heat transfer coefficient between the panel and the room:

$$F' = \frac{1/U_o}{w\left[\frac{1}{U_o[D_o + (w - D_o)F} + \frac{1}{h_i \pi D_i} + \frac{\gamma}{k_b b_w}\right]} \tag{4.4.4}$$

As heat is absorbed by the panel, the fluid temperature increases in the flow direction. The temperature distribution in the flow direction is derived by applying mass and energy balances and is given in equation (4.4.5).

$$\frac{T_f(y) - Ta}{T_{fi} - Ta} = \exp\left(\frac{-nU_0 wF'}{Mc_{p,w}} y\right) \tag{4.4.5}$$

After manipulating equation (4.4.5), the exit water temperature is calculated from the following equation where L represents the overall length of tubing.

$$T_{fo} = T_a + \left(T_{fi} - T_a\right) \times \exp\left(\frac{-U_0 wF'}{Mc_{p,w}} L\right) \tag{4.4.6}$$

The mean fluid temperature (T_{fm}) can be determined by integrating equation (4.4.5) from inlet to outlet. After integration and algebraic manipulation the mean fluid temperature is found and is expressed in equation if the chilled ceiling contains a single feed

$$T_{fm} = T_{fi} + \frac{Mc_{p,w}\left(T_{fo} - T_{fi}\right)}{A_p \times F_R \times U_0} \times \left(1 - F_R\right) \tag{4.4.7}$$

The panel heat removal factor F_R is defined in the following equation

$$F_R = \frac{Mc_{p,w}\left(T_{fo} - T_{fi}\right)}{A_p U_0 \left(T_a - T_{fi}\right)} \tag{4.4.8}$$

If the chilled ceiling contains multiple feeds, the mean fluid temperature is found by incorporating the definition of mean fluid and logarithmic mean difference. The heat transfer rate absorbed by the chilled ceiling may be expressed as

$$Q = U_0 A_p \left(T_{fm} - T_a\right) = Mc_{p,w}\left(T_{fo} - T_{fi}\right)$$

Therefore, the fluid mean temperature may be calculated by using the following equation

$$T_{fm} = T_a + \frac{Mc_{p,w}}{U_0 A_p}\left(T_{fo} - T_{fi}\right)$$

The analytical model of the chilled ceiling requires the knowledge of the overall heat transfer coefficient (U_o) which is not simple to be determined since the space temperature (T_a) is not generally at the AUST of the space enclosure during radiant cooling. The convective and radiative components of the heat flux (load per unit of area) removed by the chilled ceiling are found by using Newton's cooling law by using the equations:

$$q_c = h_c \times \left(T_a - T_{pm}\right) \tag{4.4.9}$$

$$q_r = h_r \times \left(AUST - T_{pm} \right) \tag{4.4.10}$$

The total heat flux removed by the chilled ceiling is the summation of the convective heat flux (q_c) and the radiation heat flux (q_r):

$$q_{tot} = q_c + q_r \tag{4.4.11}$$

4.4.1. Determination of the Overall U-Value of the Chilled Ceiling

To determine the overall heat transfer coefficient, the convective and radiative heat transfer coefficients shall be determined. The radiative heat transfer coefficient is found by using the following equation derived from Stefan-Boltzmann radiation law (Incropera and Dewitt 2005)

$$h_r = 5 \times 10^{-8} \times \left[\left(AUST + 273 \right)^2 + \left(T_{pm} + 273 \right)^2 \right] \times \left[\left(AUST + 273 \right) + \left(T_{pm} + 273 \right) \right] \tag{4.4.12}$$

The area weighted average temperature (AUST) is calculated by using the following correlation

$$AUST \approx T_a - d \times z \tag{4.4.13}$$

The room position index; *d*is 0.5 for an interior space, 1.0 for a room with one outdoor exposed side with fenestration less than 5% of the total room surface area, 2.0 for a room with fenestration greater than 5%, and 3.0 for a room with two or more outdoor exposed sides.

The AUST adjustment factor z is calculated by using the following set of equations

$$z = \begin{cases} -0.3684 & \text{if } T_{OA} < 26\,°C \\ \dfrac{7}{T_{OA} - 45} & \text{if } 26\,°C \le T_{OA} \le 36\,°C \\ -0.7778 & \text{if } T_{OA} > 36\,°C \end{cases} \tag{4.4.14}$$

The convective heat transfer coefficient depends on the temperature difference between the air adjacent to the panel and the temperature of the panel ΔT, the velocity of the air entering the room V, and the width of the nozzle from where air enters W. The convective heat transfer coefficient is calculated by using the following equation

$$h_c = F_c + 2.13 \times \left|\Delta T\right|^{0.31} \tag{4.4.15}$$

$$F_c = \alpha_0 + \alpha_1 (\Delta T) + \alpha_2 (V) + \alpha_3 (W) + \alpha_4 (V \times W) \tag{4.4.16}$$

The coefficients are listed in the table shown below

α_1	α_2	α_3	α_4	α_5
0.28021	-0.13931	0.11416	1.25013	1.22058

Note that since the area weighted average temperature is not necessarily equal to the panel temperature of the air; an equivalent overall U value shall be used for the model. The overall U value may be proposed by the equation

$$U_0 = h_c + h_r \tag{4.4.17}$$

A better defined equation for the overall U value of the model may be found from by using the definition of the overall U value, thus

$$U_e = \frac{q_0}{\left(T_a - T_{pm}\right)} = \frac{q_c + q_r}{\left(T_a - T_{pm}\right)} = h_c + h_r \times \frac{AUST - T_{pm}}{T_a - T_{pm}} \tag{4.4.18}$$

Note that the formulation of U_e is more precise than the formulation of U_0; nevertheless, using the effective overall heat transfer coefficient without a prior knowledge of the panel mean temperature may lead to divergence errors. Thus it is advised to use U_e after determining the mean panel temperature.

The chilled model flow chart is presented in Figure 4.2 shown on the next page.

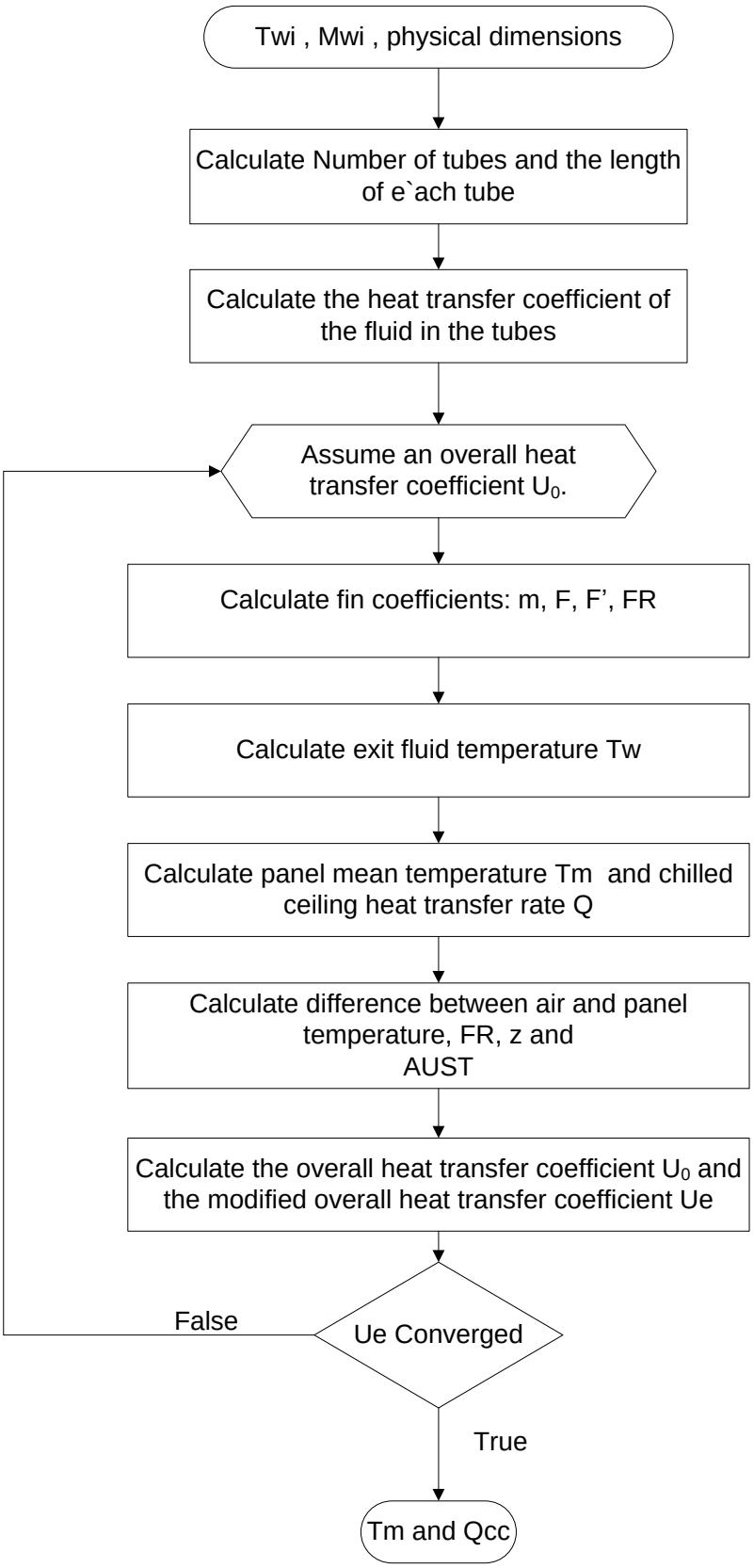

Figure 4.2: Chilled Ceiling Model flow chart

4.4.2. Chilled Ceiling Pressure Drop

To be able to calculate the chilled ceiling pressure, the head is to be calculated.

The head is defined by the following equation

$$\Delta h_{tot} = h_f + \sum h_m = \frac{V^2}{2g}\left(\frac{fL}{d} + \sum K\right) \tag{4.4.19}$$

The friction losses are evaluated by using the equation

For Laminar flow $f = \frac{64}{\mathrm{Re}_D}$ (4.4.20)

For turbulent flow $\frac{1}{f^{1/2}} \approx -1.8 \times \log\left[\frac{6.9}{\mathrm{Re}_d} + \left(\frac{\varepsilon/d}{3.7}\right)^{1.11}\right]$ (4.4.21)

CHAPTER 5

ONLINE DYNAMIC MODELS

5.1. Wall Online Dynamic Model

The thermal capacitance models are used to provide a robust calculation scheme which makes it possible to model the wall thermal storage for the simulation time interval. In the thermal capacitance model, the wall is modeled as a set of capacitors and resistors that oppose the flow of heat transfer rate due to the temperature difference.

5.1.1. First Order Lumped Capacitance Method

In the first order lumped capacitance method, the whole wall is taken as a single lumped element with internal and external air temperatures T_i and T_o as shown inFig.5.1. In the first order lumped capacitance model: r_i and r_o are the inner and outer surface thermal resistances, T_m is the uniform material temperature, C_m is the thermal capacity of the material per unit area and q_r is a radiant source term.

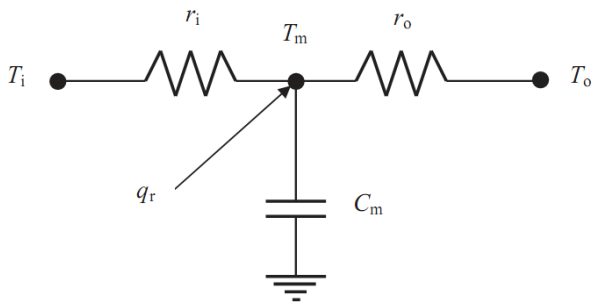

Fig.5.1: First Order Lumped Capacitance Element

Since most practical wall elements are multilayered the inner and outer thermal resistances are to be expressed in terms of the overall conductive thermal resistance r_m and capacitance C_m of the wall. Equations (5.1.3) to (5.1.6) are used to evaluate the inner and outer thermal resistances (Laret 1980).

The overall thermal resistance of the wall may be written as

$$r_m = \frac{1}{h_o} + \sum_{i=1}^{n} \frac{x_i}{k_i} + \frac{1}{h_i} \tag{5.1.1}$$

The overall thermal capacitance may be written as

$$C_m = \sum_{i=1}^{n} x_i \rho_i c_i \tag{5.1.2}$$

The parameters in equations (5.1.1) and (5.1.2) are

i	The index of the layer
x	The thickness of the layer
ρ	The density of the material of the layer
c	The thermal capacitance of the material of the layer

$$r_i = a r_m \tag{5.1.3}$$

$$r_o = (1-a) r_m \tag{5.1.4}$$

The 'accessibility factor' a is given by the equation

$$a = 1 - \frac{1}{r_m C_m} \sum_{k=1}^{n} r_k^* C_k \tag{5.1.5}$$

$$r_k^* = \sum_{j=1}^{n-1} r_j + \frac{r_k}{2} \tag{5.1.6}$$

The equation of heat conduction based on the first order lumped model may be written as shown in equation (5.1.7), in which q_r is the radiant source term per unit area.

$$\frac{dT_m}{dt} = \frac{1}{C_m}\left[q_r + \frac{(T_i - T_m)}{r_i} + \frac{(T_m - T_o)}{r_o} \right] \tag{5.1.7}$$

5.1.2. Second Order Lumped Capacitance Method

In the first order lumped capacitance method, the *whole* wall was assumed to have a single uniform temperature represented by the mean node temperature T_m. The problem is that having a single mean temperature for the whole wall surface does not give an adequate approximation of the internal surface temperature of the wall leading to deviations in approximating the long wave radiation heat exchange between the internal wall surfaces.

To incorporate the differences in surface temperatures, a second order lumped capacitance model is used with nodes $T'_m$and T''_m representing the internal and external wall surface temperatures respectively. Thus the wall element may be represented as shown inFig.5.2.

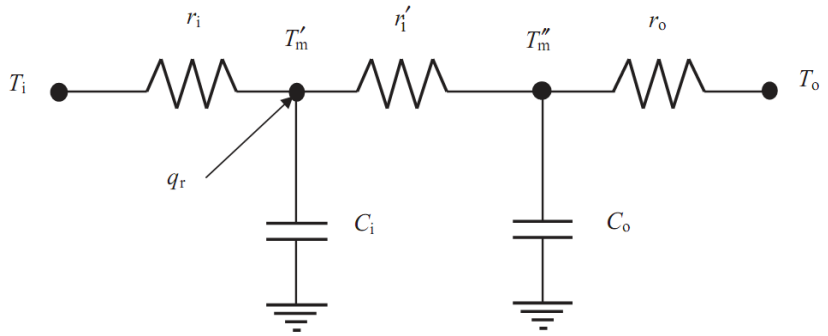

Fig.5.2: Second Order Lumped Capacitance Element

The overall element resistance may be expressed by using the ratios *f* for resistances and *g* for capacitances; therefore, the resistances r_i, r_1', and r_o may be written as shown in equations (5.1.8), (5.1.9) and (5.1.10).

$$r_i = f_1 \times r_m \tag{5.1.8}$$

$$r_1^{'} = f_2 \times r_m \tag{5.1.9}$$

$$r_o = f_3 \times r_m \tag{5.1.10}$$

The capacitance values C_i and C_o may be written as shown in equations

$$C_i = g_1 \times C_m \tag{5.1.11}$$

$$C_o = g_2 \times C_m \tag{5.1.12}$$

The five parameters f_1, f_2, f_3, g_1, and g_2 are chosen such that the response of a second order element is *nearly* identical to the response of a fully distributed element. A fully distributed element is an element with 20 different nodes (Gouda, Danaher and Underwood 2001); thus the square of the mean square error between the second order and fully distributed model is minimized by using "Kuhn-Tucker" equations for the following constraints

$$f_1 + f_2 + f_3 = 1 \tag{5.1.13}$$

$$g_1 + g_2 = 1 \tag{5.1.14}$$

$$f_1; f_2; f_3 > 0 \tag{5.1.15}$$

$$g_1; g_2 > 0 \tag{5.1.16}$$

After performing this optimization technique, it is noted that the resistive and capacitive ratios (*f* and *g*) are pretty close to each other for various wall constructions which could be divided into two categories: walls with high thermal capacitance and walls with low thermal capacitance as shown in

Table 5.1: Typical Resistance and Capacitance Fractions

Construction Element Type	f_1	f_2	f_3	g_1	g_2
External Wall with High Capacitance	0.111	0.506	0.383	0.186	0.814
External Wall with Low Capacitance	0.022	0.380	0.598	0.188	0.812
Internal Wall with High Capacitance	0.107	0.424	0.469	0.090	0.910
Internal Wall with Low Capacitance	0.111	0.477	0.412	0.198	0.802
Floor with High Capacitance	0.087	0.267	0.646	0.126	0.874
Floor with Low Capacitance	0.100	0.482	0.418	0.211	0.789

The equations of the second order lumped capacitance method may be written as shown in equations (5.1.17) and (5.1.18).

$$\frac{dT_m'}{dt} = \frac{1}{g_1 C_m}\left[q_r + \frac{(T_i - T_m')}{f_1 r_m} - \frac{(T_m' - T_m'')}{f_2 r_m}\right] \tag{5.1.17}$$

$$\frac{dT_m''}{dt} = \frac{1}{g_2 C_m}\left[\frac{(T_m' - T_m'')}{f_2 r_m} - \frac{(T_m'' - T_o)}{f_3 r_m}\right] \tag{5.1.18}$$

5.2. Chilled Ceiling Displacement Ventilation Online Dynamic Model

5.2.1. Simplified Treatment of Radiant Heat Exchange Between Internal Surfaces

Several simplified models were examined to simplify the radiant heat exchange between internal surfaces to methods simpler than adopting the conventional radiation heat transfer thermal network since it imposes a computational burden on the online dynamic model (Liesen and Pederson 1997).

The mean radiant temperature with balance (MRT/BAL) method is a compromise between accuracy and simplicity given acceptable results with a few number of computations (Walton 1980). In the MRT/BAL method, each internal wall surface is assumed to exchange long wave radiative heat transfer with a single other fictitious surface at a specified area, emissivity and temperature (mean radiant temperature) evaluated by using equations (5.2.1)to (5.2.3).

$$A_{MRT,i} = \sum_{\substack{j=1 \\ j \neq i}}^{N} A_j \tag{5.2.1}$$

$$\varepsilon_{MRT,i} = \frac{1}{A_{MRT,i}} \times \sum_{\substack{j=1 \\ j \neq i}}^{N} A_j \varepsilon_j \tag{5.2.2}$$

$$T_{MRT,i} = \frac{1}{A_{MRT,i} \varepsilon_{MRT,i}} \times \sum_{\substack{j=1 \\ j \neq i}}^{N} A_j \varepsilon_j T_j \tag{5.2.3}$$

The shape factor (view factor) between a surface and the fictitious surface with which it is exchanging radiation is given by equation (5.2.4)(Walton 1980).

$$\varepsilon_{MRT,i} F_{MRT,i} = \frac{1}{\frac{1}{\varepsilon_i} + \frac{A_i\left(1-\varepsilon_{MRT,i}\right)}{A_{MRT,i}\varepsilon_{MRT,i}}} \tag{5.2.4}$$

Therefore, the net radiative heat flux (heat gain per unit area) can be estimated by using equation (5.2.5)

$$q_{W,i,Rad} = \sigma\varepsilon_{MRT,i} F_{MRT,i}\left(T_i^4 - T_{MRT,i}{}^4\right) \tag{5.2.5}$$

The net radiative heat flux incorporates the radiation heat flux exchange between the different internal wall surfaces of the room.

5.2.2. Chilled Ceiling Displacement Ventilation Lumped Capacitance Model

A robust dynamic chilled ceiling displacement ventilation room model may be constructed by incorporating the second order lumped capacitance wall model into the cooled space lumped model to be able to develop a simple model that executes in an online dynamic fashion. The equivalent electric circuit of the whole model is shown in Fig.5.3from which a set of first order non-linear differential equations may be obtained.

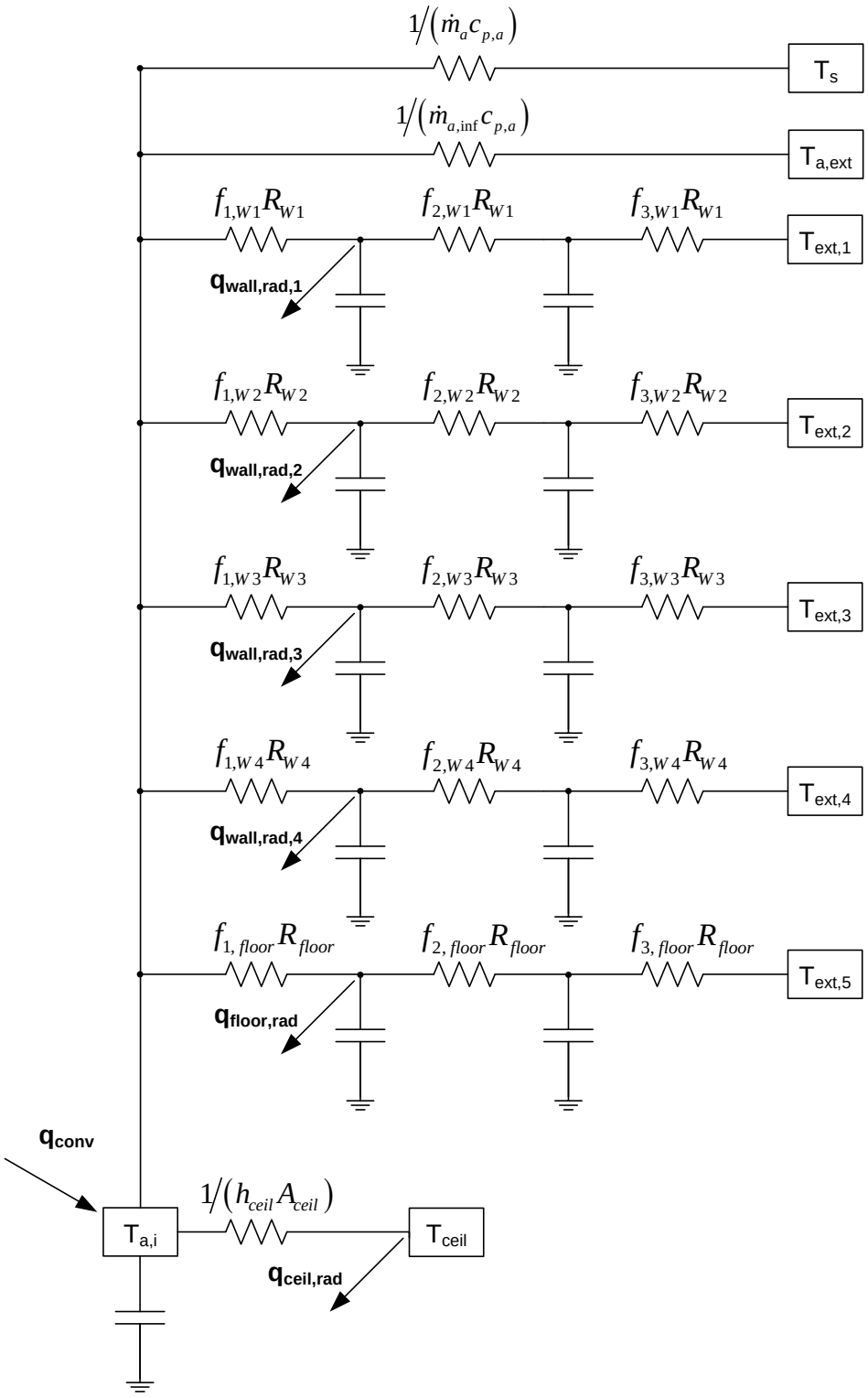

Fig.5.3: Electric equivalence of CC DV Dynamic model

The CC DV lumped system could be described by using a system of 11 ordinary differential equations with 11 unknown functions. Using the nodal analysis method to write the ordinary differential equations, these equations could be lumped into three different systems: The first system of differential equations is written at the external surface node, the second system of differential equations is written at the internal surface node and the last equation (11^{th} equation) is written at the internal room lumped air node.

At the outer node of surface *i*:

$$g_{2,i}C_i\frac{dT_{W,i,L}}{dt}=\frac{T_{ext,1}-T_{W,i,L}}{f_{3,i}R_i}-\frac{T_{W,i,L}-T_{W,i,0}}{f_{2,i}R_i} \tag{5.2.6}$$

At the inner node of surface *i*:

$$g_{1,i}C_i\frac{dT_{W,i,0}}{dt}=\frac{T_{W,i,L}-T_{W,i,0}}{f_{2,i}R_i}-\frac{T_{W,i,0}-T_{a,i}}{f_{1,i}R_i}-q_{wall,rad,i} \tag{5.2.7}$$

At the internal lumped air node:

$$m_a c_{p,a}\frac{dT_{a,i}}{dt}=\sum q_{in,conv}+\dot{m}_a c_{p,a}\times\left(T_s-T_{a,i}\right)+\sum_{i=1}^{N-1}\left(\frac{T_{W,i,0}-T_{a,i}}{f_{1,i}R_i}\right)+h_{ceil}A_{ceil}\left(T_{ceil}-T_{a,i}\right)$$
$$+\dot{m}_{a,\inf}c_{p,a}\times\left(T_s-T_{a,ext}\right) \tag{5.2.8}$$

The system of equations at the inner surface is a non-linear system of equations since the radiative heat flux leaving the surface is non-linear with respect to the inner surface temperature as indicated by Stefan-Boltzmann equations. As shown previously radiation heat exchange between the different surfaces is proportional to the difference

of the fourth power of the temperature of the surfaces exchanging radiation heat transfer.

5.2.3. Moisture and Internal Air Quality Equations

Referring to the transient simulation models, the simplified dynamic moisture and internal air quality equations are written in equations (5.2.9)and (5.2.10).

$$m_a \frac{dw_a}{dt} = G - \dot{m}_a \left(w_a - w_{a,s} \right) + \dot{m}_{a,\inf} \left(w_{a,\infty} - w_a \right) \tag{5.2.9}$$

$$\forall \frac{dC}{dt} = L + \dot{\forall}_a \left(C_s - C \right) + \dot{\forall}_{a,\inf} \left(C_\infty - C \right) \tag{5.2.10}$$

In equation (5.2.9), *G* is the rate of evaporation of water inside the cooling space (in kg/s) due to latent loads and evaporation due to contact with liquid water in the conditioned zone.

5.2.4. Discretizing the Equations

To be able to solve the equations in a fast manner, the equations are to be discretized in a forward Euler manner or in an explicit formulation to enhance the computational speed. Therefore, the system equations may be written as

$$g_{2,i} C_i \frac{T_{W,i,L}^{k+1}}{\Delta t_{sim}} = \frac{T_{ext,1}^k - T_{W,i,L}^k}{f_{3,i} R_i} - \frac{T_{W,i,L}^k - T_{W,i,0}^k}{f_{2,i} R_i} + g_{2,i} C_i \frac{T_{W,i,L}^k}{\Delta t_{sim}} \tag{5.2.11}$$

$$g_{1,i} C_i \frac{T_{W,i,0}^{k+1}}{\Delta t_{sim}} = \frac{T_{W,i,L}^k - T_{W,i,0}^k}{f_{2,i} R_i} - \frac{T_{W,i,0}^k - T_{a,i}^k}{f_{1,i} R_i} - q_{wall,rad,i}^k + g_{1,i} C_i \frac{T_{W,i,0}^k}{\Delta t_{sim}} \tag{5.2.12}$$

$$m_a c_{p,a} \frac{T_{a,i}^{k+1}}{\Delta t_{sim}} = \sum q_{in,conv}^{k} + \dot{m}_a c_{p,a} \times \left(T_s^k - T_{a,i}^k\right) + \sum_{i=1}^{N-1} \left(\frac{T_{W,i,0}^k - T_{a,i}^k}{f_{1,i} R_i} \right) + h_{ceil} A_{ceil} \left(T_{ceil} - T_{a,i}^k\right) + \dot{m}_{a,\inf} c_{p,a} \times \left(T_s^k - T_{a,ext}^k\right) + m_a c_{p,a} \frac{T_{a,i}^k}{\Delta t_{sim}}$$

(5.2.13)

$$m_a \frac{w_a^{k+1}}{\Delta t_{sim}} = G^k - \dot{m}_a \left(w_a^k - w_{a,s}^k\right) + \dot{m}_{a,\inf} \left(w_{a,\infty}^k - w_a^k\right) + m_a \frac{w_a^k}{\Delta t_{sim}} \quad (5.2.14)$$

$$\forall \frac{C^{k+1}}{\Delta t_{sim}} = L^k + \dot{\forall}_a \left(C_s^k - C^k\right) + \dot{\forall}_{a,\inf} \left(C_\infty^k - C^k\right) + \forall \frac{C^k}{\Delta t_{sim}} \quad (5.2.15)$$

5.2.5. Evaluating the Systems Loads

In order to use equations (5.2.8), (5.2.9), and (5.2.10) the internal heat moisture and contaminant loads are to be evaluated, to evaluate these loads, two previous measurements would be used, these measurements are taken during time steps *k* and *k*+1. These loads are evaluated using equations

$$\sum q_{in,conv} = m_a c_{p,a} \left(\frac{T_i^k - T_i^{k-1}}{\Delta t_{smp}} \right) - \dot{m}_a c_{p,a} \times \left(T_s^k - T_{a,i}^k\right) - \sum_{i=1}^{N} h_{ceil} A_{ceil} \left(T_{W,i}^k - T_{a,i}^k\right) - \dot{m}_{a,\inf} c_{p,a} \times \left(T_s^k - T_{a,ext}^k\right) \quad (5.2.16)$$

$$G = m_a \left(\frac{w_a^k - w_a^{k-1}}{\Delta t_{smp}} \right) + \dot{m}_a \left(w_a^k - w_{a,s}^k\right) - \dot{m}_{a,\inf} \left(w_a^k - w_{a,\infty}^k\right) \quad (5.2.17)$$

$$L = \forall \left(\frac{C^k - C^{k-1}}{\Delta t_{smp}} \right) + \dot{\forall}_a \left(C^k - C_s^k\right) + \dot{\forall}_{a,\inf} \left(C^k - C_\infty^k\right) \quad (5.2.18)$$

Equations (5.2.16), (5.2.17) and (5.2.18) are used to evaluate the current load at a specified time interval.

5.2.6. Statistical Correlations of CC/DV Inherent Parameters

Ghaddar et al. (2008) charts considered the sensitivity of the chart to room area and height parameters and concluded that their effect does not significantly affect feasible design regions. For the current work, the charts were generated from simulations of a 25 m^2 space area of typical height of 3 m. For a *CC/DV* system and conditioned space of total cooling load *Q*, the design parameters are the chilled ceiling temperature (T_c), supply air temperature (T_s), supply air flow rate ($\dot{m}_s$), and supply air humidity ratio (w_s). For a given total sensible load Q_s, the user of the chart should be able to select the supply conditions and the chilled ceiling temperature and make out the effect of the selected parameters on *dT/dZ* and stratification height. With the exception of humidity ratio, all operational parameters, stratification height and acceptable thermal comfort conditions are either included or will be possible to deduce from the design charts (Ghaddar et al. 2008). The CC/DV design charts were developed for six load ranges from 40 to 100 W/m^2 at increments of 10 W/m^2. The selected range of study falls within the recommended operation of the combined *CC/DV* air conditioning system (Rees and Haves, 2001). The considered range of values of supply air and chilled ceiling temperatures is between 15 °C and 22 °C. The constraint on the supply air temperature arises from the risk of cold drafts in the occupied region and from maintaining sufficient density gradient to keep the fresh air in the occupied zone. The supply mass flow rate is constrained by the fresh air minimum requirement for

acceptable IAQ with the condition that air velocity is less than 0.15 m/s to reduce draft for thermal comfort (ASHRAE, 2005). The design parameters appearing in each chart are T_s, T_c, load ratio R equal to chilled ceiling cooling load to the total sensible load, the displaced air parameter ($P = Q_s / \dot{m}_s$) equal to the total sensible load ratio to the supply air mass flow rate, H and dT/dZ.

The stratification height is mainly dependent on mass flow rate parameter and its incremental value of 0.05m has been traced on all the constant P-line for various values of T_c and T_s. The equal increment lines of ΔH are connected and shown on the same graph as dotted lines. The stratification height can be obtained from the chart by reading the reference value of the stratification height H_o at the top of each constant P-line. The dotted line connects the points where the stratification height is incrementally higher by dH = 0.05 m from the value H_o. The charts show that the stratification height is strongly correlated to and is weakly correlated to supply air and ceiling temperatures. By definition the stratification height is the height at which the supply flow rate is equal to upward plume flow in the space. The incremental increase in stratification height for a given P is affected by both T_c and T_s. The plume rise depends on the temperature difference between the heat source and the surrounding air. At fixed sensible load, a higher supply flow rate (smaller P value) leads to higher stratification height while a higher room air temperature at fixed supply flow rate lowers the stratification height. At high flow rate (low P), the effect of supply temperature on changing the stratification height is more important than its effect at lower flow rate (high P).

Equations for predicting stratification height Hand vertical temperature gradients dT/dZ were developed by conducting linear regression analyses using the

mass flow rate parameter P, the CC load ratio R, the chilled ceiling temperature T_c, and the supply temperature T_s as independent variables. All linear multi regression equations were developed using SPSS statistical commercial software. A significance level of $p < 0.01$ is used. The same data used for developing the design charts were used for developing the H and dT/dZ correlations. A step-wise statistical model is used in the regression model satisfying the assumptions on linearity dependence of the dependent variable, the constant variance error terms, the independence of the error terms, and the normality of the error term distribution. This step-wise method starts with the simplest regression model in which only the one independent variable that is mostly correlated to the dependent variable is used. Then the partial correlation coefficients are examined to find an additional term that would significantly explain the dependent variable. A new model including the two new variables is built and the former step is checked until we are sure that the remaining variables do not have significant influence on the dependent variable. The predictability of the linear regression equations was judged by the comparing the magnitude of the R^2-value and the significance level p. The R^2-value of the model indicates the percent variance in the predicted dependent variable that is accounted for by the independent variable entered into the regression equation.

The stratification height correlation is calculated for all load ranges of the CC/DV system as a function of Q_s, T_s, T_c, P, and R by

$$H = 0.017 \times T_c + 0.034 \times T_s - 0.036 \times P + 0.007 \times Q_s - 0.084 \times R + 0.374 \qquad (5.2.19)$$

The correlation R^2-valueis 0.865. The stratification height *H,* according to the correlation shown in equation (5.2.19), increases weakly with increase of both the chilled ceiling temperature T_c and the supply air temperature T_s. It also decreases with

the increase in displacement air parameter P and the chilled ceiling load ratio R while H increases with increase of total sensible load Q_s. The trends in variation of the stratification height with the system and load parameters are consistent with published trends by other researchers [13]. The vertical temperature gradient correlation at CC/DV load ranges is also developed in terms of the system parameters and room sensible load as

$$\frac{dT}{dz} = -0.136 \times T_c - 0.008 \times T_s + 0.052 \times P + 0.006 \times Q_s - 0.213 \times R + 2.946 \quad (5.2.20)$$

5.3. Cooling Coil Online Dynamic Model

The simulation cooling coil equations were presented under the simulation model heading; nevertheless, the generalized model may be simplified such that the models could be used for online optimization.

To simplify the equations, the overall energy balance is applied on each row rather than on a differential element reducing the computational time used to solve the generalized partial differential equations. Therefore a new simplified set of ordinary differential equations may be written for each row.

Moreover, overall heat transfer coefficients (U-values) are assumed to vary with the mass flow rates of air and water on their respective sides to simplify the computations rather than computing them using correlations and calculating fin and surface efficiencies.

5.3.1. Generalized Online Dynamic Coil Model Equations

5.3.1.1. Dry Row

For a dry row

$$m_w c_w \frac{dT_{w,l}}{dt} + \dot{m}_w c_w \left(T_{w,l} - T_{w,e}\right) + \frac{1}{R_w}\left(T_{w,in} - T_c\right) = 0 \tag{5.3.1}$$

$$m_c \times c_c . \frac{dT_c}{dt} + \frac{1}{R_a^*}(h_{s,c} - h_{a,in}) + \frac{1}{R_w}(T_c - T_{w,in}) = 0 \tag{5.3.2}$$

The water side heat resistance for each row is determined by using the equation

$$R_w = \frac{1}{\varepsilon_w \dot{m}_w c_w} \tag{5.3.3}$$

Note that the effectiveness on the water side ε_w is related to the number of transfer units as shown in equation (5.3.4)

$$\varepsilon_w = 1 - e^{-NTU_w} \tag{5.3.4}$$

The number of transfer units is calculated by using the relation

$$NTU_w = \frac{UA_w}{\dot{m}_w c_{p,w}} \tag{5.3.5}$$

The air side thermal resistance for eachrow is calculated by using the equation

$$R_a = \frac{1}{\varepsilon_a \dot{m}_a c_{p,a}} \tag{5.3.6}$$

Note that the effectiveness on the air side ε_a is related to the number of transfer units as shown in equation (5.3.7)

$$\varepsilon_a = 1 - e^{-NTU_a} \tag{5.3.7}$$

5.3.1.2. Wet Row

For a wet row, the air side dry equation is replaced with a modified equation that includes heat and mass transfer between the coil material and air.

$$m_c c_{p,c} \frac{dT_c}{dt} + \frac{1}{R_a^*}(h_{s,c} - h_{a,in}) + \frac{1}{R_w}(T_c - T_{w,in}) = 0 \tag{5.3.8}$$

The air side resistance for heat and mas transfer for each row is calculated by using the equation

$$R_a = \frac{1}{\varepsilon_a^* \dot{m}_a} \tag{5.3.9}$$

Note that the effectiveness on the air side ε_a^* is related to the number of transfer units as shown in equation (5.3.10)

$$\varepsilon_a = 1 - e^{-NTU_a^*} \tag{5.3.10}$$

The number of transfer units for a wet row is evaluated by using equation (5.3.11)

$$NTU_a = \frac{\eta_a^* h_a A_a}{\dot{m}_a c_{p,a}} \tag{5.3.11}$$

5.3.2. Evaluating the Coil Heat Transfer Coefficients

To evaluate the coil heat transfer coefficients, it is assumed that the dry coil fin efficiency is constant and known. For a wet row, the dry coil fin efficiency is corrected

as shown in the section *Determination of the Fin and Surface Efficiencies* in the simulation coil model found on page 83.

To evaluate the convective heat transfer coefficients, the following relations are assumed based on the dimensions and properties of the coils

For the internal convective heat transfer coefficient based on the water side

$$h_w = \alpha_w \dot{m}_w^{\beta_w} \tag{5.3.12}$$

For the external convective heat transfer coefficient based on the air side

$$h_a = \alpha_a \dot{m}_a^{\beta_a} \tag{5.3.13}$$

Note that the correlations stated in equations (5.3.12) and (5.3.13) are dependent on the dimensions of the coil, fin configuration, number of rows, and other geometric parameters; nevertheless, it is assumed that the correlations do not vary with the variation of temperature of air and water streams. Thus, for a given coil, the constants α_a, α_w, β_a, β_w are unique.

CHAPTER 6

ONLINE SYSTEM OPTIMIZATION

The main concern is to find the optimum value for each design parameter for each prediction period for a total simulation time of 24 hours. The simulation is performed on the selected system based on the optimization timeframe with an acceptable accuracy and the optimization process is applied for a prediction period of one hour in accordance with the dynamic load which is changing on an unknown basis. The value of a single design parameter and internal loads are fixed during a prediction period and may vary from one prediction period to another.

6.1. Genetic Algorithm

Modeling the CC/DV system is complex task with multi-variables involved, several equations are coupled and indirect relations between different parameters are present. Since the chilled ceiling displacement ventilation model is treated as a black box where several non-linear equations are solved, it is advised to use a revolutionary derivative free optimization tool that follows the direct search technique. The simplest optimization tool that could be used for the proposed case is the genetic algorithm optimization tool because it is derivative free, based on numerical analysis, and is somehow efficient if compared with other derivative based optimization schemes. Moreover, it fetches the global minimum of a specific function.

Our choice of using a derivative free algorithm to solve the optimization problem is implemented by the evolutionary genetic algorithm. Genetic algorithms are

adaptive methods which may be used to solve search and optimization problems, and are based on the genetic process of biological organisms. Genetic algorithms are growing more and more popular and extending from simple design optimization to online process control. The power of the genetic algorithm arises from its robustness, being acceptably good in finding the near optimum solution and being relatively quick (Chen 1994). An efficient optimization technique uses two techniques to find the optimal solution, exploration and exploitation, and this is what genetic algorithm does.

6.1.1. Genetic Algorithm main features

Genetic algorithm is an evolutionary technique because it is inspired from the biological evolution. It is based on searching points or solution candidates in a randomly selected population.

Advantages (Beasly 1993):

- Fast convergence to near global optimum.
- Deals with complex and noisy searching surface.
- Applicability to the searching space where we cannot use gradient information of the space.

Disadvantage (Ruan 1997):

- The tuning of the genetic algorithm parameters are sometimes an exhaustive task to accomplish.
- Its convergence speed near the global optimum becomes slow, thus increasing the need to apply hybrid optimization.

6.1.2. Applications of the Genetic Algorithm

Genetic Algorithms have been successfully applied to problems in a variety of studies in almost all disciplines, and their popularity continues to increase because of their effectiveness, applicability and ease of use(Karr and Freeman 1999). Genetic algorithm may be applied to various industrial problems such as procedures and strategy optimization, equipment optimization, controls optimization, process, plant optimization, etc… Genetic algorithms extends to the problem of tuning the parameters of the PID controller and decision making codes.

6.1.3. The Genetic Algorithm terminology

- The algorithm starts by seeding a set of trial combinations of the variables to be optimized and calculating the numerical value of the objective function for each combination selected. This set is called the "*Initial Population*".

- The set of numerical values calculated for the objective function from the first trial, is then evaluated according the "*Fitness Criteria***"**. The fitness criteria can be defined as the condition for the objective function numerical value to be better convenient than its pears.

- Based on their fitness, some combinations in the previously seeded set are chosen to be "**Parents".** Parents then undergo either "*Crossover***"** or "*Mutation***"** procedure to produce "**Children**". Most fitted parents simply jump to the next generated population without any change; such parents are referred as "*Elite***"**.

- The current population is replaced by children from the next population.

- **Elite children** are the individuals in the current generation with the best fitness values. These individuals automatically survive to the next generation. *Crossover children* are created by combining the vectors of a pair of parents. *Mutation children* are created by introducing random changes, or mutations, to a single parent.
- The algorithm stops when the "*Tolerance*" in the objective function values between two generations is less than a certain set error value, or when the maximum number of **"Generations"** is exceeded, or by any other defined **"***Stopping Criteria***"**.

6.1.4. The Genetic Algorithm procedure

1. Randomly initialize a population of individuals, such that each individual represents the random combination of the design variables.
2. The objective function is calculated for each individual.
3. The fitness of each individual is then evaluated using the information from the objective function.
4. The individuals are sorted by their fitness.
5. The best individual is saved as elite member so that it will continue to exit in the next generated population.
6. Now the top individuals are selected to be parents for reproduction.
7. A couple of parents from the selected individuals are randomly chosen for the reproduction process.
8. New children are generated by crossover, creep and mutation.
9. The elite member and the new children represent the next generated population.
10. The process repeats itself until reaching the stopping criterion.

11. Randomly initialize a population of individuals, such that each individual represents the random combination of the design variables.
12. The objective function is calculated for each individual.
13. The fitness of each individual is then evaluated using the information from the objective function.
14. The individuals are sorted by their fitness.
15. The best individual is saved as elite member so that it will continue to exit in the next generated population.
16. Now the top individuals are selected to be parents for reproduction.
17. A couple of parents from the selected individuals are randomly chosen for the reproduction process.
18. New children are generated by crossover, creep and mutation.
19. The elite member and the new children represent the next generated population.
20. The process repeats itself until reaching the stopping criterion.

A flow chart representing the basic execution of the genetic algorithm is presented in Fig.6.1.

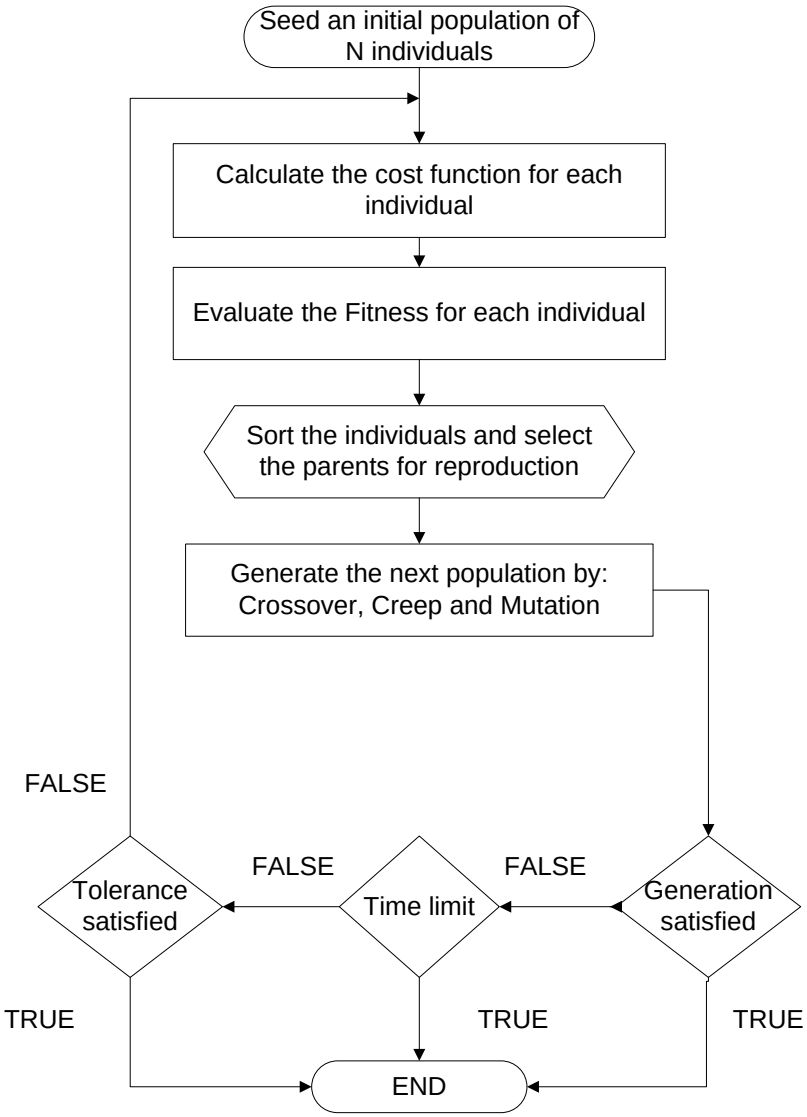

Fig.6.1: Basic Genetic Algorithm Flowchart

6.2. Optimization Variables

For the optimized control strategy used for the chilled ceiling, displacement ventilation system the variables of the chilled ceiling and displacement ventilation are varied; this variation leads to a minimal optimal cost that results in the minimum cost that could be attained in the system.

Referring to the system figure and considering the optimal control strategy, the variables that may be used for cost optimization are:

- The mass flow rate of water supplied to the coil and ceiling $\dot{m}_{w,supp}$ represented by the valve ratio χ_1.
- The mass flow rate of water passing through the cooling coil $\dot{m}_{coil}$ represented by the valve ratio χ_2.
- The mass flow rate of water passing through the chilled ceiling $\dot{m}_{ceil}$ represented by the valve ratio χ_3.
- The amount of reheat added to meet the inlet air temperature conditions expressed in terms of reheat ratio χ_{reheat}.
- The supply air mass flow rate $\dot{m}_a$.

Thus it is noticed that five variables are optimized online using dynamic models in this procedure. In order to enhance the speed of the optimization process, the corresponding valve ratios are taken as optimization variables.

6.3. Optimization Variable Bounds

6.3.1. Global Bounds

Each variable in the optimization routine has a lower and an upper bound. These bounds define the interval where the genetic algorithm searches for the optimal cost and are based on physical considerations. The bounds for the different variables are:

- The mass flow rate of water entering the coil and/or chilled ceiling is lower than the mass flow rate of water given by the chiller.
- The supply air temperature is considered to vary between 17 and 23 °C.

- The supply air mass flow rate is considered to vary between 0.08 and 0.26 kg/s such that the carbon dioxide content inside the room is within ASHRAE's recommendations.
- The supply chilled water temperature is considered to vary between 7 and 14 °C.

6.3.2. Online changing bounds

To further enhance the speed of the genetic algorithm process, it is preferred to roughly estimate the bounds of the optimized variables to minimize the search space. This is done by using two different methods which result in two different search spaces; note that the optimization search space taken into consideration is the *intersection* of the search spaces obtained from both methods.

6.3.2.1. First Method: Rough Computations Method

In this method, it is assumed that all of the system models operate at steady state conditions, and the air leaving the cooling coil is saturated with water. These assumptions will be compensated by introducing a safety factor for the lower and upper bounds to include the effects of transients and capacitance models.

From the steady state humidity model

$$w_{a,s,\max} = w_{a,\max} - \frac{ACH}{\dot{m}_a}\left(\frac{\rho \forall}{3600}\right)\times\left(w_{a,\max} - w_{a,\infty}\right) - \frac{1}{\dot{m}_a}\left(\sum \dot{m}_{w,\text{int}} + \frac{q_{\text{int},lat}}{h_{fg}}\right) \qquad (6.3.1)$$

From the steady state carbon dioxide model

$$\dot{m}_{a,\min} = \frac{\rho\left[L + \frac{ACH \times V}{3600}\left(C_{\infty} - C_{\max}\right)\right]}{C_{\max} - C_s} \tag{6.3.2}$$

The mass flow rate of air entering the room may be determined from the maximum carbon dioxide content inside the room directly since the carbon dioxide content is of fresh air may be roughly estimated (for fresh air, the carbon dioxide concentration is 360 ppmv).

From the knowledge of the coil leaving air humidity and assuming that the air exiting from the coil is already saturated, the temperature at the exit of the coil may be evaluated by calculating the dew-point temperature at the humidity ratio of the air exiting from the cooling coil this calculation is performed using equations (6.3.3) and (6.3.4).

The partial water pressure may be calculated using the equation

$$p_w = p_{ws} = \frac{p \times w}{0.62198 + w} \tag{6.3.3}$$

The dew point temperature may be calculated using the equation

$$t_{coil,l,est} = 6.54 + 14.526 \times \alpha + 0.7389 \times \alpha^2 + 0.09486 \times \alpha^3 + 0.4569\left(p_w\right)^{0.1984} \tag{6.3.4}$$

In equation (6.3.4), $\alpha = ln(p_w)$.

Since the mass flow rate of air and the exit air psychrometric conditions are estimated, the load removed from the air stream in the cooling coil may be determined

noting that fresh air with known psychrometric conditions is entering the coil. Thus the load removed from the air stream may be written as

$$q_{coil,est} = \dot{m}_a c_{p,a}\left(T_{c,e} - T_{c,l}\right) + \dot{m}_a h_{fg}\left(w_{c,e} - w_{c,l}\right) \tag{6.3.5}$$

Assuming that the heat load removed from the air side is added to the water side, equation (6.3.6) may be written after performing an energy balance on the water side of the cooling coil.

$$q_{coil} = \dot{m}_{w,coil} c_{p,w}\left(T_{w,l} - T_{w,e}\right) \tag{6.3.6}$$

Thus a relation between the mass flow rate and temperature difference between the inlet and exit water streams in the coil is obtained. The water temperature difference inside the coil may be obtained from a previous measured value; nevertheless, to be safe, the temperature difference is inflated by 10% and the appropriate mass flow rate of water into the coil may be calculated.

The chilled ceiling is assumed to have a constant effective overall heat transfer coefficient (convective and radiative) equal to a conservative value of 10 W/m^2-K. Since the minimum mass flow rate of water into the chilled ceiling is being calculated, it is safe to assume that the temperature difference of water is equal to a previously measured value inflated by 20%. Therefore the following equation may be written for the chilled ceiling

$$\dot{m}_{w,ceil} = \frac{U_{eff} A_{ceil}\left(T_p - T_{a,in}\right)}{c_{p,a} \times \Delta T_{w,ceil}} \tag{6.3.7}$$

The panel and space air temperature are obtained from a previous measurement.

The minimum mass flow rate supplied to the coil and ceiling $\dot{m}_{w,supp}$ is bounded to be at least equal to the maximum of the mass flow rates of the coil $\dot{m}_{coil}$ and ceiling $\dot{m}_{ceil}$.

6.3.2.2. Second Method: Bounding Method

When the optimization tool finds the minimum for the first time interval, the successive time interval optimization variable is seeded to be within a 40% bound from the previous time step optimal value (the upper bound is taken to be 20% greater than the optimal variables of the previous iteration and the lower bound is taken to be 20% less than the previous iteration). Note that these bounds shall not exceed the physical bounds of the system defined in the problem.

6.4. Optimization Constraints

There are several non-linear constraints that are applicable to the system. These constraints are related to thermal comfort issues, condensation inside the room and physical constraints. The constraints may be redefined in the following list

- The Percent People Dissatisfied inside the occupied zone is less than 10%. This condition is required for the human thermal comfort. The closer the PPD is to zero, it is assumed that the occupants inside the room would be more comfortable noting that the smallest percent people dissatisfaction is 5%.

- The temperature gradient shall not be greater than 2.5 K/m or 2.5 °C/m.

This condition is required so that there would not be any large gradients in the human body. Large gradients cause thermal discomfort for living beings.

- The stratification height inside the room is greater than 1 m. This condition is required so that the stratified air does not mix with the breathing zone.

- The relative humidity inside the occupied zone is greater than 30% and less than 85%.

- The fresh air supply mass flow rate shall comply with the ventilation standards inside the conditioned zone meaning that the acceptable CO_2 concentration inside the conditioned space is less than 1000 ppm according to the ASHRAE standard.

6.5. The Fitness Function

To be able to enhance the speed of the genetic algorithm, the electrical cost function and constraints are combined in a single cost function by using penalty functions, thus the fitness cost function may be written as:

$$J_{fitness} = \alpha_{elec} \times C_{elec} + \alpha_{tGrad} \times C_{tGrad} + \alpha_{stratH} \times C_{stratH} + \alpha_{ppd} \times C_{PPD} + \alpha_{rh} \times C_{rh} + \alpha_{IAQ} C_{IAQ} \quad (6.3.8)$$

Note that in equation (6.3.8), the penalty values are set according to the system parameters before installing the controller in the given system in an offline mode.

6.5.1. The Electrical Cost Function

The objective function that is to be optimized is the total operational cost of the system; this cost may be divided into:

- The cost of running the chiller.
- The cost of running the pump.
- The cost of running the fan.
- The cost of reheating the air inside the room.

In the sub-sections methods would be presented to calculate the chiller, pump, fan, and reheat cost inside the room. The cost unit is in KW. To convert the cost to KW-h, multiply the results by a factor of 3600; to convert to energy in GJ, multiply the total cost over a whole day by a factor of 0.108.

Note that in this work the cost is given in units of KW.

6.5.1.1. Chiller Cost

The chiller cost is expressed in terms of the part load ratio. The part load ratio is defined as the ratio of the current load on the chiller divided by the design load that the chiller could handle. Mathematically, the part load ratio is found from the equation

$$PLR = \frac{\dot{m}_{w,chiller} \times c_{p,w} \times \left(\Delta T_{w,chiller}\right)}{P_{chiller}} \qquad (6.3.9)$$

Note that in equation (6.3.9), it is computationally exhaustive to predict the load by predicting the water temperatures entering and leaving the chiller, thus it is preferred to estimate the chiller cost without referring to the water circuit, this is done by applying a first law energy balance on the overall piping system indicating that the current load on the chiller may be expressed by the relation

$$q_{chiller} = q_{coil} + q_{ceiling} \tag{6.3.10}$$

Therefore, the part load ratio may be written as

$$PLR = \frac{q_{coil} + q_{ceiling}}{P_{chiller}} \tag{6.3.11}$$

The coefficient of performance of the chiller is correlated to the load equation by using the following correlation

$$COP = 7.9275 \times PLR^3 - 21.194 \times PLR^2 + 16.485 \times PLR + 2.2139 + 0.1 \times (T_{chiller} - 6) \tag{6.3.12}$$

The cost of the chiller is calculated by using the following equation

$$C_{chiller} = \frac{q_{coil} + q_{ceiling}}{1000 \times COP_{chiller}} \tag{6.3.13}$$

To get a physical insight on the cost of the chiller, the coefficient of performance of the chiller is plotted versus the part load ratio of the chiller based on equation (6.3.12) for a chiller supply water temperature equal to 11 °C. The plot is shown in Fig.6.1.

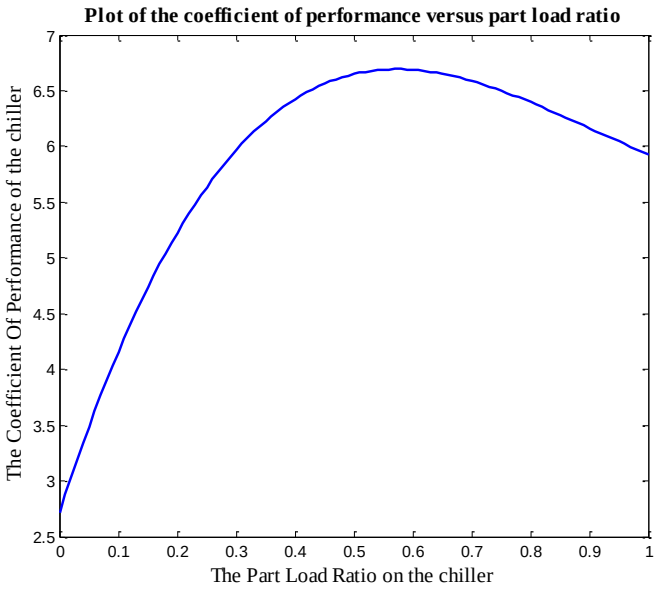

Fig.6.1: The coefficient of performance versus part load ratio.

In Fig.6.1, it is noticed that the maximum coefficient of performance that could be extracted from the chiller occurs at a part load ratio equivalent to 0.58, thus the chiller cost is a minimum at an optimal part load ratio equal to 0.58.

As the value of the part load ratio deviates from the optimal, the cost of the chiller increases and the coefficient of performance decrease. Thus at very high and very low loads, the coefficient of performance is very low. In other words it is not necessary that the chiller cost at a low load be lower than the chiller cost at a higher load.

6.5.1.2. Pump Cost

The pump cost is related to the pump head, mass flow rate, and the efficiency of the pump. The power of the pump is evaluated by multiplying the pressure

difference by the volumetric flow rate and dividing the result by the pump efficiency; mathematically the pump cost equation may be written as

$$C_{pump} = \frac{\dot{V} \times \Delta p}{1000 \times \eta_{pump}} = \frac{\dot{V} \times \rho \times g \times H_p}{1000 \times \eta_{pump}} = \frac{\dot{m}_{chiller} \times g \times H_p}{1000 \times \eta_{pump}} \tag{6.3.14}$$

The pressure difference on the pump is variable and depends on the piping system and valve openings and minor losses. Note that each valve opening corresponds to a certain pressure drop, thus the work of the pump is not constant due to the change in pressure difference.

6.5.1.3. Fan Cost

The fan cost is directly related to the air mass flow rate by using the following equation

$$C_{fan} = \left(\frac{200}{3600}\right)\left(\frac{\dot{m}_{air}{}^3}{1.29}\right) \tag{6.3.15}$$

6.5.1.4. Reheat Cost

The reheat cost is dependent on the temperature difference between the supply air temperature and the fan coil exit temperature. The reheat cost is evaluated by evaluating the sensible reheat heat transfer that occurs to heat air from the exit coil temperature to the supply room temperature. Note that resistivity efficiency also affects the cost. Mathematically, the equation is

$$C_{reheat} = \frac{\dot{m}_{air} \times c_{p,a} \times \left(T_s - T_{fc,l}\right)}{1000 \times \eta_{reheat}} \tag{6.3.16}$$

If the reheat cost is to be related to inlet air temperature, then equation (6.3.16) is recommended where the reheat cost may be calculated after determining the coil exit air temperature from the dynamic coil model. However, it is more efficient to relate the reheat cost to the reheat ratio that is given from the optimization variable: the reheat ratio is given by the equation

$$C_{reheat} = \frac{\chi_{reheat} P_{reheat}}{\eta_{reheat}} \tag{6.3.17}$$

The minimum amount of reheat is determined according to the optimized fitness function that relates the amount of reheat to the reheat ratio, dynamic cooling coil model and chilled ceiling displacement ventilation space model.

Therefore, the total electric cost is evaluated by using the expression

$$C_{elec} = C_{chiller} + C_{pump} + C_{fan} + C_{reheat} \tag{6.3.18}$$

6.5.2. The Constraints Cost Functions

The cost function for the constraints may be written such that they could be incorporated into the online cost function in a simple manner. These constraints are related to their respective threshold values such that when the constraints are violated, the fitness function would have a very large value.

For the predicted person dissatisfied, the cost function may be simply written as

$$C_{PPD} = PPD \tag{6.3.19}$$

The internal air quality cost function may be written as

$$C_{IAQ} = \exp\left(\frac{C}{C_{thld}}\right) - 1 = \exp\left(\frac{C}{1000}\right) - 1 \tag{6.3.20}$$

The relative humidity cost function may be bounded from the upper side by using the relation

$$C_{rh} = \exp\left(\frac{RH_i}{RH_{\max}}\right) - 1 = \exp\left(\frac{RH}{80}\right) - 1 \tag{6.3.21}$$

The stratification height cost is bounded to be larger than 1m, thus the stratification height cost is

$$C_{stratH} = \exp\left(\frac{H_{\min}}{H}\right) - 1 = \exp\left(\frac{1}{H}\right) - 1 \tag{6.3.22}$$

The temperature gradient is to bounded to be less than 2.5 K/m, thus the temperature gradient cost function may be written as

$$C_{tGrad} = \exp\left(\frac{dT/dz}{dT/dz|_{\max}}\right) - 1 = \exp\left(\frac{dT/dz}{2.5}\right) - 1 \tag{6.3.23}$$

The penalty or scaling functions are used to scale the each constraint penalty function to be of the same magnitude as the objective (fitness) functions that are to be minimized; nevertheless, in the given case and for the given function, the fitness and constraint functions are already at the same magnitude, thus all scaling factors are chosen to be equal to 1.

6.6. Optimization Routine

6.6.1. Genetic Algorithm Generation Step

First the genetic algorithm randomly seeds four operational parameters (for the optimal case): the water mass flow rate needed for the cooling coil, the water mass flow rate needed for the reheat, the amount of reheat added to the system represented by the reheat ratio, and the required fresh air mass flow rate of air added to the system. The variables generated and seeded in the genetic algorithm are shown in Fig.6.2.

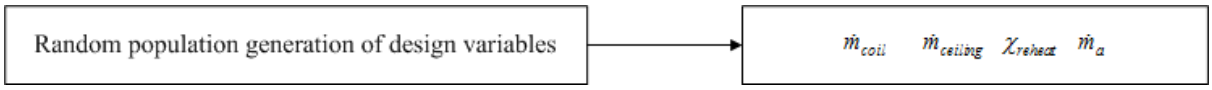

Fig.6.2: Genetic algorithm seed for operational parameters

Note that when the optimization tool finds the minimum for the first time interval, the successive time interval optimization variable is seeded to be within dynamically updated bounds. Note that these bounds shall not exceed the physical bounds of the system defined in the problem. If the optimization tool does not find an optimal within the stated constraints, then the bounds are reset and the optimization tool behaves as if it were in the first iteration. The inclusion of this algorithm reduces the oscillations found in the optimization variable with respect to time and greatly minimizes the run time required.

6.6.2. Genetic Algorithm Circuit Optimization Steps

After generating the seed values for the genetic algorithm, the optimization variables enter into the model to calculate the different parameters in the different selected components. The water exiting the chiller (at a certain chiller temperature)

enters into the cooling coil and the chilled ceiling via a pump to pump the water flow. On the other hand, air passes through the cooling coil via a fan and is reheated to enter the room at an acceptable supply air temperature.

Step 1: Cooling Coil Model

The dynamic cooling coil model uses the chilled water temperature value $T_{chiller}$, the water flow rate into the cooling coil $\dot{m}_{coil}$ and the air flow rate $\dot{m}_a$, as well as the ambient dry and wet bulb temperatures as an input and implements the model shown in page 114 to calculate the air temperature leaving the coil $T_{exit,coil}$ and humidity ratio of air leaving the coil w_s as well as the exit chilled water temperature T_4 as an output for the first time step using a numerical iterative procedure.

Step 2: Chilled Ceiling Model

At this stage the chilled ceiling model receives the temperature T_6 and the mass flow rate of the water $\dot{m}_6$entering the chilled ceiling as well as the room air temperature near the chilled ceiling. The chilled ceiling model predicts the mean plate temperature T_{pm} and the exit water temperature T_7 by solving the chilled ceiling model presented in page 36. The chilled ceiling model is solved as steady state model at each time step, but it is updated with data calculated transiently at each step such as the room air temperature at the fourth zone $T_{a,4}$. Now the other piping system equations are algebraically solved knowing that mixing occurs between the water exiting the chilled ceiling and water by-passed from the chilled ceiling to determine the water temperature returning to the chiller T_{10}.

Thus for each simulation step the cooling coil model and the chilled ceiling model as well as the chilled water circuit equations are solved as a steady state models,

and the main parameters needed for the plume multi-layer model are calculated (T_s, M_a, W_s, T_c).

Step 3: CC DV Space Dynamic Lumped Model Accompanied with Correlations

The dynamic plume multi-layer model receives the information for the input (T_s, M_a, W_s, T_c) for each simulation period and simulates the thermal conditions inside the conditioned zone for each simulation period in a transient fashion in time using the forward finite difference method.

The plume multi-layer model is simulated for a prediction period of 10 minutes several times (number of generations) until reaching the optimal design parameters for this prediction period. At each prediction period the cost function is integrated using the trapezoidal method with an increment time step of one simulation period. The genetic algorithm checks the total cost function (equation (6.3.8)) of the system space response generated by the space model during this prediction period and takes the decision for a new seed of the design variables for the next generation until reaching the optimal design parameters for the current prediction period.

The plume multi-layer model is used again using the optimal design parameters for the current prediction period and the final conditions are taken as initial conditions for the next prediction period. The procedure is repeated for the next prediction period and continues to be repeated until the end of the overall simulation time of 24 hours. The final conditions are checked and compared with the initial conditions assumed for the first minute, the whole process is simulated again using an initial condition values from the previous simulation until reaching the periodic solution where the initial and

final values are the same. The cycle is repeated four times and the results reveal that the simulation is periodic after the four cycle run.

A necessary condition for the explicit finite difference scheme to converge is satisfied for a simulation time step of 60 seconds and a space increment of 100 divisions for a wall thickness of 23 cm, the condition is presented in equation ((6.3.24)).

$$\alpha \times \left|\frac{\Delta t}{\Delta x^2}\right| < \frac{1}{2} \qquad (6.3.24)$$

Step 4: Chilled Water Circuit

The chilled water plumping circuit is an important component of the simulation that could not be over passed; i.e. it represents the connection between the fundamental parts of the circuit (chiller, coil, and chilled ceiling). In short referring to Fig.3.1, water exiting the chiller enters the cooling coil, and then passes to the chilled ceiling returning to the chiller. This flow process is initiated by a water pump connected to the system and controlled by a number of three way valves: these valves control the mass flow rate of chilled water that enters into the circuit $\dot{m}_2$, the mass flow rate of chilled water that enters into the cooling coil $\dot{m}_3$, and the amount of water that enters into the chilled ceiling $\dot{m}_6$. Moreover, after exiting the cooling coil and the chilled ceiling, there are mixers that mix the exiting water with the bypassed chilled water.

6.6.2.1. Optimization Procedure

The CC/DV system is simulated using a set of governing equations for the mass and energy balance on the assumed layers of air and for the heat source plumes and wall plumes. The time step solution for the CC/DV is solved using an iterative method to calculate the temperature distribution in the conditioned space based on an

initial assumption and on an assumed curve fitting for the wall air temperature difference. The iterative procedure updates the curve fitting until the convergence for the temperature distribution is reached.

The cooling coil model is simulated with a transient model at each time step. On the other hand, since the response time of the metallic chilled ceiling is less than 5 minutes, the chilled ceiling model is simulated for a quasi- steady conditions at each time step. The energy balance equations for the chilled water circuit simple equations are algebraic and are solved for each time step.

In the cooling coil model the fraction of the coil that is dry depends on the exit water temperature for the combined analysis, while for the wet analysis the exit water temperature depends on the average saturation specific heat, for this reason the exit water temperature is determined using an iterative method. The overall heat transfer coefficient for the chilled ceiling depends on the mean plate temperature, also an iterative procedure is needed to solve for the overall heat transfer coefficient.

The iterative solution that is needed for the CC/DV room as well as for the cooling coil model and the chilled ceiling model is started by assuming an initial value for the targeted parameter to be solved. The simulation runs and new values for the parameters are calculated, the new value replaces the assumed value or replaces the value from the previous iteration, and the simulation runs again. The procedure repeats itself until reaching a minimum desired error between an old value and the new calculated value.

For the transient solution of the CC/DV system, a forward first order finite difference scheme is adopted. The equations are explicit in time. The forward finite

difference method needs an initial value for the system to be solved. This initial value is assumed and the simulation for a whole cycle of solutions is repeated for adjusting the first assumption so that the initial value at the end of the simulation is equal to the final value for a steady periodic solution.

CHAPTER 7

CONTROL PROCESSES

The main aim of this work is to be able to control the undergoing processes in an efficient and online way. To be able to control the system effectively; the control signal is to be determined.

The pump is considered to work at a constant speed and the chiller is considered to work at a constant temperature, thus these two elements cannot be controlled.

For the fan and reheat, the response time of these two elements is pretty fast and there is no need to implement a sophisticated controller on this elements, a PID controller is more than sufficient.

For the fan, a flow sensor may be installed if carbon dioxide control is not made, or the mass flow rate of air may be calculated using the dynamic carbon dioxide model. The open loop driving voltage is determined from the fan modulation curve.

For the reheat, the feedback is represented by the supply room temperature where the current heat added by the reheat is calculated from the enthalpy difference between air entering the reheat and air entering the conditioned zone.

For the three way control valves, due to hysteresis and the non-linearity induced by the cooling coil, non-linear traditional model predictive control is used where the supply voltage is optimized to reduce the signal error in an online fashion. The square of the RMS mean error is reduced in a dynamic fashion to determine the optimal operating voltage.

7.1. Reheat Control

The reheat is considered as a simple resistance that operates on AC voltage converting the voltage into heat. The conversion is expressed mathematically by using Ohm's law as shown in equation (6.3.25)

$$q_{reheat} = V \times I \tag{6.3.25}$$

To be able to control the resistance effectively, the voltage supplied to the resistance is decreased to decrease the output resistance heat, thus controlling the heat generated by the reheating resistance. The voltage is controlled by pulse width modulation (PWM).

Since the reheat heat the supply air stream in a sensible (constant humidity ratio) fashion, the temperature difference between the entering air and leaving air can be taken as a feedback for the controller. Knowing the flow rate of air (from the fan control or via measurement), the heat generation is equal to the heat added to the air stream, the following mathematical relation may be written

$$q_{reheat} = \dot{m}_a c_{p,a} \Delta T_a \tag{6.3.26}$$

7.2. Fan Control

The flow rate of supply air is related to the speed of the fan blades supplying air to the system, thus changing the speed of the fan results in changing the flow rate of air supplied to the conditioned zone. In general, the pressure in the flow is controlled by using motorized dampers and variable air volume mixers that induce a change in the pressure of air inside the air circuit.

The pressure is related to the mass flow rate by a system curve that could be obtained after calculating the different pressure and friction losses (minor and friction losses) in the system. The fan characteristic curve relates the pressure difference of air before and after the fan to the flow rate of air in the fan. If the fan characteristic curve is plotted with the system curve on the same plot, it is noted that these two curves intersect at a single operational point for a single fan speed, for multiple fan speeds the intersection is a curve named as the *fan modulation curve*. The fan modulation curve is illustrated in Fig.7.1.

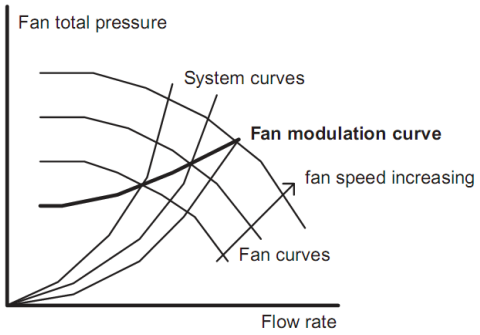

Fig.7.1: Fan Modulation Curve Illustration

The fan modulation curve relates the fan speed to the flow rate of air passing through the system, for most HVAC applications, this curve may be considered to be linear; thus the flow rate of air is related to the fan speed by a linear function. This linear function enables the usage of the PID controller.

7.3. Three Way Valve Control

The control of a three-way valve is not as simple as controlling the fan speed or the reheat because of the inclusion of the different non-linear elements, these elements include the dead time of the actuator, delay time for the valve to operate, and hysteresis.

7.3.1. Non-linear Valve Effects

The dead time is the minimal time required for the actuator to initiate to open or close the valve; typical three-way valve actuators used in HVAC applications have a time delay of two minutes.

Valve hysteresis occurs due to the fact that according to Fig.7.2to open the valve, you need a smaller force than to close the valve due to pressure difference and buoyancy effects. Thus the voltages given to the actuator to open the three-way valve are different than the voltages given to close these three-way valves resulting in a hysteresis effect as shown for a sample used valve shown in Table 7.1.

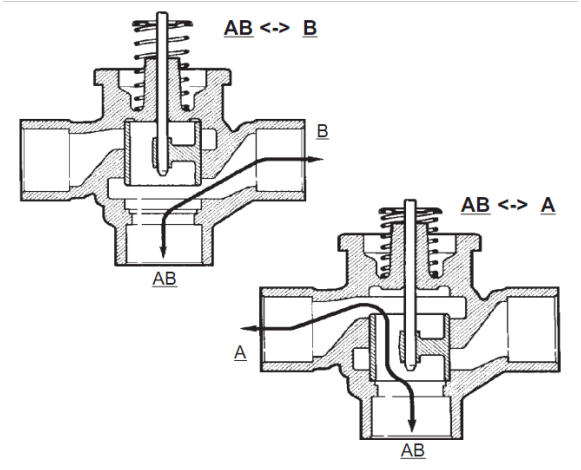

Fig.7.2: Valve Schematic

Table 7.1: Voltage values for opening and closing a typical three-way valve

Voltage [V]	Going Up [LPM]	Going down [LPM]
0	0	0
0.5	0	0
1	0	0
1.5	0	0
2	0	0
2.5	0	0
3	0	1.25
3.5	0	2.5
4	2.5	3.5
4.5	3.5	4.25
5	4.25	5
5.5	5	6.2
6	6	7.5
6.5	7	9
7	8	10.2
7.5	10	12
8	11.5	14
8.5	13.5	17
9	15.6	21
9.5	20	23
10	23	23

The non-linear effects render the usage of the PID controller to be impractical, thus other non-linear control methods are to be devised. Moreover, the valves are linked with sophisticated dynamic models for the cooling coil and the chilled ceiling complicating the control process in the frequency domain since it is not easy to compute the Laplace transform of these non-linear functions. Thus a non-linear time domain controller is required and the model predictive control method is chosen.

7.3.2. Model Predictive Control

Model predictive control relies on online dynamic models to predict the future measurement in the future predictive and control periods. It is worth to distinguish

between the prediction and control periods: the prediction period is the period upon which the set-point variables (loads) are assumed to be constant (equivalent to the optimization set-period); on the other hand, the control period is the period over which the voltage setting on the valve actuator is to be changed. For an illustration, refer to Fig.7.3.

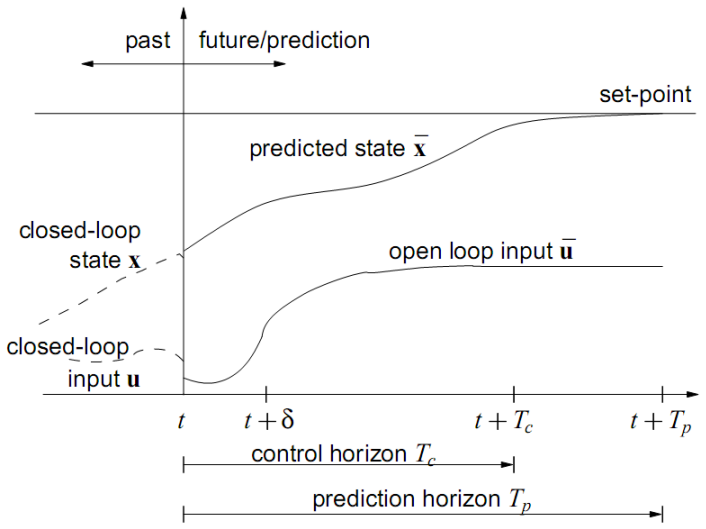

Fig.7.3: Model predictive control illustration

7.3.2.1. Advantages of model predictive control

- Concepts of model predictive control are very intuitive and are relatively easy to understand.
- It can be used to control a great variety of processes from relative simple dynamics to more complex systems that include hysteresis.
- Dead times and delay times are already compensated.
- It is very useful when future references are known or could be predicted.

7.3.2.2. Model Predictive Control Procedure

For each three-way valve, the voltage is optimized in an online fashion using the genetic algorithm to determine the dynamic operational voltage at each control time interval. As shown in Fig.7.4, the voltage (control variable) is optimized in an online fashion using the genetic algorithm to minimize the mean square error between the predicted and set control values. The fitness function is different for each valve since the sensor feedback of each valve is different than other valves.

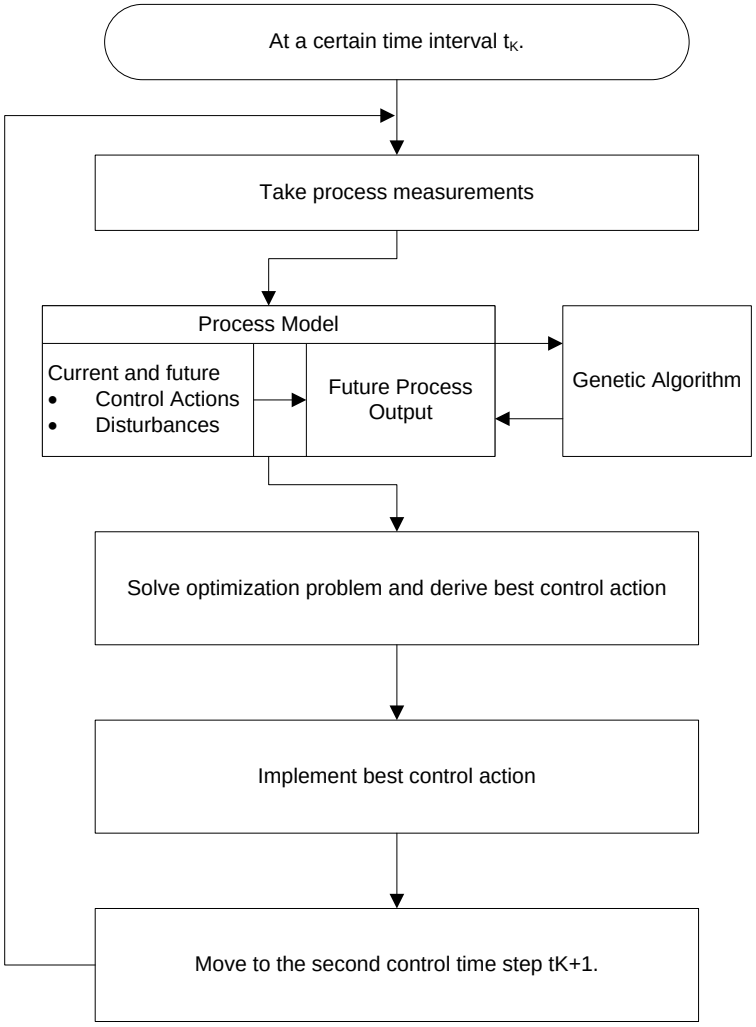

Fig.7.4: Model predictive control flowchart

It is recommended to install an electronic flow meter for the first valve that reads the flow in an electronic fashion to feedback the controller, thus the fitness function of the first valve may be stated as

$$F = \left(\dot{m}_{w,\text{sup}} - \dot{m}_{w,\text{sup},set} \right)^2 \tag{6.3.27}$$

It is worth to note that in equation (6.3.27), the fitness function is non-linear since there is a time delay in the actuator to function and that is taken into consideration.

For the second three way valve, the enthalpy difference between the air stream entering the coil and that exiting the coil is used as a driver for the controller, thus the fitness function may be defined as

$$F = \left(\Delta i_{a,coil} - \Delta i_{a,coil,set} \right)^2 \tag{6.3.28}$$

For the third three-way valve, the panel temperature is taken as a driver for the controller thus, the fitness function may be written as

$$F = \left(T_{panel} - T_{panel,set} \right)^2 \tag{6.3.29}$$

It is noted that for the second and third three-way valves, the online models of the coil and ceiling are used to calculate the predicted coil enthalpy difference and chilled ceiling panel temperature respectively adding to the complexity and non-linearity of the controller. The chilled ceiling panel temperature and coil enthalpy difference are preferred since it is not practical to install flow rate meters noting that the aim of changing the three-way valve setting is to control the chilled ceiling panel temperature and coil enthalpy difference.

CHAPTER 8

CASE STUDY

A case study is selected to illustrate the procedure used to select and optimize the chilled ceiling and displacement ventilation systems. The system consists of a single room conditioned by using the chilled ceiling and displacement ventilation system. The room consists of two external walls with two partitions and is considered to be located above conditioned space at 25 °C.

The wall configuration is a widely used wall configuration that consists of the layers listed in Table 8.1.

Table 8.1: Wall Layer Properties

Layer Number	Layer Material	Thickness [mm]	Density [kg/m^3]	Specific Heat [kJ/kg-K]	Thermal Conductivity	R-Value [m^2-K/W]
1	Gypsum Board	15.88	800.9	1.09	0.161	0.09862
2	LW Concrete Block	101.590	608.7	0.84	0.38	0.26681
3	Face Brick	101.59	2002.3	0.92	1.33	0.07626

The overall thickness of the wall is 219.06 mm, and the overall U-value of the wall is 1.28 W/m^2-K. The room walls orientations are summarized in Table 8.2.

Table 8.2: The orientation of the wall with the accompanying overall U values

Wall Number	Orientation	Overall U Value
1	South	1.28
2	West	1.28
3	Partition (East Direction)	1.28
4	Partition (North Direction)	1.28

The room is considered to be a 5 x 5 x 3 room where the floor area is 25 m^2 and the height of the room is 3m. Note that in the test case, windows are not considered inside the room since the model for spaces cooled by chilled ceiling and displacement ventilation does not support the inclusion of windows, this is a reasonable assumption for offices that do not include windows.

The mechanical HVAC (heating, ventilation and air condition) ducting and piping circuit is shown in Fig.8.1. Note that the layout consists of some key parameters in control:

- The three-way valves located in the water circuit. These valves control the flow rate of water exiting from the chiller, and entering to the cooling coil and chilled ceiling. Note that the exiting coil properties and ceiling temperature depend on the input water mass flow rate that is determined by the valves.
- The reheat that is used to reheat the sub-cooled air to reach an optimum supply air temperature.
- The fan that is used to supply cooled air into the conditioned space.

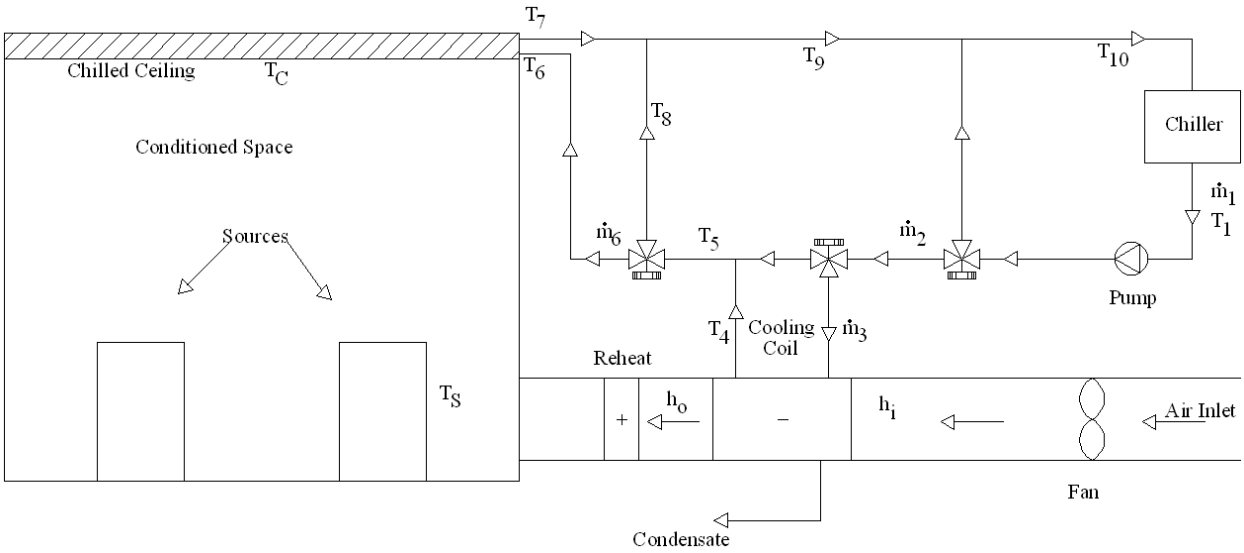

Fig.8.1: Duct and Piping layout for the CCDV system.

The occupants schedule is given in Table 8.3 and Fig.8.2.

Table 8.3: The occupants schedule

Hour	0	1	2	3	4	5	6	7	8	9	10	11
Occupants	0	0	0	0	0	0	0	2	2	4	5	5

12	13	14	15	16	17	18	19	20	21	22	23
5	6	6	6	3	4	3	4	3	2	0	0

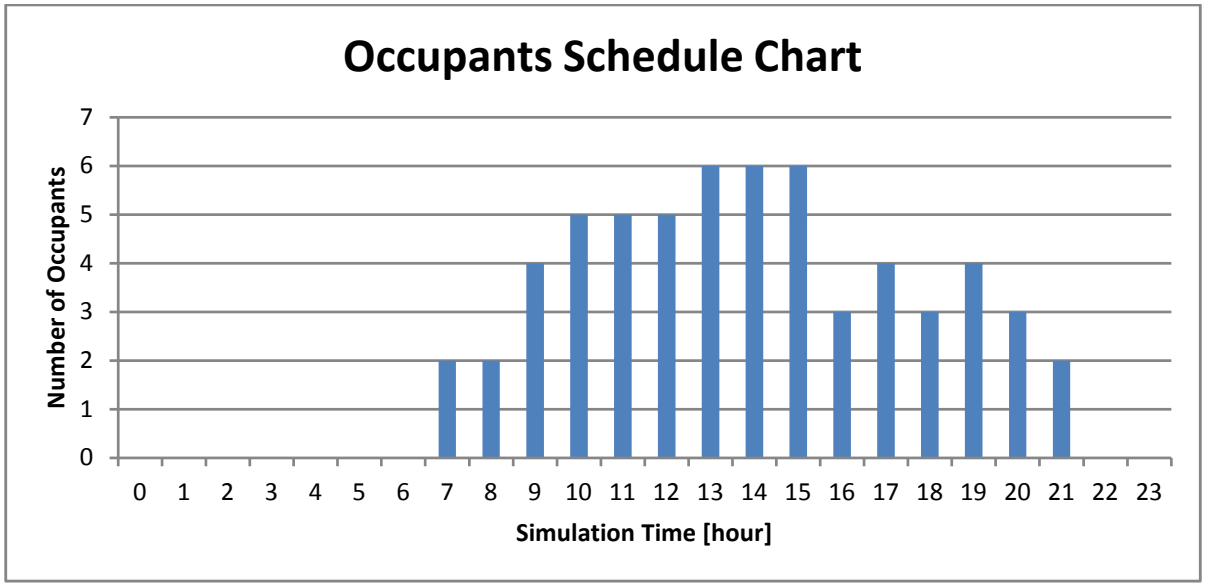

Fig.8.2: Occupants Schedule Chart

The sensible load is shown in the Table 8.4 and Fig.8.3.

Table 8.4: The sensible load schedule

Hour	0	1	2	3	4	5	6	7	8	9	10	11
Load	0	0	0	0	0	0	0	512	640	1280	1280	1280

12	13	14	15	16	17	18	19	20	21	22	23
1280	1280	1280	1280	640	512	512	512	512	512	0	0

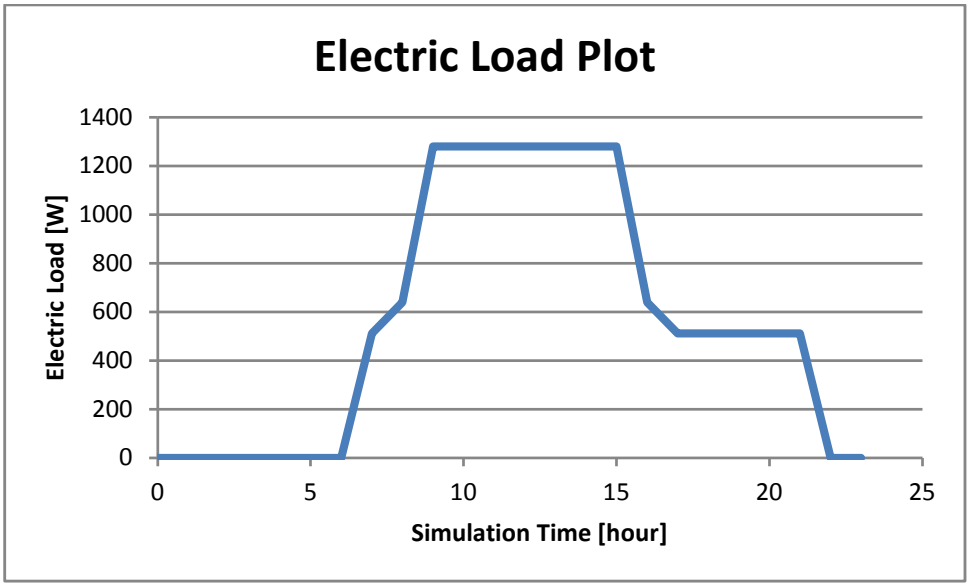

Fig.8.3: Sensible Load Schedule Chart

The lighting load is taken as shown in Table 8.5 and Fig.8.4

Table 8.5: The Lighting load schedule

Hour	0	1	2	3	4	5	6	7	8	9	10	11
Load	0	0	0	0	0	0	0	200	200	200	200	200

12	13	14	15	16	17	18	19	20	21	22	23
200	200	200	200	200	200	200	200	200	200	0	0

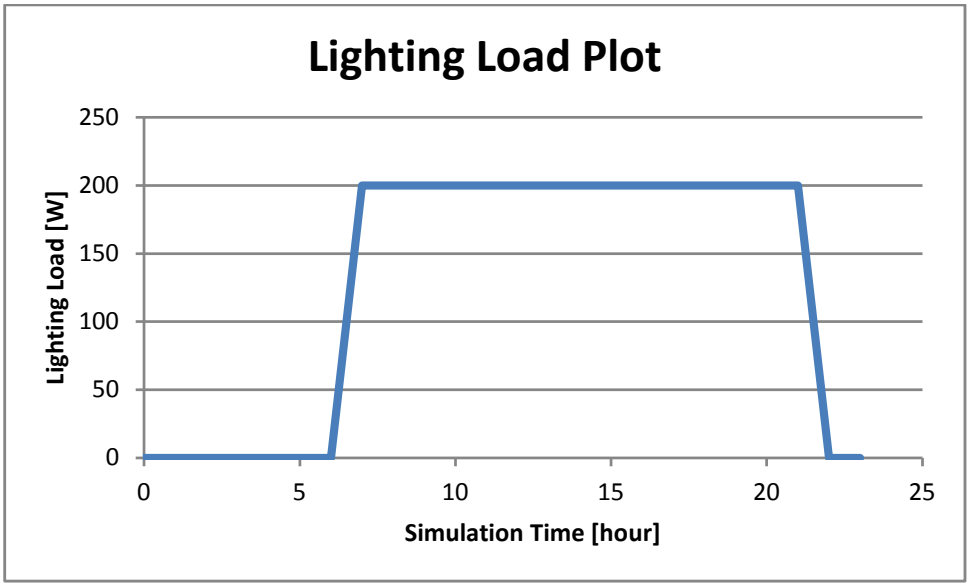

Fig.8.4:Lighting Load Schedule Chart

Therefore, the calculated convective sensible load, radiative load, latent load and carbon dioxide generation are shown in the following tables

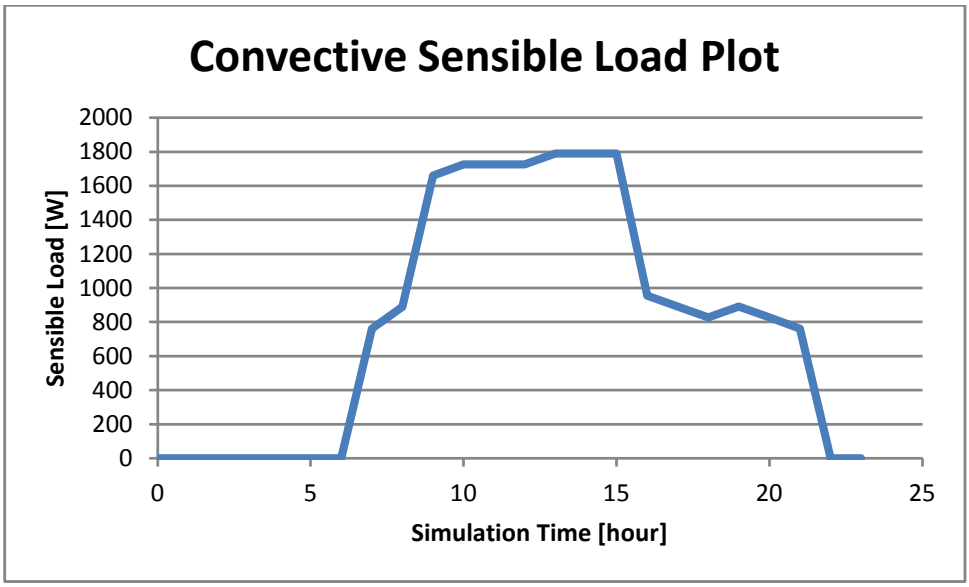

Fig.8.5: Convective Sensible Load Plot

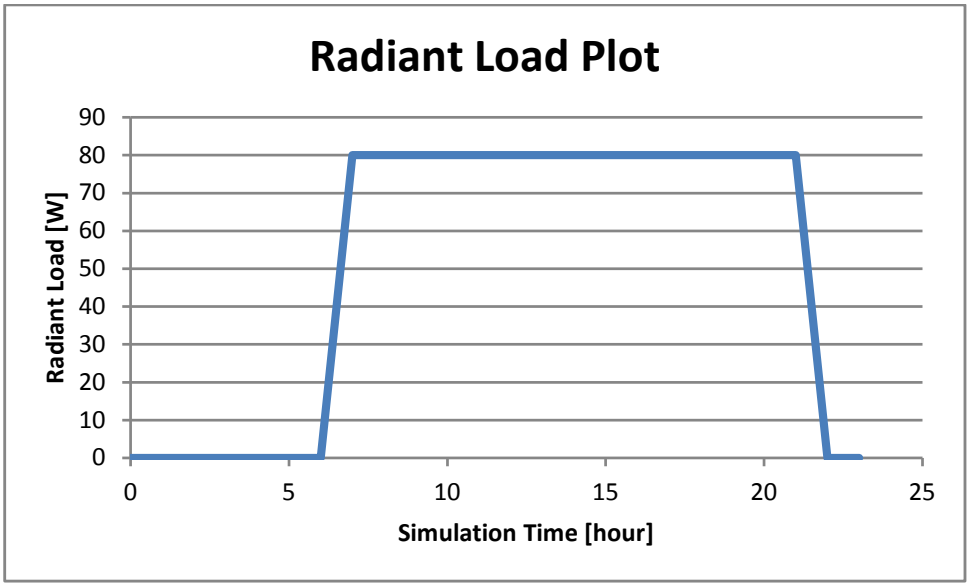

Fig.8.6: Radiant Load Plot

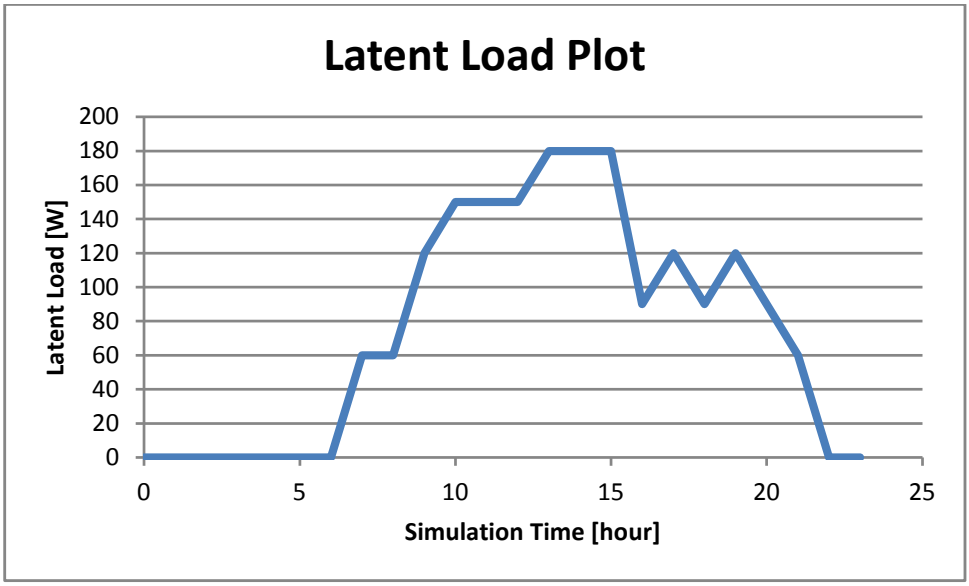

Fig.8.7: Latent Load Plot

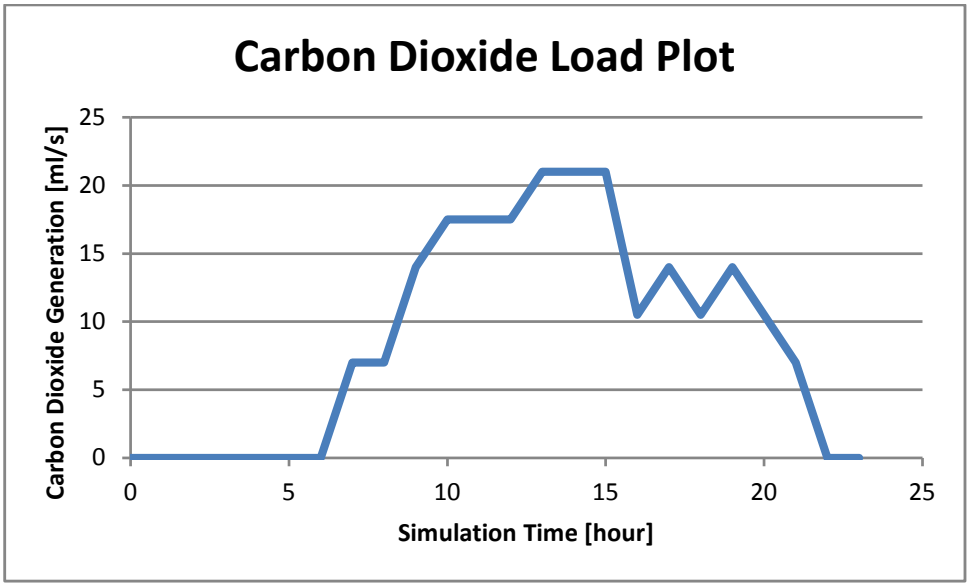

Fig.8.8: Carbon Dioxide Load Plot

In the analysis presented in this text, it is assumed that the load inside the cooled region is unknown; nevertheless, the load profile is given in the foregoing figures. The given load profile is used for the simulation function to generate the appropriate *"measurement"* values that are used in the online functions to predict the future cost values.

In a similar fashion, the dimensions of the selected cooling coil and the selected chilled ceiling are needed to be able to generate the appropriate measurement values.

The cooling coil used in the study has the following properties

Property	Value
Number of rows	3
Number of tubes	8
Number of feeds	3
Serpentine	1
Nominal tube Diameter	0.5”
Row Spacing	1.083”
Tube Spacing	1.25”
Number of Fins per Inch	14
Finned Height	8”
Finned Length	3 ft = 36”
Tubing Material	Copper
Fin Material	Aluminum

The chilled ceiling has a tube spacing of 20 cm with 0.5” copper tubes connected at the exit of the coil as shown in Fig.8.1.

CHAPTER 9

RESULTS AND DISCUSSION

After performing the online optimization, the simulated results are shown in this chapter. Namely, the opening valve ratios, reheat ratio, air mass flow rate into the room, supply, return and chilled ceiling temperatures, the temperature gradient, predicted mean vote, stratification height, carbon dioxide content and cost functions are plotted in this chapter.

The openings of the valves are shown in Fig.9.1.

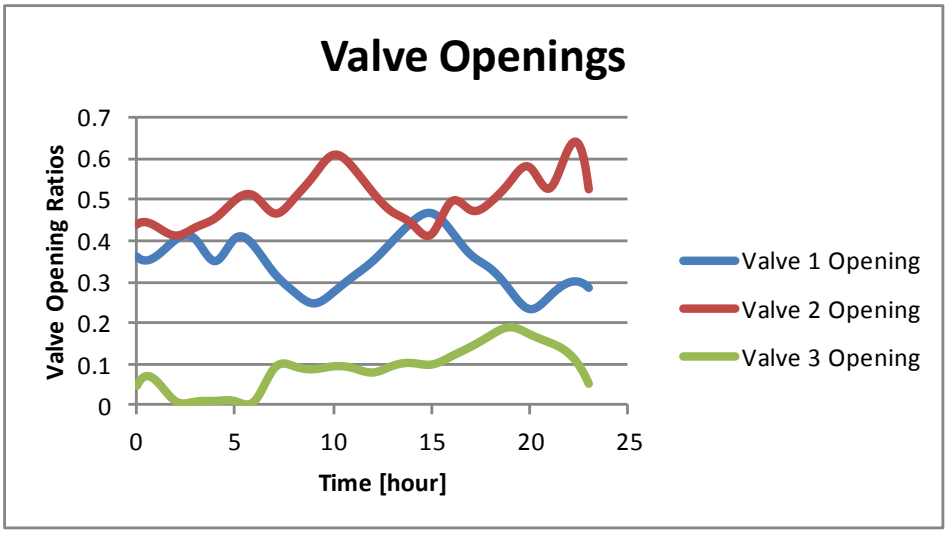

Fig.9.1: Valve Opening Ratios

Referring to Fig.9.1, it is noted that as the load varies, the opening ratios in the three three-way valves vary simultaneously in each prediction period.

The reheat ratio is plotted in Fig.9.2.

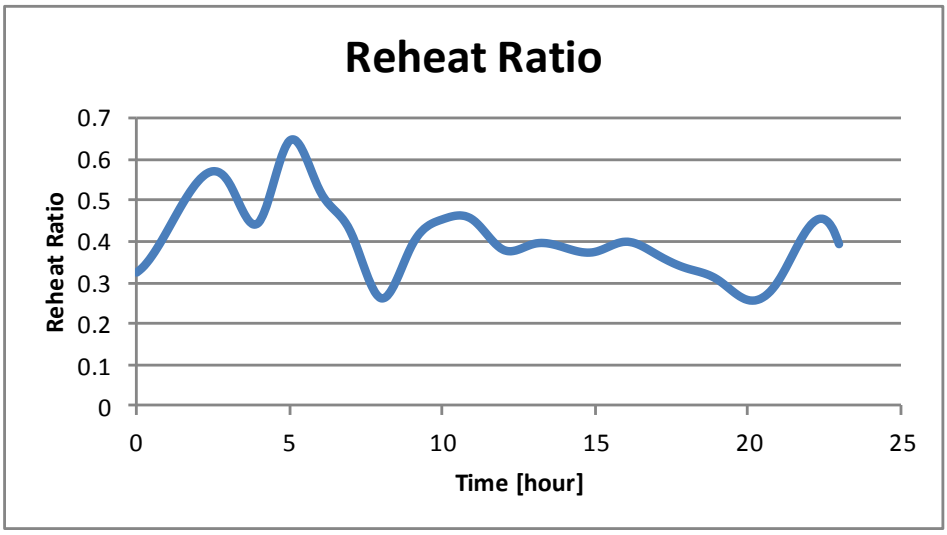

Fig.9.2: The reheat ratio of the system

The mass flow rate of fresh air supplied to the room is shown in Fig.9.3.

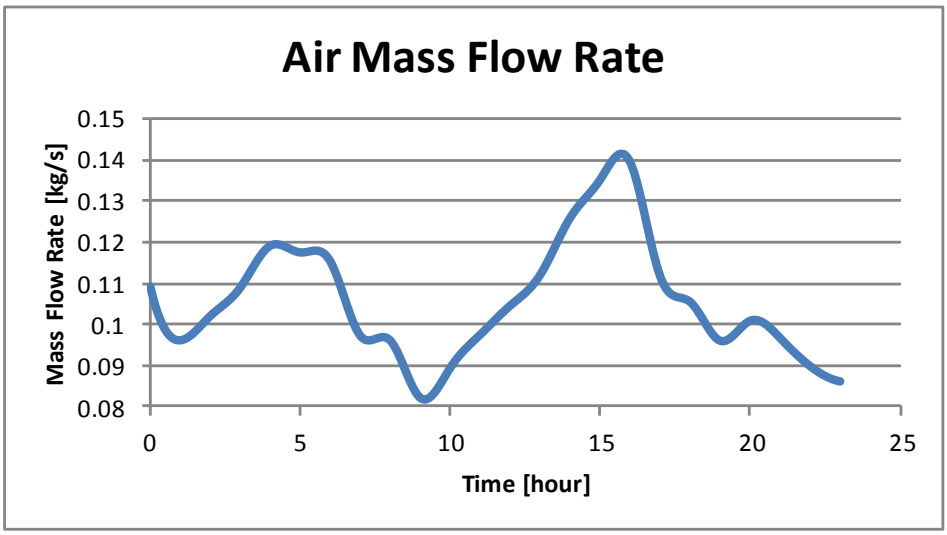

Fig.9.3: The mass flow rate of air

The supply and return air and chilled ceiling temperatures are shown in Fig.9.4.

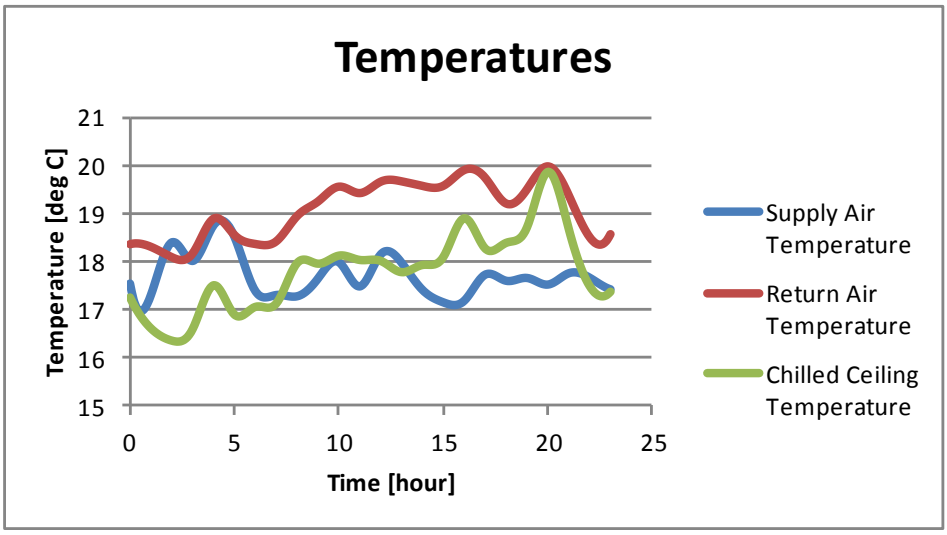

Fig.9.4: Plot of the supply, return and chilled ceiling temperatures

The electrical chiller, pump, reheat and fan cost are shown in Fig.9.5.

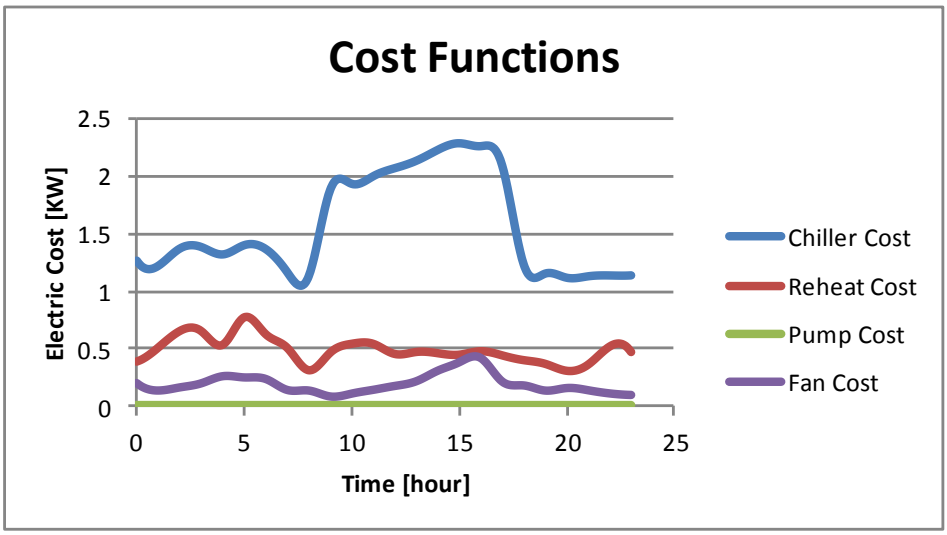

Fig.9.5: The electrical cost functions

The temperature gradient is shown in Fig.9.6.

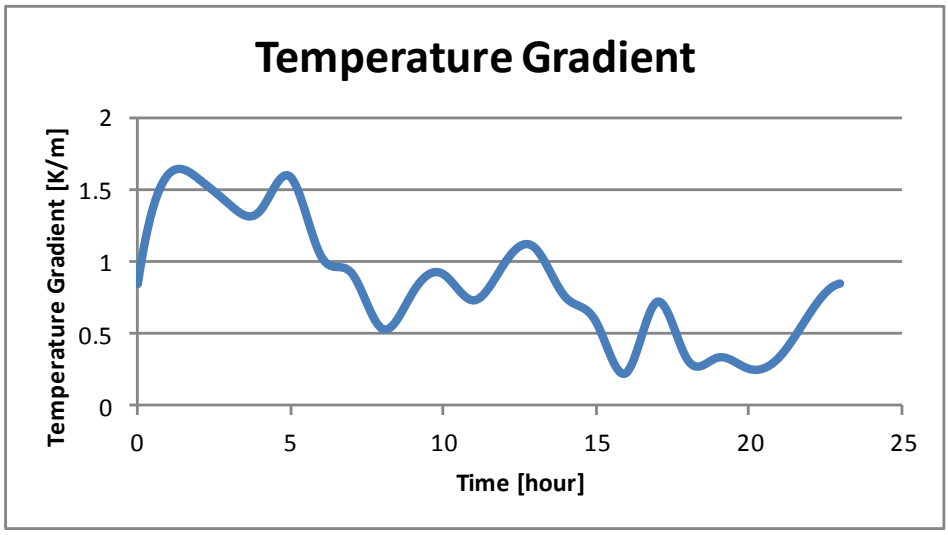

Fig.9.6: Temperature Gradient

The stratification height is shown in Fig.9.7.

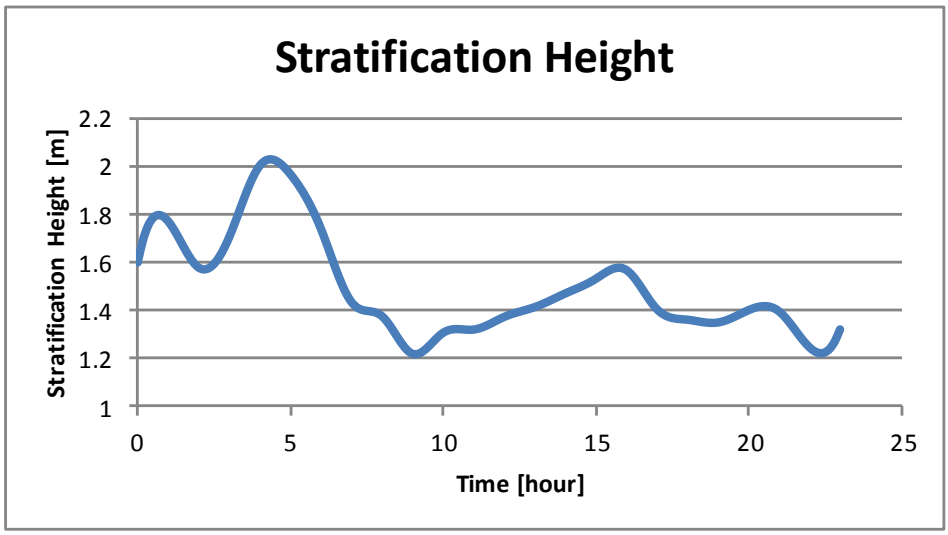

Fig.9.7: Plot of the stratification height

The Predicted Mean Vote is shown in Fig.9.8.

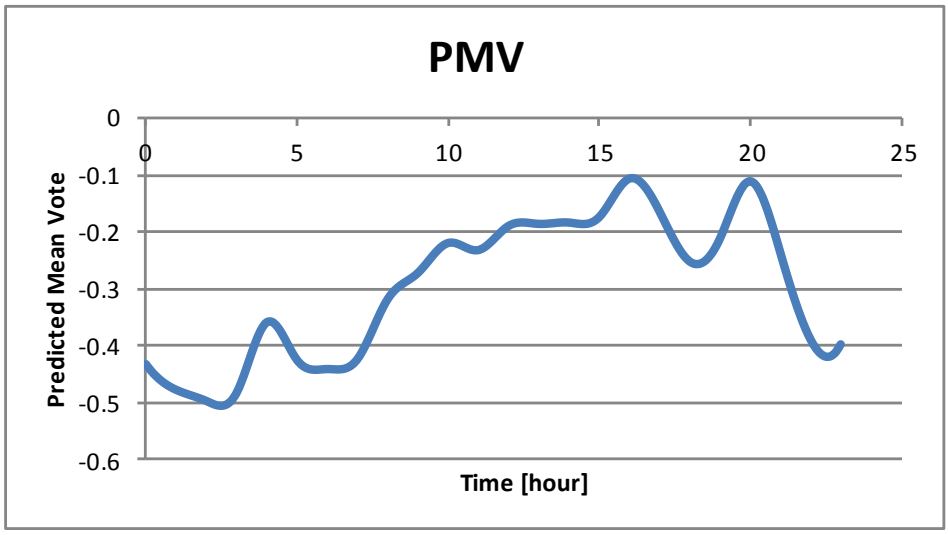

Fig.9.8: The predicted mean vote

The relative humidity inside the conditioned zone is shown in

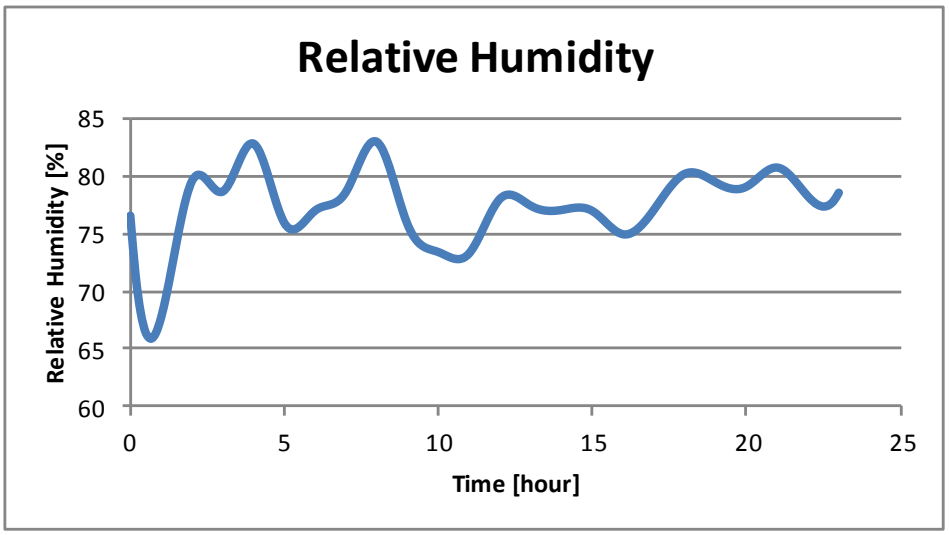

The Carbon Dioxide concentration by volume is shown in Fig.9.9.

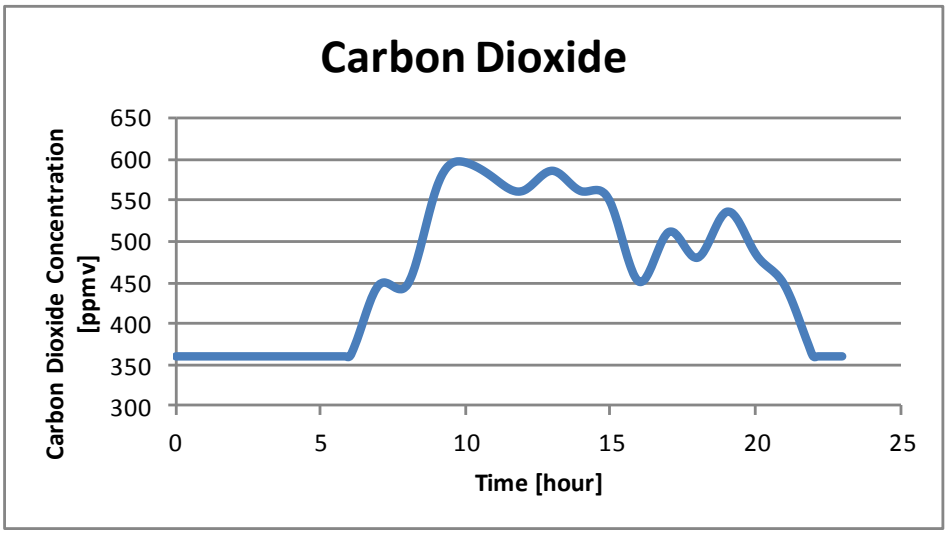

Fig.9.9: Carbon dioxide concentration inside the room

REFERENCES

Beasly, D. *An Overview of Genetic Algorithms, Part1 Fundamentals.* University Computing, 1993.

Chen, Q. "Performance evaluation and development of design guidelines for displacement ventilation." *ASHRAE RP-949*, 1994.

Coilmac Coil. "Water Cooling Coils 1/2" OD Tube." 2000.

Conroy, C. L., and Stanley A. Mumma. "Ceiling radiant cooling panels as a viable distributed parallel sensible cooling technology integrated with dedicated outdoor air systems." *ASHRAE Transactions*, 2001: 578–585.

Ghaddar, N., K. Ghali, R. Saade, and A. Keblawi. "Design charts for combined chilled ceiling displacement ventilation systems." *ASHRAE Transactions*, 2008: 574-587.

Gouda, M. M., S. Danaher, and C. P. Underwood. "Building thermal model reduction using nonlinear constrained optimization." *Building and Enviroment*, 2001: 1255-1265.

Hottel, H. C., and A. Whillier. "Evaluation of flat-plate collector performance." *Transactions of the Conference on the Use of Solar Energy*, 1958: 74.

Incropera, Frank P., and David P. Dewitt. *Fundamentals of Heat and Mass Transfer, Fifth Edition.* John Wiley and Sons, 2005.

Jeong, Jae-Weon, and Stanley A. Mumma. "Simplified cooling capacity estimation model for top insulated metal ceiling radiant cooling panels." *Applied Thermal Engineering*, 2004: 2055-2072.

Karr, C., and M. Freeman. "Industrial applications of Genetic Algorithms." *CRC Press LLC*, 1999.

Keblawi, A., N. Ghaddar, K. Ghali, and L. Jensen. "Chilled ceiling displacement ventilation design charts correlations to employ in optimized system operation for feasible load ranges ." *Energy and Buildings*, 2009: 1155-1164.

Keepright Refrigeration. "Water Cooling Coils." Ontario, Canada, 2007.

Kuehn, Thomas H., James W. Ramsey, and James L. Threlkeld. *Thermal Enviromental Engineering, Third Edition.* Prentice Hall, 1998.

Laret, L. "Use of general models wih a small number of parameters: Part I - theoritical analysis." *Procedings of 7th Internaltional Congress of Heating and Air Conditioning CLIMA 2000.* Budapest, 1980.

Liesen, R. J., and C. O. Pederson. "An evaluation of inside surface heat balance models for cooling load calculations." *ASHRAE Transactions*, 1997: 61-75.

McQuiston, F. C. "Correlations for heat, mass and momentum mass transport coefficients for plate-fin-tube heat transfer surfaces with staggered tubes." *ASHRAE Transactions*, 1978: 294-309.

N., H. Kim, B. Youn, and R. L. Webb. "Air-side heat transfer and friction correlations for plain fin-and-tube heat exchangers with staggered tube arrangements." *ASME Journal of Heat Transfer.*, 1999: 662-667.

Novoselac, A., and J. Srebric. "A critical review on the performance and design of combined cooled ceiling and displacement ventilation systems." *Energy and Buildings*, 2002: 497-509.

Ruan, Da. *Intelligent Hybrid Systems.* Kluwer Academic Publishers, 1997.

Tan, H., T. Murata, K. Aoki, and T. Kurabuchi. "Cooled ceilings/displacement ventilation hybrid air conditioning system-design criteria." *Proceedings of Roomvent'98*, 1998: 77-84.

Underwood, Chris P., and Francis W.H. Yik. *Modelling Methods for Energy in Buildings.* Blackwell Publishing, 2004.

Vardhan, Abhay, and P. L. Dhar. "A new procedure for performance prediction of air conditioning coils." *International Jounal of Refrigeration*, 1998.

Walton, G. N. "A new algorithm for radiant interchange in room load calculations." *ASHRAE Transactions*, 1980: 190-208.

Wang, Jianfeng, and Eiji Hihara. "Prediction of air coil performance under partially wet and totally wet cooling conditions using equivalent dry-bulb temperature methos." *International Journal of Refrigeration*, 2002.

Wang, Shengwei, and Xinqiao Jin. "Model-basel optimal control of VAV air-conditionig system using genetic algorithm." *Building and Enviroment*, 1999: 471-487.

Yazdanian, M., and J. H. Klems. "Measurement of the exterior convection film coefficient for windows in low rise buildings." *ASHRAE Transactions*, 1994.

Zhou, Xiaotang, James E. Braun, and Qingfan Zeng. "An Improved Method for Determining Heat Transfer Fin Efficiencies for Dehumidifying Cooling Coils." *HVAC&R Research*, September 2007: 769-783.